EQUIPMENT ROOT CAUSE OF FAILURE ANALYSIS

CLASS 1E 125 VDC POWER SYSTEM BATTERIES

2EPKAF11, 2EPKBF12, 2EPKCF13, 2EPKDF14

May 9, 1997

Revision 0

ERCFA Investigator: [signature] 5/13/97

Co-Authors: [signature] 5-9-97

[signature] 5-9-97

[signature] 13 MAY 97

Section Leader: [signature] 6/4/97

Department Leader: [signature] 6-10-97

ERCFA Program Manager: [signature] 5/13/97

Nuclear Assurance: [signature] 6/24/97

TABLE OF CONTENTS

1.0 EXECUTIVE SUMMARY

The 60 month battery discharge test (32ST-9PK04) was performed on 2EPKAF11 and 2EPKCF13. The capacity of 2EPKCF13, which was performance tested on March 22, 1996, was equal to 88.3%. On March 23, 1996, the capacity for 2EPKDF14 was predicted to equal approximately 88%. 2EPKCF13 and 2EPKDF14 were declared inoperable because the capacity of both batteries was below the Technical Specification Surveillance Requirement 4.8.2.1.e limit of 90%.

Based on performance test results, the apparent cause for the AT&T (Lucent Technologies) Round Cell capacity loss was string related as shown below.

STRING	APPARENT ROOT CAUSE CAPACITY LOSS
HG-14	positive plate passivation - PCL
HG-16	negative plate sulfation (crystals) - aggravated by cell mixing and borderline polarization (double platinum)
HG-18	negative plate sulfation (crystals) positive plate degradation

To verify the failure mode, cells from PVNGS and Braidwood were sent to Argonne National Laboratory. The results of the destructive analysis are summarized in Attachment 1. Based on the examination of six high gravity Round Cells, Argonne concluded capacity loss was caused by changes in the corrosion layer that normally develops between the positive plate active material and positive plate grid. According to discussions with Lucent Technologies, the changes in the PbO_2 scale were not significant enough to cause a loss in cell capacity. The scale morphology of the "good" cell (SN 59942) was different from that of the other cells examined. These differences may be due to the maintenance history of cell SN 59942 (a spare cell stored on open circuit prior to one modified performance test) compared to the "bad" cells (installed cells had three or more capacity discharge/recharge cycles). The Argonne report did not specify what caused the changes in the corrosion layer. The root cause of the capacity loss could not be determined conclusively from destructive examination analysis of the cells.

The HG-14 and HG-16 cells were removed and replaced. The capacity of each of the newly configured battery banks is greater than 100%. The Unit 2 battery banks have been reconfigured as follows:

2EPKAF11: HG-1
2EPKBF12: HG-10 (new cells)
2EPKCF13: HG-16
2EPKDF14: Braidwood cells

Testing to determine the charge recovery for low and high gravity Round Cells following multiple shallow discharges has been completed. Test results indicate that recharging Round Cells at float potential following multiple shallow discharges does not fully restore battery capacity. The capacity loss for high gravity Round Cells was greater than low gravity Round Cells. The average high and

low gravity Round Cell capacity loss was 17.9% and 6.4%, respectively. This result is consistent with premature capacity loss (PCL) seen in previous high gravity performance testing. Considering that the maximum required capacity by design basis for the batteries is 53%, even assuming a maximum capacity loss of 22.3% (based on high gravity test results, Section 6.2), there still remains considerable safety margin for Unit 2 batteries. Assuming that there is a capacity loss problem, it can be shown that due to significant safety margin, a worst case projected capacity loss would not significantly impact the PVNGS batteries ability to perform their safety function. This conclusion also applies to the Unit 1 & 3 batteries.

Lucent Technologies Inc., Microelectronics Group - Power Systems Division has decided to discontinue manufacturing high gravity Round Cells and discontinue "marketing and sales activities of all power products into the nuclear utility market." This decision was based on several key issues: past and current customer concerns about long term battery performance, premature capacity loss of high gravity cells, amount of technical support required and Lucent Technologies' business decision to focus on their more profitable telecommunications market.

Since the high gravity Round Cell battery may not deliver the long term performance results that we require, the installed Round Cells will be replaced with qualified batteries that have had a proven history of reliable performance. Design and implementation will be tracked in CATS under CRDR 2-6-0050.

2.0 EQUIPMENT DESCRIPTION

Four Class 1E 125 Vdc power subsystems designated A, B, C and D are provided in each Unit. Subsystem A and B provide control power for alternating current load groups 1 and 2, respectively. These subsystems also provide vital instrumentation and control power for channels A and B, for Reactor Protection, Engineered Safety Features (ESF) systems, and diesel generators A and B. Subsystems C and D provide vital instrumentation and control power for channels C and D, for Reactor Protection, ESF systems and other safety-rated loads as referenced in UFSAR, Table 8.3-6, Class 1E DC System Loads. Each Class 1E DC subsystem consists of one 125 Vdc battery composed of 60 cells, one battery charger and one control center, which is supplied with 480 VAC power from separate motor control centers. The battery chargers are designed to supply at least 400 Amps for battery banks A and B, and 300 Amps for banks C and D at 125 volts for at least eight hours. Four inverters, which are supplied from the DC subsystems, provide four independent 120 VAC vital instrumentation and control power supplies for the banks of Reactor Protection and ESF systems. The Class 1E 125 Vdc power system has two backup chargers. Backup charger "AC" is capable of providing 125 Vdc power to battery bank A or C. Backup charger "BD" is capable of providing 125 Vdc power to battery bank B or D.

The Class 1E 125 Vdc systems are designed for normal operation at a charger float voltage of 135 DC. During normal operation, the normal battery charger supplies power to its associated 125 Vdc control center. In addition to carrying the loads on the DC control center, the normal battery charger provides a float charge to the battery to keep the battery fully charged. The battery is available as a standby DC source to carry the control center load automatically in case of loss of the charger. The common backup battery charger is connected through a manual transfer switch to the DC control

center. In case of loss of AC power to the normal battery charger, or unavailability of the normal battery charger due to maintenance or testing, the backup battery charger is manually connected to the control center to supply control loads and provide a float charge to the battery. In case of complete loss of AC power, each DC control center will be fed by its battery for a minimum of two hours. Upon restoration of AC power, the battery charger is operated in the equalize mode to supply all the steady state loads and the charging current required to restore the battery from the design minimum charge state to the fully charged state within 12 hours.

Each Unit has four batteries EPKAF11, EPKBF12, EPKCF13 and EPKDF14. Each battery is compromised of 60 AT&T LINEAGE® 2000 Round Cells, model KS-20472, List 1SH. Each is a high specific gravity, 1850 ampere-hour (8 hour rate) lead-acid battery. At PVNGS, 60 cells are series connected to provide a nominal 125 Vdc battery bank voltage. Each Unit has four spare cells, which are located in the bank A battery room. The spares are tested and maintained the same as the four battery banks. The spares are recharged following testing on a separate charger. The spare battery chargers are designed to supply 50 Amps at 125 volts.

The primary application for the Round Cell battery is to provide float duty reserve energy. It is not suitable for high cyclic rate discharges. UPS applications are generally acceptable because the depth of discharge, which is usually quite shallow, will not modify the active plate material to any great extent. Repeated deep discharges (> 80%) cause the active material in all lead-acid cells to lose its crystalline structure and shed from the plates. One or two discharges of 100% capacity each year over the battery life would be the expected maximum for any lead-acid battery designed for float duty backup power.

Overall battery performance is defined by two types of tests: a capacity (or performance) test and a service (load profile) test. During a capacity test, the battery is discharged at a constant current to a specified terminal voltage. A capacity discharge test is performed on a new battery (a string of 72 cells connected in series) prior to shipment (acceptance test) to verify it meets specifications or manufacturer's ratings. A capacity discharge test (performance test) of the battery bank is performed, during shutdown, within the first 2 years of service and at 5 year intervals thereafter. The purpose of the performance test is to detect any degradation of capacity and to determine remaining battery life. Annual performance discharge tests are given to any battery that shows signs of degradation or has reached 85% of the service life expected for the application (ref. Tech Spec 4.8.2.1.f). For the Round Cells, degradation is indicated when the battery capacity drops more than 5% of rated capacity from its average on previous performance tests or is 95% of the manufacturer's rating (ref. Tech Spec 4.8.2.1.f).

At 18 month intervals, during shutdown, a service test is performed to verify battery capacity is adequate to supply all emergency loads for the design accident duty cycle. The battery is tested to a defined load profile based on the expected loading on the batteries during an actual accident condition.

2.1 Battery Description

The AT&T LINEAGE® 2000 Round Cell has a conventional pasted plate construction similar to other lead-acid batteries. Figure 1 shows the major Round Cell components.

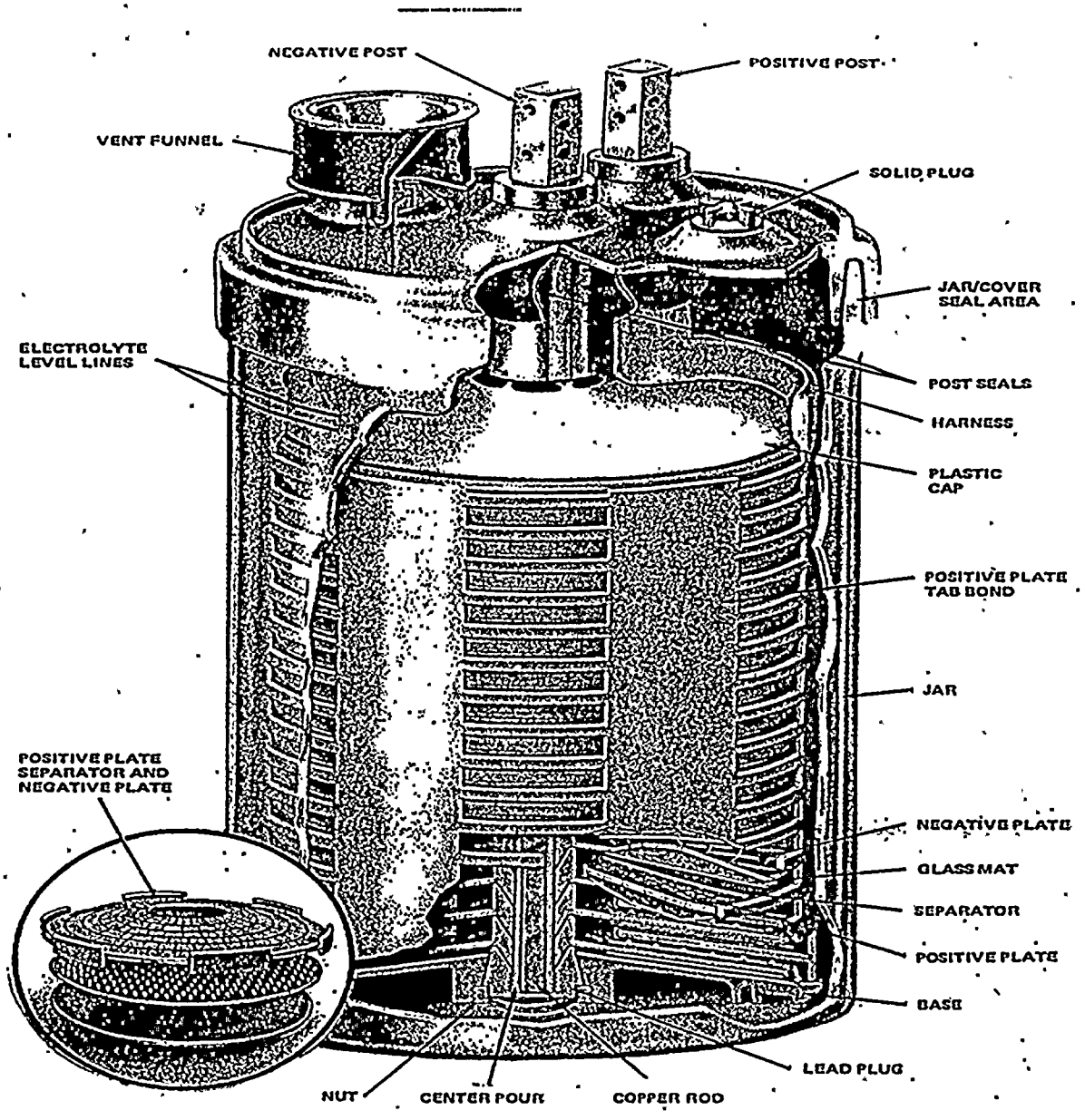

Figure 1. AT&T Round Cell

The plates are conical at a 10 degree angle and stacked vertically. Microporous separators and fiberglass mats separate the plates to provide electronic insulation and prevent shorting while allowing ionic transport and gas transmission. The plate stack rests on a conical shape hard

rubber base. After stack assembly and insertion of a copper rod for conductivity down the center of the stack, the entire negative group is interconnected by a center pouring process. The positive plates have vertical connector tabs that are joined after assembly by a welding process. Gas and electrolyte is allowed to percolate via a chimney around the center of the negative post and through the spaces between the tabs on the positive plates. The ten degree angle of the positive plates allows for efficient circulation of gas.

The jar is made of PVC with a cover that is connected using a heat sealed shear bond for maximum strength. For ease of maintenance a dam is provided at the outer edge of the jar cover to contain any electrolyte leakage. Post seals incorporate a long leakage path which is coupled to the cover by a rubber flexible bellow backed up by a piston-cylinder, accordion ring type seal to allow for vertical movements such as vertical element growth.

At the factory, after the Round Cell is assembled, a group of 72 cells is connected in series. This group of cells is referred to by the manufacturer as a battery "string". The battery string is then condition cycled. The purpose of the conditioning cycle is to saturate the plates with acid to allow for positive plate conversion. The string is charged and discharged according to the customer's specific discharge test requirements before the cell is packed and shipped.

The circular design of the grid structure was a result of the design objective of Bell Labs to minimize corrosion and control positive plate growth. The pancake stacked design of the Round Cell allows for minimal loading on the plates and provides the opportunity to make use of the superior growth characteristics of pure lead grids. In addition, the circular plate allows for better control of contact between the pure lead grid and the positive paste pellets. Capacity loss due to corrosion generally occurs due to loss of contact between the grid structure and the active positive paste material.

AT&T Round Cells operate in the same manner as conventional lead-acid storage batteries. The 60 cell battery provides electrical power by converting its stored chemical energy into electrical energy. The energy conversion is achieved by a chemical reaction in the battery that releases electrons. The process is reversible in a stationary battery; electrical energy directed into the battery reverses the chemical reaction and restores the battery to a fully charged condition.

The generation of electrical current from a battery cell originates from a difference in electrochemical potential between two compounds (the positive and negative plates) inside the battery that are not in direct contact, but are connected by an electrically conducting medium (electrolyte). The electrochemical process between the plates and electrolyte creates a voltage difference between the positive and negative plates of the cell. The voltage difference between the plates constitutes an electromotive force that causes electrons to flow from the negative to the positive plates, if connected together by an external load. The battery continues to generate electrical current until the materials involved in the reaction are depleted or the external connection is removed. In a lead-acid battery, the positive plate (active) material is lead dioxide (PbO_2) and the negative plate material is lead (Pb). The chemical reaction in a lead-acid cell is in terms of the reaction occurring at each plate. From left to right, these equations represent the discharge process (from right to left, the charging process):

Positive Plate $PbO_2 + SO_4^{2-} + 4H^+ + 2e^- \Leftrightarrow PbSO_4 + 2\,H_2O$

Negative Plate $Pb + SO_4^{2-} \Leftrightarrow PbSO_4 + 2e-$

3.0 FAILURE DESCRIPTION

The 60 month battery capacity discharge test (32ST-9PK04) was performed on 2EPKAF11 and 2EPKCF13 (battery banks A and C) during the Unit 2 sixth refueling outage (U2R6). The test was performed on the Class 1E batteries to satisfy the IEEE-450 requirement to perform a capacity discharge test on new batteries within the first two years of service. 2EPKAF11, which was performance tested on March 20, 1996, had a capacity of 106.7%. The capacity of 2EPKCF13, which was performance tested on March 22, 1996, was equal to 88.3%. On March 23, 1996, the capacity for 2EPKDF14 was predicted to equal approximately 88%. The 2EPKDF14 battery predicted capacity was derived using data from battery bank A and C performance tests. The predicted capacity for 2EPKBF12 was approximately 104%. 2EPKCF13 and 2EPKDF14 were declared inoperable because the capacity of both batteries was below the Technical Specification Surveillance Requirement 4.8.2.1.e limit of 90%. Fuel movement was suspended, until Tech Spec 4.8.2.1.e. was temporarily modified. The modification specified the provisions of Specification 4.0.1 and 4.0.4 were not applicable to the battery capacity requirements until entry into Mode 4 coming out of the sixth refueling outage or upon any deep discharge of the battery. The change to the Tech Specs allowed PVNGS to declare the Unit 2 batteries operable based on current battery capacities without having to satisfy the surveillance requirements of Tech Spec 4.8.2.1.e. Each train of the class 1E battery had sufficient capacity to independently supply the required design basis accident loads for 2 hours. The PVNGS design exceeds the 25% margin sizing requirement specified in IEEE-450. 2EPKCF13 and 2EPKDF14 have design capacity of 348% and 684% of the required end-of-life capacity, respectively. Since the capacity is based on the manufacturer's rating, the degradation experienced by the Unit 2 batteries had resulted in capacities that were still in excess of that required for the batteries to perform their safety related function. Calculations performed demonstrated that the projected capacities provided greater than 200% margin above that required for safety related loads.

To date, Units 1 and 3 have experience the expected capacity from the installed Round Cells.

4.0 SEQUENCE OF EVENTS (SOE)

DATE	SEQUENCE OF EVENTS
10/19/94	manufacturer string HG-14 first factory acceptance test, capacity = 110% recharge: factory method *
11/1/94	manufacturer string HG-14 second factory acceptance test, capacity = 102% jumpers used instead of intercell connectors, problems with charger prior to discharge recharge: factory method *
11/21/94	manufacturer string HG-14 third factory acceptance test, capacity = 108% recharge: factory method *

11/30/94	manufacturer string HG-18 first factory acceptance test, capacity = 115% recharge: factory method *
12/20/94	manufacturer string HG-18 second factory acceptance test, capacity = 110% recharge: factory method *
12/22/94	manufacturer string HG-14 fourth capacity discharge test (first performance test at PVNGS), capacity = 105% recharge: factory method *
1/5/95	manufacturer string HG-18 third factory acceptance test, capacity = 108% recharge: factory method *
1/17/95	manufacturer string HG-16 first factory acceptance test, capacity = 115% recharge: factory method without trickle charge *
1/18/95	manufacturer string HG-1 first factory acceptance test, capacity = 115% recharge: factory method without trickle charge *
1/25/95	manufacturer string HG-16 second factory acceptance test, capacity = 113% recharge: factory method *
1/26/95	manufacturer string HG-1 second factory acceptance test, capacity = 115% recharge: factory method *
2/19/95	replaced 2EPKBF12 cells in accordance with Calc. 02-EC-PK-210 (New AT&T Round Cells installed)
2/19/95	replaced 2EPKDF14 cells in accordance with Calc. 02-EC-PK-210 (New AT&T Round Cells installed)
3/1/95	replaced 2EPKAF11 cells in accordance with Calc. 02-EC-PK-210 (New AT&T Round Cells installed)
3/2/95	replaced 2EPKCF13 cells in accordance with Calc. 02-EC-PK-210 (New AT&T Round Cells installed)
4/6/95	1EPKDF14 passed performance test, capacity = 107% recharge: PVNGS method **
4/7/95	1EPKBF12 passed service test recharge: PVNGS method **
4/19/95	1EPKAF11 passed service test recharge: PVNGS method **
4/19/95	1EPKCF13 passed service test recharge: PVNGS method **
8-9/95	battery 2EPKDF14 equalize charge
10/17/95	3EPKAF11 passed service test recharge: PVNGS method **
10/18/95	3EPKCF13 passed service test recharge: PVNGS method **
10/29/95	3EPKBF12 passed service test recharge: PVNGS method **
10/31/95	3EPKDF14 passed service test recharge: PVNGS method **
11/30/95	Lucent Technologies Round Cell Nuclear Utility User's Council meeting in Mesquite, TX

1-2/96	battery 2EPKCF13 equalize charge
2/96	battery 2EPKBF12 equalize charge
2/14/96	Braidwood cells acceptance test, manufacturer drop 40 capacity = 112% manufacturer drop 41 capacity = 116% Cells shipped to Byron Nuclear station, then to Braidwood Nuclear Station.
3/20/96	**battery 2EPKAF11 performance test, capacity = 106.7%** **capacity was approximately 6% less than the previous capacity (ref. Calc. 02-EC-PK-210) - degradation is indicated when the battery capacity drops more than 5% of rated capacity from the average of its previous performance tests (Tech Specs SR 4.8.2.1.f)** battery recharge: 71 A for 20 hours spares recharge: current limit setting = 50 A (spare charger) for 28 hours
3/22/96	**battery 2EPKCF13 performance test, capacity = 88.3%** **battery bank declared inoperable - capacity below Technical Specification Surveillance Requirement 4.8.2.1.e limit of 90%** recharge: 59 A for 22 hours, 5 A for 48 hours
3/23/96	**battery 2EPKDF14 predicted capacity = 88%** **battery bank declared inoperable**
3/23/96	**NRC issued emergency Tech Specs change allowing PVNGS to declare the Unit 2 batteries operable based on current battery capacities**
4/10/96	manufacturer string HG-10 (new) 2 hour acceptance test, average ICV at end of discharge = 1.88 V (discharge end criteria - when average ICV = 1.75 V or 2 hour duration, whichever occurred first) recharge: factory method *
4/11/96	Lucent Technologies Round Cell Nuclear Utility User's Council meeting in Gulf Shores, AL
4/13/96	battery 2EPKDF14 performance test, test equipment malfunction, cells discharged 42 minutes, test aborted
4/17/96	**60 Braidwood cells installed in battery 2EPKDF14**
4/18/96	**60 manufacturer string HG-10 (new) cells installed in battery 2EPKBF12**
4/18/96	Lucent Technologies Round Cell Nuclear Utility User's NRC presentation in Washington, DC
4/19/96	**battery 2EPKDF14 passed service test** recharge: 75A for 3 hours, 9 A for 2 hours
4/20/96	performance test 17 HG-1 and 34 HG-16 cells in PK storage facility, manufacturer string HG-1 battery capacity = 108% manufacturer string HG-16 battery capacity = 102%
4/21/96	**battery 2EPKBF12 passed service test** recharge: 60A for 8 hours
4/24/96	**battery 2EPKCF13 reconfigured, HG-16 cells installed** **battery 2EPKAF11 reconfigured, HG-1 cells installed**
4/26/96	surveillance test credit taken for manufacturer strings HG-1 and HG-16 performance tests on 3/22/96, 3/24/96 and 4/20/96

	surveillance test credit taken for Braidwood and manufacturer string HG-10 factory acceptance tests
4/27/96	battery 2EPKBF12 connected to portable charge for high rate charge (2.8 Vpc {volts per cell}, charge at 20 A for 6 hours)
	battery 2EPKDF14 connected to portable charge for high rate charge (2.8 Vpc, charge at 20 A for 6 hours)
5/22/96	Lucent Technologies Round Cell Nuclear Utility User's Council meeting in Charlotte, NC

* Factory method of recharge: constant current method - 130% of the ampere-hours removed during the discharge is replaced (recharged) within 20 hours (typical recharge rate = 60 to 70 A for 20 hours), followed by a trickle charge of 5 A for 3 days.
** PVNGS method of recharge; constant voltage method - 2.33 Vpc until current < 10 A, 2.5 Vpc for 8 hours and specific gravity is above 1.290.

5.0 FAILURE MODE INVESTIGATION

5.1 Unit 2 Battery Performance Prior to U2R6 Performance Testing

Prior to performance testing, the 2EPKBF12, 2EPKCF13 and 2EPKDF14 individual cell voltages (ICVs) were varying (primarily based on data reviewed from 92 day STs). The ICVs had deviated from a nominal 2.25 Vpc to 2.21-2.28 Vpc. Because Round Cells are so uniform in performance, by design the voltage difference between the lowest and highest floating cell is usually less than 40 mV. The ICV deviations seemed to correlate with manufacturer string. Since installation, the ICVs of HG-18 cells were decreasing. HG-18 factory and installed data showed declining negative half-cell potentials.

The specific gravity of the lower voltage cells dropped an average of 9 points (.009) since installation. The following table shows the average specific gravity by manufacturer string.

STRING	NUMBER OF DISCHARGES	INITIAL AVERAGE SPECIFIC GRAVITY	FINAL AVERAGE SPECIFIC GRAVITY
HG-1	2	1.308	1.303
HG-14	4	1.307	1.305
HG-16	2	1.306	1.299
HG-18	3	1.302	1.293

Equalization of the batteries is the corrective action to reduce cell voltage variations and reverse a decreasing trend in specific gravity. 2EPKBF12, 2EPKCF13 and 2EPKDF14 were placed on equalize charge (ref. Section 4.0, Sequence of Events). Cell voltages, which temporarily improved following an equalize charge, were not permanently corrected.

5.2 Unit 2 Battery Bank Composition

The Unit 2 Class 1E batteries were replaced and configured, in accordance with Calc. 02-EC-PK-210, at the end of the fifth refueling outage. As shown in the tables below, capacity and capacity loss/gain, from 2EPKAF11 and 2EPKCF13 U2R6 performance tests, can be correlated by string.

2EPKAF11 Capacity and Capacity Loss/Gain					
STRING	NUMBER OF CELLS	CAPACITY 3/20/96 (AVERAGE)	CAPACITY STANDARD DEVIATION	CAPACITY LOSS/GAIN FROM TEST PRIOR TO 3/20/96	CAPACITY LOSS/GAIN STANDARD DEVIATION
HG-1	43	114.2%	4.9%	- 4.1%	4.5%
HG-14	6	83.5%	5.7%	- 22.3%	6.1%
HG-16	10	102.3%	3.0%	- 15.1%	3.1%
HG-18	1	110.3%	N/A	- 7.5%	N/A

2EPKCF13 Capacity and Capacity Loss/Gain					
STRING	NUMBER OF CELLS	CAPACITY 3/20/96 (AVERAGE)	CAPACITY STANDARD DEVIATION	CAPACITY LOSS/GAIN FROM TEST PRIOR TO 3/22/96	CAPACITY LOSS/GAIN STANDARD DEVIATION
HG-1	4	114.4%	4.4%	+ 0.4%	4.5%
HG-14	15	90.6%	4.6%	- 17.4%	4.2%
HG-16	18	105.3%	3.2%	- 8.1%	3.1%
HG-18	23	83.0%	12.4%	- 29.4%	9.7%

5.3 Additional Discharge Tests

5.3.1 Unit 2 Spares

Each Unit has four spare cells, which are located in the bank A battery room. The spares are tested and maintained the same as the four battery banks. The Unit 2 spares, which are from manufacturer string HG-14, were discharged with 2EPKAF11 on March 20, 1996. The spare recharge method used approximated a constant current recharge by setting the spare charger current limit to 50 A. The spares were recharged for approximately 28 hours and retested on March 24, 1996 to determine whether the capacity loss was reversible.

DATE	SPARE 1 SN 74970	SPARE 2 SN 74861	SPARE 3 SN 74859	SPARE 3 SN 74912
12/22/94	104%	103%	103%	103%
3/20/96	75%	77.5%	77.5%	75.8%
3/24/96	82.5%	85.8%	85.8%	85.8%

5.3.2 Single Cell Testing

Single cell discharge testing was performed on several cells removed from Unit 2. The results are summarized below.

BATTERY	SN	CAPACITY [1]	3/96 CAPACITY	SINGLE CELL CAPACITY [2]	HALF CELL VOLTAGE [5] + TO REF. / - TO REF.
2EPKCF13 cell 25	77722 HG-18	113%	80%	59% 3/31/96	+ 1.286 / - 0.973
2EPKCF13 cell 39	78056 HG-18	102%	46%	39% 4/3/96	+ 1.281 / - 0.967
2EPKCF13 cell 43	78060 HG-18	103%	48%	35% 4/3/96	+ 1.287 / - 0.966
2EPKCF13 cell 47	77661 HG-18	113%	97%	78% 4/6/96	+ 1.275 / - 0.971
2EPKCF13 cell 55	78025 HG-18	113%	95%	68% 4/8/96 [3]	+ 1.275 / - 0.973
2EPKCF13 cell 9	77904 HG-18	113%	93%	63% 4/8/96 [4]	+1.273 / - 0.973
2EPKCF13 cell 44	78105 HG-18	114%	89%	28% 4/8/96	+ 1.275/ - 0.973
2EPKDF14 cell 6	76822 HG-16	112%	N/A	100% 4/9/96	+ 1.287/ - 0.966
2EPKDF14 cell 60	78023 HG-18	109%	N/A	74% 4/12/96	+ 1.295/ - 0.968

[1] capacity of last discharge test, prior to installation

[2] single cell performance test, cell removed from installed battery bank

[3] modified performance test: 1st min. at 2 hr. discharge rate, next 3 hrs 59 mins. at 4 hr. rate

[4] modified performance test: 1st min. at 2 hr. discharge rate, next 4 hrs 59 mins. at 5 hr. rate

[5] half cell voltage measurements taken on float prior to single cell performance test

5.4 Observations

Cell voltage or specific gravity, by itself, is not an indication of battery state of charge. However, failure of a cell to hold a charge, as shown by cell voltage and specific gravity readings, is a good indicator that battery replacement may be needed. The following

characteristics were observed in cells with catastrophic capacity loss:

1. Low negative half cell voltage (low cell voltage)
2. Specific gravity loss
3. Crystal growth on negative (center) post

STRING	OBSERVATIONS SUMMARY
HG-1	2 factory acceptance (performance) prior to installation
	performed well, no adverse behavior
HG-14	4 factory acceptance (performance) prior to installation
	capacity loss consistent: - 2EPKAF11 capacity loss = 22.3% - 2EPKCF13 capacity loss = 17.4%
	no specific gravity loss
	high positive plate polarization
	capacity improved after constant current recharge (4 spares)
	float current normal (approximately 100 mA)
HG-16	2 factory acceptance (performance) prior to installation
	capacity consistent and greater than 100%: - 2EPKAF11 capacity = 102.3% - 2EPKCF13 capacity = 105.3%
	average specific gravity loss less than HG-18 cells
	average polarization greater than HG-18 cells
	negative plate sulfation (crystals)
	HG-16 single cell performance test: - 11% capacity loss - negative plate limited - within 3% of predicted capacity
HG-18	3 factory acceptance (performance) tests prior to installation
	catastrophic capacity loss: - 2EPKCF13 capacity loss = 29.4%
	specific gravity loss more than HG-1, HG-14 and HG-16
	polarization lower than HG-1, HG-14 and HG-16
	negative 1/2 cell voltage declined at factory
	negative plate sulfation (crystals)
	positive plate degradation, positive plate limited
	float current high (approximately 300 mA)

5.5 Most Probable Failure Modes

The following table summarizes the most probable failure modes that were evaluated as part of the equipment root cause of failure investigation.

FAILURE MODE	EFFECTS ON CELL	CAUSE
low impedance short	cell does not fully recharge	shedding of positive active material
	float voltage near or under OCV	
	sulfation (crystals) on positive strap	
high negative polarization	positive electrode does not fully recharge	deactivation of platinum (normally a function of cycling)
	crystals on positive strap	
	negative electrode floats at > 50 mV above open circuit negative potential (.97V with $Hg/HgSO_4$ electrode)	
	float voltage may be higher than other cells	
low negative polarization	negative electrode does not fully recharge	metal impurities or organic contamination
	crystals on negative post (sulfation)*	
	negative electrode floats below OC	
	increased gassing	
	increased float current (if all cells in one string affected)	
premature capacity loss (PCL)	cells show high positive polarization	formation of poorly conductive $PbSO_4$ and PbO_2 layers at active material/grid or particle/particle interface
	positive electrode builds up high resistance	
	process can be reversed by special conditioning cycling or recovery charge **, but not through on-line cycling	
	failure mode more severe with higher discharge rates combined with low recharge rates and higher electrolyte concentrations	
grid corrosion	disconnection of positive active material from corroded grid	occurs after a very long time on float
	increased rate of capacity loss	

* Sulfation structurally damages the plates, causing irreversible capacity loss.

** Recovery charge eliminates high impedance on the positive plate. The cells are placed on open circuit for approximately 8 weeks to increase the plate's porosity and reactivity (recrystallization of the active material) then recharged at 2.6 Vpc for 100 hours.

5.6 Historical Problems

5.6.1 Previous Unit 2 Class 1E Battery Capacity Loss

Comparison of the capacity loss for the Round Cells tested during U2R5 and U2R6 are shown as follows:

COMPARISON OF PROBLEMS WITH INSTALLED UNIT 2 CELLS	
1994 OBSERVATIONS	1996 OBSERVATIONS
capacity loss after first performance test	capacity loss after 3 - 4 performance tests
specific gravity remained constant	specific gravity decreased
ICVs remained constant	ICVs varied
capacity loss recoverable	irreversible capacity loss
all cells had capacity > 50%	many cells had capacity < 50%
no lead sulfate crystals on negative post (plate)	lead sulfate crystals on negative post (plate)

5.6.2 Manufacturer Changes

5.6.2.1 Platinum (Pt)

When first introduced, the Round Cell had problems recharging at float potential after a discharge. Reference electrode measurements indicated the positive plates were at or near the reversible $PbO_2/PbSO_4$ potential, i.e., positive plates were at open circuit potential. Optimally, the Tafel characteristics of a cell on float will have a positive plate slope of approximately 80 mV/decade. In the linear region, the negative plate slope should be approximately 120 mV/decade. Ideally the positive plates should be floating with at least 70 mV overpotential with the remainder on the negative plates. Examination of the Tafel characteristics showed the non-linearity of the negative plate polarization was not achieved and the current remained too low to charge the positive plates. To shift the negative plate polarization intercept to the right (higher current), Lucent Technologies added Pt as a depolarizing agent, as follows:

DATE	QUANTITY OF Pt ADDED FOR LIST 1S ROUND CELL
2/79	3 mg (tank formation)
6/85	0.12 mg (changed from tank to jar formation)
9/94	0.24 mg

5.6.2.2 Separator

Until the mid-80's, the Round Cell was manufactured using microporous rubber

separators. As part of an evaluation to determine the feasibility of replacing rubber separators with microporous polyethylene separators, prototype cells with microporous polyethylene separators were connected in series with cells with rubber separators. On float, the negative plate polarization was substantially less for cells with polyethylene separators. Subsequent field experience showed that this difference disappears over time. The separator material was changed from rubber to polyethylene for List 1S Round Cells in November 1989. The separator changes occurred prior to PVNGS purchase of cells, consequently all PVNGS cells have the same separator material.

5.7 Contaminants

Cells at PVNGS exhibit copper contamination in amounts that should not adversely affect cell performance, according to Lucent Technologies and Vinal (Reference 1). If the copper plates on the negative post in sufficient quantity, it can contribute to depolarization of the cell if other contaminates are present. Though, qualitative electrolyte samples from HG-18 cells contained a predominance of Zn, quantitative results indicated concentration levels were not significant enough to impair cell capacity. According to Vinal, the presence of Cu and Zn in a cell has a synergistic effect. Cells with twice as much Pt (0.12 mg vs. 0.24 mg) could be more susceptible to this affect. The Unit 1 and 3 cells have half the amount of Pt and more visual indication of copper contamination, but a much greater average negative overpotential than the Unit 2 cells that were replaced in U2R6.

6.0 TROUBLESHOOTING PLAN/RESULTS

6.1 Destructive Testing

To verify the root cause, three PVNGS cells (described in the table below) and three Braidwood cells were sent to Argonne National Laboratory for destructive analysis. Two of the Braidwood cells had severe capacity loss, the third was a "good" cell.

AT&T Serial Number: 76712		**Production String:** HG-16
Installed Battery Bank: 2EPKBF12		**Installed Cell Position:** 47
Apparent Root Cause: negative plate sulfation (crystals) aggravated by cell mixing and borderline polarization (double platinum)		
Cell History		
1/17/95 discharge @ factory cell capacity = 116%	constant current recharge: 130% of amp-hrs removed replaced within 20 hours	placed on float after recharge
1/25/95 discharge @ factory cell capacity = 115%	constant current recharge: 130% of amp-hrs removed replaced within 20 hours, 5 amps for 3 days	placed on float after recharge

2/96	equalized battery bank	
4/17/96	Cell removed from 2EPKBF12, placed in PK battery warehouse	placed on float
4/20/96 discharge @ PVNGS cell capacity = 95%	constant current recharge: 135% of amp-hrs removed replaced within 24 hours	placed on float after recharge

AT&T Serial Number: 74975		**Production String:** HG-14
Installed Battery Bank: 2EPKCF13		**Installed Cell Position:** 30
Apparent Root Cause: positive plate passivation (cycling)		
Cell History		
10/19/94 discharge @ factory cell capacity = 117%	constant current recharge: 130% of amp-hrs removed replaced within 20 hours, 5 amps for 3 days	placed on float after recharge
11/1/94 discharge @ factory cell capacity = 113%	constant current recharge: 130% of amp-hrs removed replaced within 20 hours, 5 amps for 3 days	placed on float after recharge
11/21/94 discharge @ factory cell capacity = 120%	constant current recharge: 130% of amp-hrs removed replaced within 20 hours, 5 amps for 3 days	placed on float after recharge
12/22/94 discharge @ PVNGS cell capacity = 108%	constant current recharge: 130% of amp-hrs removed replaced within 20 hours, 5 amps for 3 days	placed on float after recharge
1-2/96	equalized battery bank	
3/22/96 discharge @ PVNGS cell capacity = 89%	constant current recharge: 135% of amp-hrs removed replaced within 22 hours, 5 amps for 2 days	placed on float after recharge
4/24/96	cell removed from 2EPKCF13, placed in PK battery warehouse	placed on float

AT&T Serial Number: 77773		**Production String:** HG-18
Installed Battery Bank: 2EPKDF14		**Installed Cell Position:** 32
Apparent Root Cause: negative plate sulfation (crystals) positive plate degradation contamination and/or factory defect		
Cell History		
11/30/94 discharge @ factory cell capacity = 119%	constant current recharge: 130% of amp-hrs removed replaced within 20 hours, 5 amps for 3 days	placed on float after recharge
12/20/94 discharge @ factory cell capacity = 113%	constant current recharge: 130% of amp-hrs removed replaced within 20 hours, 5 amps for 3 days	placed on float after recharge
1/5/95 discharge @ factory cell capacity = 109%	constant current recharge: 130% of amp-hrs removed replaced within 20 hours, 5 amps for 3 days	placed on float after recharge
8-9/95	equalized battery bank	
4/12/96	constant current charge: 7 amps for 72 hours	placed on float after charge
4/15/96 discharge for 42 mins @ PVNGS (test equipment malfunctioned, test aborted)	cell removed from 2EPKDF14, placed in PK battery warehouse	
6/6/96	boost charge cell at 2.6v for 22 hours, current limit 120 amps	
6/7/96 discharge @ PVNGS cell capacity = 41%	recharge on float	

The six Round Cells were disassembled, and the components were evaluated following appropriate analytical procedures. Specific gravities and inorganic impurities in the electrolyte were determined. Microscopy studies were conducted on positive and negative electrodes from each cell. Interpretation of the electrode morphologies was augmented by intrusion porosimetry measurements. The microscopy studies also included examination of corrosion of the positive electrode grids.

Data synthesis using change analysis techniques focused on similarities and differences between cell 59942 ("good" cell), which showed no capacity loss, and the remaining cells from Braidwood and PVNGS, which demonstrated the capacity loss phenomenon.

6.1.1 Examination Procedure

The six Round Cells were placed on periodic float charge to insure the cells were maintained at a comparable state-of-charge (approximately 100%) prior to cell teardown. Prior to removal of a cell from float, a small hole was drilled in the cell lid and 50 mL electrolyte samples were extracted via an inserted length of tubing. In each cell, the first sample was extracted approximately 3 cm below the electrolyte level. The tubing was then lowered to approximately 3 cm from the cell bottom, and after waiting approximately 30 minutes, a second sample was extracted. These samples were analyzed for specific gravity and trace elements. The bulk of the trace element analysis was performed by the System Material Analysis Department of Commonwealth Edison.

Each cell teardown followed the same steps.

1. The electrolyte was pumped out of the cell and the cell interior was purged briefly with nitrogen.
2. The cell lid was removed and the electrode assembly was lifted free of the container.
3. The perimeter bonds between positive lugs were severed with a reciprocating saw.
4. The negative electrodes were separated from the central post by severing the radial grid elements adjacent to the post.
5. All electrodes were removed and inspected, but electrode samples were taken only from four preselected electrodes:
    - uppermost positive electrode (P1)
    - second negative from the top (N2)
    - lowest positive electrode (P18)
    - second negative from the bottom (N18)
6. The sediment at the bottom of each cell was also collected

Samples of electrodes were prepared in the following manner. The preselected electrodes underwent repeated immersions in water over several days to remove sulfuric acid. Sections were then removed from the neutralized electrodes, and these sections were vacuum dried for over a day.

The subsequent electrode studies included intrusion porisimetry, limited X-ray diffraction, and optical and scanning electron microscopy. Standard metallographic procedures were employed to prepare four different microscopy samples from each electrode. These samples were cross sections near the inner and outer perimeters of the circular electrodes, and surface sections from the same general areas.

6.1.2 Teardown Observations

No serious defects were noticed in the construction of the six cells. All welded connections were sound; the various insulating and sealing components were intact; and

the electrodes were relatively free of serious imperfections. Cell specific comments can be found on the cell worksheets attached to the Argonne National Laboratory Report (Attachment 1).

6.1.2.1 Positive Electrodes

The positive electrodes retained a number of earmarks from the pasting and formation processes. The top surfaces were highly textured, while the bottom surfaces were relatively smooth. The top-surface texture consisted of deep grooves and high ridges, with some finer structure overlaid on this alternating pattern. The "burlap" texture was evidently imparted to the electrodes by a coarse fabric shortly after the pasting operation. The smoother undersides had little surface texture other than minor pasting flaws. The slight bowing of the axial grid elements in the direction of pasting were clearly discernible on this side of the electrodes.

The positive paste-to-grid adhesion was deemed good. Pellet loss was minor in most cells and was represented by the loss of individual pellets or pellet fragments, usually at the outer perimeter. The worst incidence of pellet loss involved cell 59941 (Figure 2). Two sizable indentations were found on the outer perimeter rims. One extended from the third positive electrode to the sixth positive electrode, and the other extended from the twelfth positive electrode to the fifteenth positive electrode. Apparently, the welded electrode stack was hit twice before insertion in the cell jar. As a consequence, several perimeter pellets were dislodged in the immediate area of impact, and hairline gaps were opened between the grid and paste several centimeters in from the impact zone.

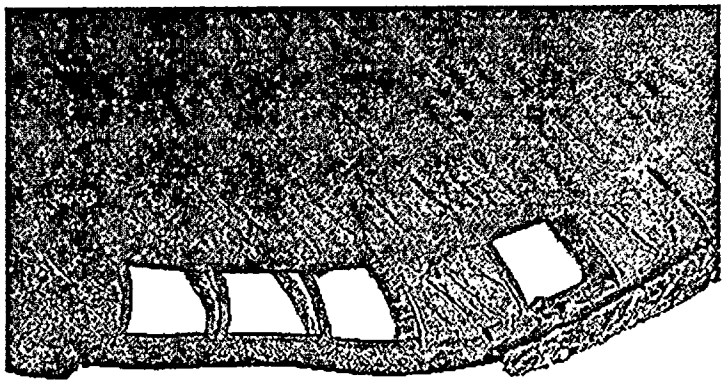

Figure 2. Cell 59941 - Multiple Pellet Loss with Outer Rim Indentations

The only consistent difference noted between the Braidwood and PVNGS cells pertained to the physical dimensions of the positive electrodes, as shown in the table below. The average of the mean diameters was 317.3 mm for the Braidwood positive electrodes but 316.5 mm for the PVNGS counterparts. The trend in thickness measurements was the opposite. The average thickness for the Braidwood and

PVNGS positive electrodes were 6.4 and 6.7, respectively. Both of these trends were interpreted as outcomes of a difference in service time. The larger diameters for the Braidwood electrodes reflected greater positive electrode expansion, a time-related corrosion phenomenon. The reduced thickness of Braidwood electrodes was a consequence of positive active-material shedding, also a usage-dependent degradation process. Sediment, which is a measure of active-material shedding, corroborated this premise. The sediment found in the bottoms of the Braidwood cells weighed 250% more on average than the sediment from the PVNGS cells. Performance differences related to these dimensional differences would be expected to be second-order effects and have little impact on usable capacity.

Positive and Negative Electrode Dimensions

Cell SN	Electrode	Thickness (mm)	Diameter (mm)
59941	P1	6.0	317.2
	P18	6.0	317.2
59942	P1	6.6	317.8
	P18	6.5	318.0
59936	P1	6.5	316.7
	P18	6.6	317.0
76712	P1	6.5	315.7
	P18	6.6	317.5
74975	P1	6.9	316.2
	P18	6.6	316.7
77773	P1	6.7	316.3
	P18	6.8	316.7
59941	N2	5.0	292.6
	N18	4.6	292.6
59942	N2	4.7	292.4
	N18	4.6	292.6
59936	N2	4.6	293.8
	N18	4.6	293.3
76712	N2	4.9	292.4
	N18	4.7	292.4
74975	N2	4.5	292.6
	N18	4.5	292.1
77773	N2	4.6	293.7
	N18	4.7	294.1

6.1.2.2 Negative Electrodes

The negative paste-to-grid adhesion was adequate, but the type and quantity of minor imperfections was greater than for the positive electrodes. These imperfections were again traceable to electrode fabrication, especially the pasting process. For the

negative electrodes, the burlap texture was evident on the bottom surfaces, and the top surfaces were relatively smooth, in a sense a mirror reversal of the positive electrodes. The grooves and ridges of the burlap pattern were not as pronounced for the negative electrodes. The presence of this pattern on both electrodes suggested that a common coarse separator was used during the formation process.

The most consistent pasting flaw for the negative electrodes was a mild tendency to underpaste (Figure 3). Once the paste was applied, it was not completely worked into contact with the grid elements. The end result was intermittent areas with surface gaps along the grid interface. On the top surfaces, these interfacial gaps ranged from fairly broad, shallow separations to slight hairline breaks. On the electrode undersides, the gaps tended to be wider and deeper and were commonly found near either the outer or inner perimeter. These separations generally occurred at only one or two interfaces of a given pellet, and the pellets remained in place. The only loose negative pellet was found in cell 59941, and it was dislodged from one of the areas where the electrode assembly had been struck and dented.

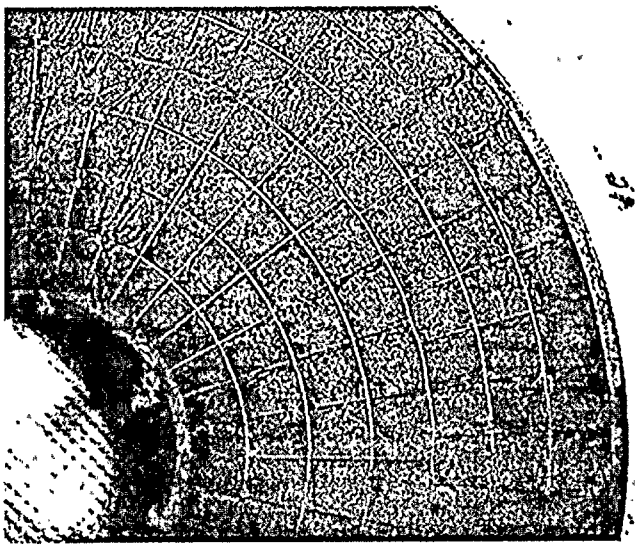

Figure 3. Cell 76712 - Negative Electrode, Mild underpasting

Other pasting flaws were less prevalent. Areas of overpasting due to the application of too much paste or due to intentional patching were found on the undersides of a few electrodes (Figure 4). Drops of excess paste were also inadvertently bonded to the top surfaces of other electrodes. "Doctor-blade" marks were also discernible. Breaks in the leveling action left slight ridges on individual pellets, and incomplete blade travel across the electrode left larger raised ridges along the outer perimeter.

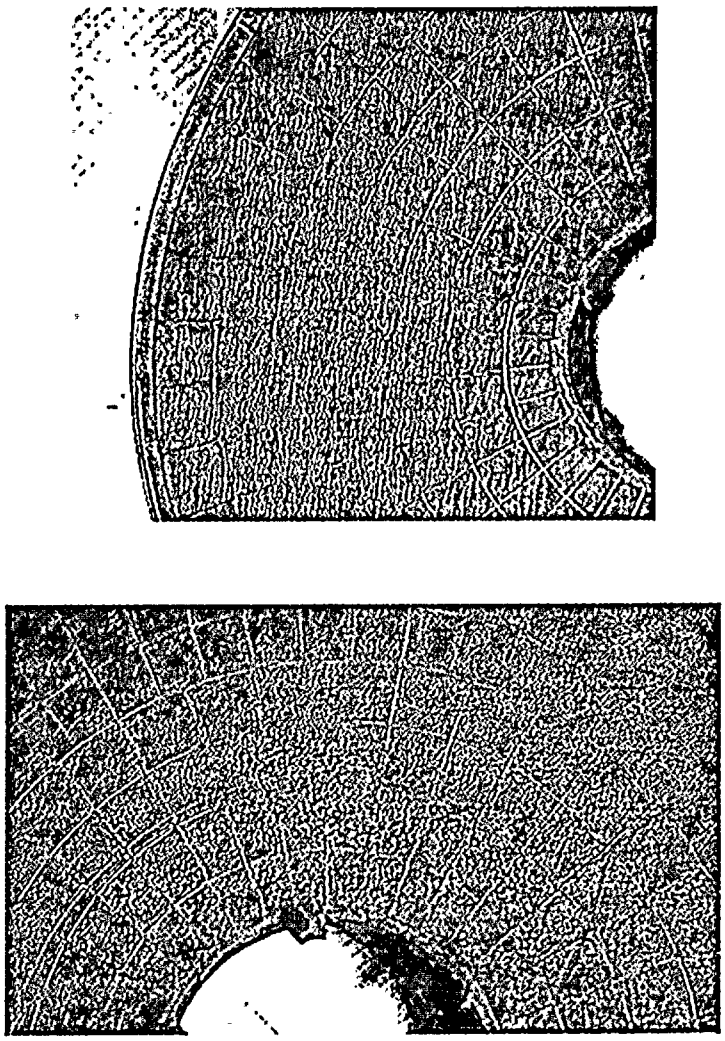

Figure 4. Cell 76712 - Negative Electrode, Overpasting (top) and Intentional Patch (bottom)

Two other flaws, blistering and "dimpling," were observed on the negative electrodes. Examples of blisters were found in every cell. They commonly develop during formation when hydrogen gas is entrapped in localized pockets just beneath the surface. In some, but not all cells, individual pellets had shallow indentations. These dimpled pellets were often found in a series of consecutive pellets along an electrode perimeter and were an apparent artifact of pasting or handling.

6.1.2.3 Electrolyte Analyses

The electrolyte in each cell met specifications in terms of quantity and composition. In each cell, the electrolyte meniscus fell between the level lines marked on the sidewall of the container. The specific-gravity measurements are summarized below. The average of the two measurements made for each cell ranged from the design density of 1.300 g/cc to 1.307 g/cc. The slightly higher gravities probably reflected water loss due to electrolysis.

Electrolyte Specific Gravity Measurement

Cell No.	Specific Gravity (g/cc)		
	@ Top	@ Bottom	Cell Average
59941	1.298	1.302	1.300
59942	1.295	1.305	1.300
59936	1.307	1.307	1.307
76712	1.304	1.308	1.306
74975	1.304	1.306	1.305
77773	1.303	1.304	1.304
Averages	**1.302**	**1.305**	**1.304**

The results of the sample submissions for impurity analysis are presented in Argonne National Laboratory Report, Appendix 2 (Attachment 1). No trace element was present in concentrations greater than 15 ppm. Typical concentrations were 12 ppm Ca, and approximately 5 ppm for Al, Fe, and Mg, with all other reported contaminants (Ba, Cd, Cl, Cu, Mn, Ni, Pt, and Zn) present in concentrations of 2 ppm or less. Cadmium levels showed the greatest variability, ranging from below detectable limits to under 2 ppm, but these results were consistent for duplicate samples submitted to both analytical services. None of these impurities were found in concentrations high enough to impair cell performance.

The electrolyte samples, which were collected under float charge, did show a slight location dependence in specific gravity. As shown in the table above, the electrolyte samples collected near cell bottoms averaged 0.003 g/cc more in density than the average for the samples collected near the tops. This density gradient was insufficient to induce discernible differences in the electrodes. The electrode design was thus deemed adequate to avoid electrolyte stratification and the consequent impairment of cell capacity.

6.1.3 Electrode Assessment

Scanning electron microscopy (SEM) was the primary tool used to evaluate the condition of both the negative and positive electrodes. Interpretation of the electrode microstructures by this method is qualitative, but comparisons made across common electrode samples from the different cells revealed some distinctive differences, especially concerning the morphology of the corrosion scale formed on the positive-electrode grids. The intrusion porosimetry performed on selected samples was less comprehensive, but it did provide a more quantitative view of the pore structure available for transport of sulfate ions.

6.1.3.1 Negative Electrodes

The microstructure of the negative electrodes was consistent from cell to cell. In the interior, these electrodes consisted of a sintered network of 2 μm to 5 μm lead particles. The sintered connections between particles were well formed, but the lead particles still possessed high surface area. The void volume was ample and essentially free of $PbSO_4$ crystals. The upper half of the table below summarizes the intrusion porosimetry results for three pairs of electrodes from three of these cells. The findings for pore volume, pore area, pore diameter, and bulk density are very comparable, especially for full-capacity cell 59942 and low-capacity cell 76712. The data for low-capacity cell 59941 suggested that its electrodes were slightly more porous and had more internal surface area. If these limited samplings truly represent these electrodes, the enhanced porosity and area would be beneficial, not detrimental, to electrode performance.

Porosimetry Data for Negative and Positive Electrodes

Cell-Electrode Identification	Pore Volume (cc/g)	Pore Area (m^2/g)	Pore Diameter (μm)	Bulk Density (g/cc)
59941-N2	0.179	2.06	0.346	3.68
59941-N18	0.178	2.19	0.337	3.71
59942-N2	0.156	1.88	0.330	3.89
59942-N18	0.151	1.67	0.362	3.88
76712-N2	0.145	1.64	0.353	3.99
76712-N18	0.157	1.82	0.345	3.85
Averages	**0.161**	**1.88**	**0.346**	**3.83**
59941-P1	0.108	3.24	0.134	4.64
59941-P18	0.118	2.51	0.188	4.30
59942-P1	0.111	2.44	0.182	4.40
59942-P18	0.116	3.52	0.132	4.32
76712-P1	0.121	3.54	0.137	4.21
76712-P18	0.117	2.39	0.196	4.20
Averages	**0.115**	**2.94**	**0.162**	**4.35**

Differences in appearance were limited to the surfaces of the negative electrodes. A common characteristic was coarsening of the surface particles. The surface morphology was better described as partial aggregates with a characteristic dimension of approximately 10 μm. The only cell-to-cell difference for the negative electrodes was the degree of surface sulfation. This condition was directly related to

the time between termination of float charging and cell disassembly. When a cell was examined immediately after charging termination, no $PbSO_4$ was evident. When a multi-day period elapsed, small needles and platelets of $PbSO_4$ grew in both size and concentration. After four days, the $PbSO_4$ particles averaged 5 μm along their major growth axis. True sulfation results when large (>100 μm), difficult-to-reconvert crystals develop within as well as on the negative electrodes. Weeks of inactivity are generally required to develop this type of microstructure.

In each of these cells, the critical grid interface showed good contact between the negative active material and the grid. Physically, the negative-electrode paste maintained close proximity to the grid elements except where underpasting resulted in areas of broad, V-shaped gaps. Adherence was promoted by the formation of a sintered metallurgical bond between the grid and adjacent lead particles. The good conductivity of the grid to the active material, coupled with the open structure of interconnected, high-interfacial-area lead particles, made the negative electrodes a most unlikely source of capacity loss problems.

6.1.3.2 Positive Active Material

The microstructure of the positive active material also proved to be very consistent from cell to cell. PbO_2 was essentially the sole constituent. Within the core of an electrode pellet, these particles typically ranged from 2 μm to 5 μm in dimension and were identifiable as discrete particles, but still appeared to form good particle-to-particle contact between adjoining particles. At the surface, the morphology differed. Finer particles with greater surface area tended to merge into larger 20 μm to 30 μm aggregates. This change in structure was evident in every cell and was discernible not only for the fresh surfaces exposed by breaking pellets, but also for polished cross sections.

Intrusion porosimetry also found no significant differences in the positive electrodes. These results are summarized in the lower half of the table in Section 6.1.3.1. Given the variation for electrodes from the same cell, the values for pore volume, pore area, and mean pore diameter were virtually indistinguishable for full-capacity cell 59942 and low-capacity cells 59941 and 76712. The bulk density of the last cell appeared to be 5% to 10% less than that of the other two cells. In essence, the porosimetry results confirmed the qualitative impression from the microscopic studies. None of the physical changes in the positive active material were deemed great enough to cause the reported capacity decline.

6.1.3.3 Corrosion of Positive-Electrode Grid

Corrosion of the positive-electrode grids is an expected (and undesired) reaction for lead-acid cells. Prolonged conversion of metallic lead to PbO_2 weakens the structural integrity of the grid as it simultaneously increases the stresses imparted by the

expanding mass of active material. None of these cells experienced sufficient corrosion to fail because of grid growth. The modest growth reported in Section 6.1.2.1 supports this premise. Our microscopy studies, however, found differences in scale morphology and composition that clearly delineated the high-capacity cell from the low-capacity cells.

The PbO_2 scale formed on the positive grids of high-capacity cell 59942 followed the expected stages of growth and development (Figure 5). A dense scale formed and thickened over time. A limiting thickness of 30 μm to 40 μm was reached as the outermost scale broke up under normal service and formed particle masses that were indistinguishable from original active material. The PbO_2 scale remained adhered to the lead substrate for all examined samples. No separations were evident in the dense scale; only a few occasional hairline cracks developed in the outer scale regions. When separated from the active material, the exterior surface of the scale was highly textured and particle-like, and when the scale was removed, it cleaved very clearly at the substrate, revealing the lead substrate.

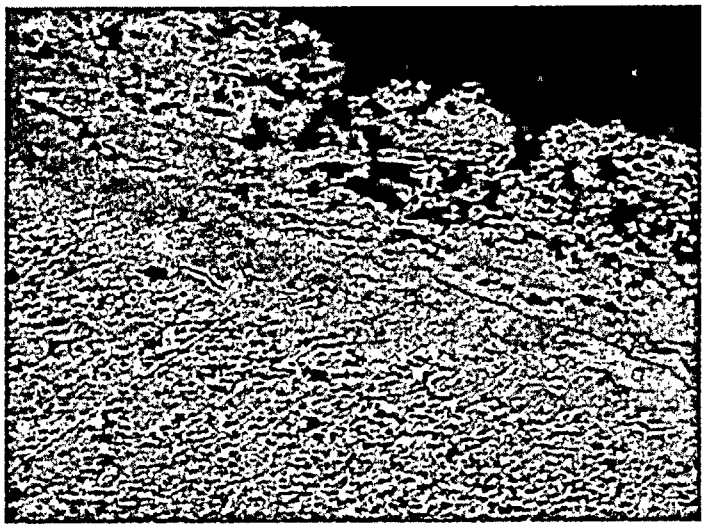

Figure 5. Cell 59942 - Dense PbO_2 Formed on Positive Grids

In every capacity-impaired cell, the structure of the scale was altered. The monolithic nature of the scale was destroyed by the development of extended separations within the PbO_2 scale (Figure 6). These separations presumably started as fine hairline cracks that propagated laterally to the grid interface. The separations were offset from this interface and were most pronounced in the outer half of the once-intact scale. In some instances, multiple lateral separations were evident. The gaps between scale sections consistently ranged between 2 μm and 5 μm. The new scale morphology was not the result of increased scale thickness; the combined thickness of the scale sections was still in the range of 30 μm to 40 μm, which was the same thickness range found for the 59942 grids. Cracks in the scale do not have a severe impact on cell performance if they are perpendicular to the grid interface. A relatively uniform electron flux can then be maintained in all radial directions. The

lateral separations in these scales, however, severely inhibited electron transfer between grid and active material by forcing electrons to channel along sparse bridges across semicontinous gaps.

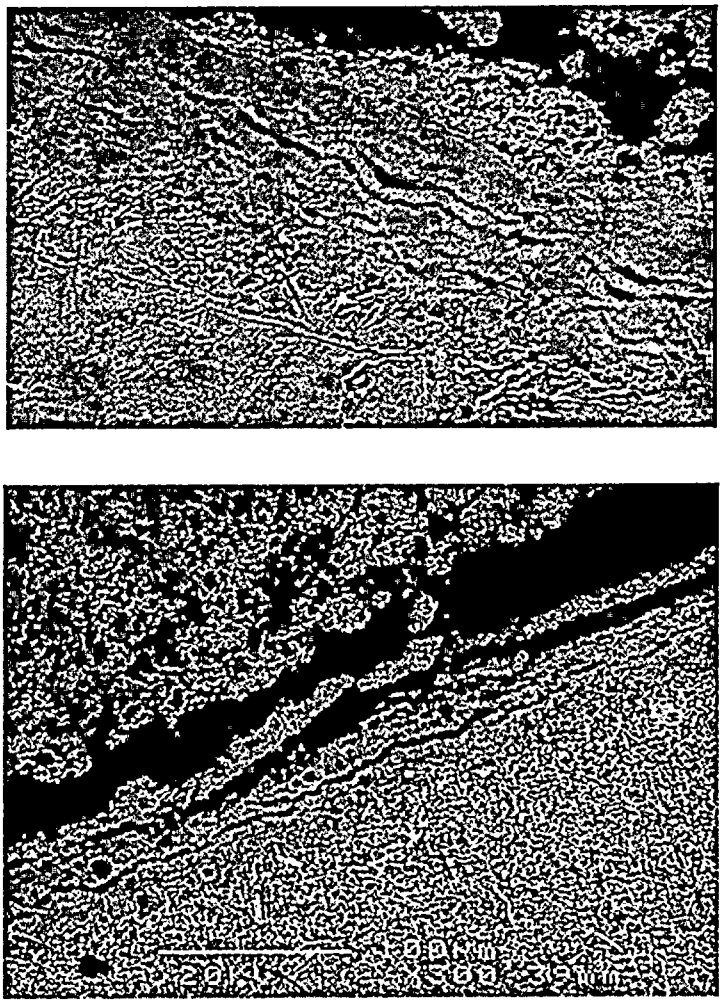

Figure 6. Cell 74975 (top) and 59941 (bottom) - Lateral Separations in the PbO_2 Scale for Positive Grid

Further examination of these scale separations revealed that $PbSO_4$ crystals had formed within them. On occasion, these crystals could be discerned by looking down into scale separations. They could be seen much more clearly after sections of the outer scale were removed. The removal process was relatively easy because in the affected cells, the scale would preferentially cleave along the existing lateral separations rather than at the grid interface. All of these crystals were relatively flat (1 μm to 3 μm) because of the geometric constraints imposed by the narrow gaps. In the plane of the separation, however, some crystals reached 30 μm in major dimension. The planar growth was variable and resulted in crystals with distinct shapes. Most often, simpler and much thinner disc-shaped crystals formed (Figure 7). On occasion, these crystals developed in pairs (Figure 8). In other instances, both

rounded crystals and intersecting linear platelets were observed for grid samples from the same cell (Figure 9).

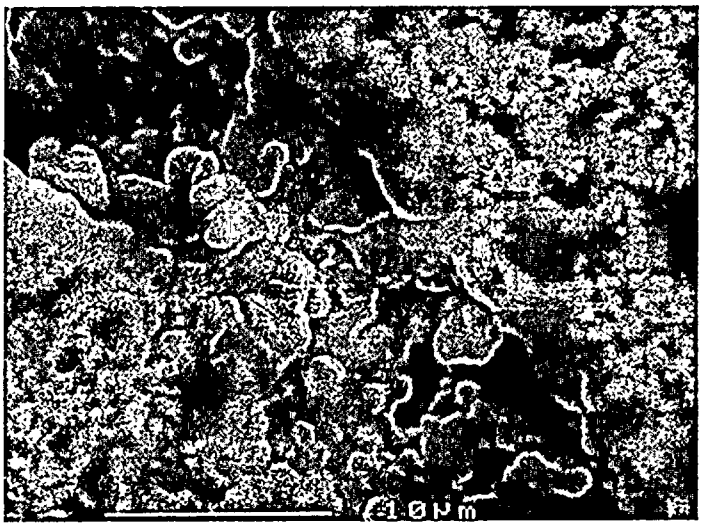

Figure 7. Cell 59941 - Small, Disk-Shaped $PbSO_4$ Crystals

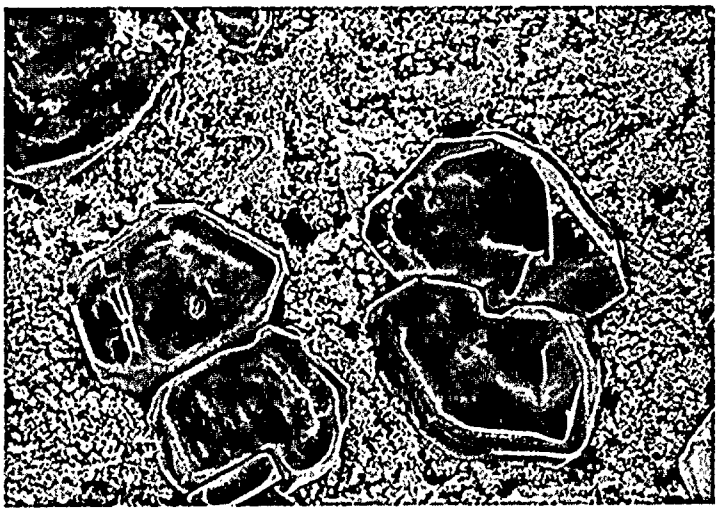

Figure 8. Cell 77773 - $PbSO_4$ Crystals

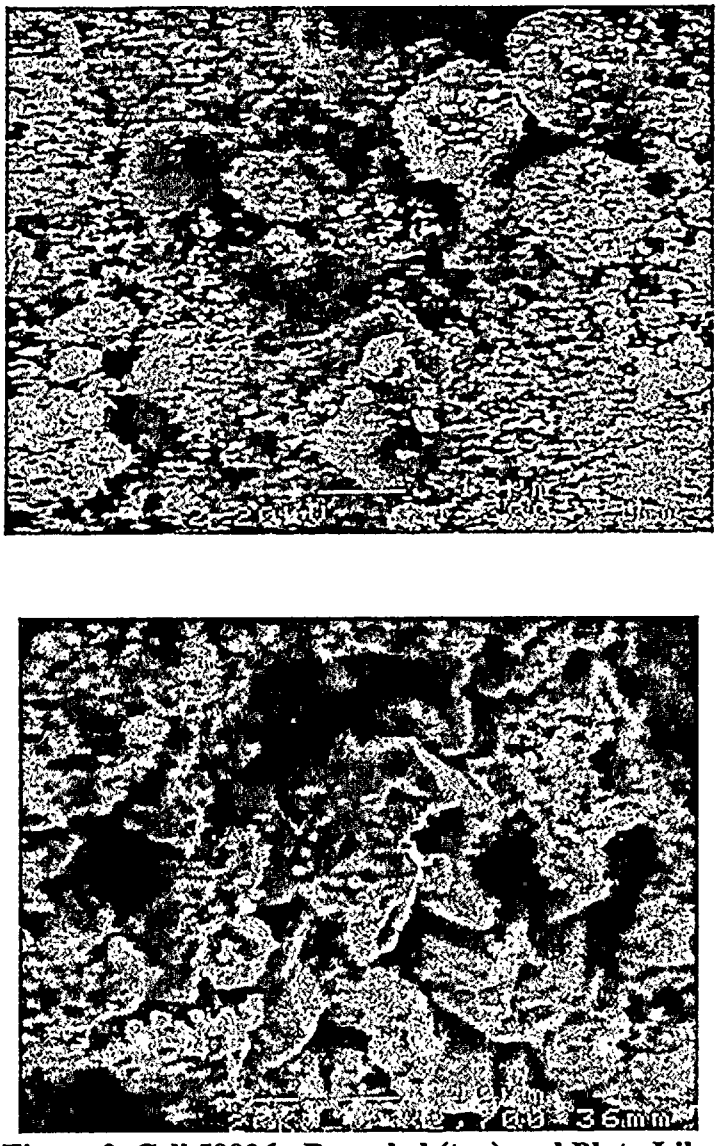

Figure 9. Cell 59936 - Rounded (top) and Plate-Like (bottom) $PbSO_4$ Crystals

The $PbSO_4$ crystals illustrated the severity of the lateral scale separations in two ways. First, their virtually exclusive presence in these restricted regions attested to the localized impairment in electrochemistry. The bulk of the positive electrodes, including those from the capacity-impaired cells, were nearly free of these crystals. Second, their occupation of the scale separations physically reinforced the stability of the defective scale structure. With active cycling, the outer scale region would be expected to convert into a mass of PbO_2 particles. Effective electrical continuity would require intimate contact of these new particles with the remaining grid scale. However, as the outer scale breaks down, the blocking action of the $PbSO_4$ crystals would impede inward movement of the newly formed PbO_2 particles to create new contacts. Chemical conversion of the insulating $PbSO_4$ into conductive PbO_2 would

occur only when the outer scale is completely converted and sufficient electrolytic pathways opened. The critical scale-to-active-material interface would be restored only after this last conversion process has occurred.

6.1.4 Correlating of Performance Data with Examination Findings

Argonne National Laboratories reviewed the discharge curves provided by Braidwood and PVNGS for the five cells that suffered capacity losses (Argonne National Laboratory Report - Attachment 1). The curves were reviewed for indications of changes in cell impedance. These curves showed an increase in the pure resistance component of impedance for the discharges where the capacity was lost. While other sources of ohmic loss cannot be ruled out through this type of "black box" analysis, the findings were definitely consistent with the development of resistance-enhancing changes in the structure and composition of corrosion scale present on the positive-electrode grids.

Argonne National Laboratories provided an interpretation based on load currents of 600 A and 714 A for the ComEd and PVNGS cells, respectively. The current rating Argonne used for the PVNGS cells was incorrect. The rated current for the PVNGS cells is actually 514 A. For subsequent discharges where the capacity loss became evident, the voltage curves showed progressively greater voltage depression as the discharges progressed. At 15 minutes into the discharge, which was the first common time provided for all five cells, the voltage depression ranged from 15 mV to 45 mV, a 8% to 25% increase in resistance. Internally, the suppressed voltage meant that the potential between the electrodes was reduced. With a reduced potential to drive ionic transport, polarization of the reactions occurring at the electrodes became more difficult to overcome and caused a further decline in the effective potential. In effect, a negative feedback loop was established that accelerated the voltage decline with depth of discharge. After 60 minutes, voltage suppression ranged from 35 mV to 115 mV, depending on the particular cell.

This scenario appeared to be valid for all five cells, although further interpretation was needed to bring the voltage curves for cell 74975 into compliance. Instead of overlaying, the early discharges trended upwards with successive discharges, rising approximately 30 mV from the first to fourth cycle. The voltage improvement very likely occurred because formation of this cell was incomplete and continued during early cycling. The fourth discharge was still consistently lower in voltage for a given time than the early discharges of the other cells. When this added complexity is considered, the fifth voltage curve showing the loss of capacity in cell 74975 is seen to be consistent with the other discharges showing capacity losses and similar to the last discharge of cell 76712.

Correlating the performance data with examination findings, Argonne concluded the following:

1. *The capacity impairment would persist on subsequent discharges as long as the detrimental scale condition existed.*

Argonne, however, could not provide an explanation for the cause of the detrimental scale. Argonne concluded the capacity loss was due to adverse changes in the PbO_2 scale formed on the positive grid. This conclusion was derived from the observation that the morphology of cell 59942, which showed no capacity loss, was different. Based on discussions with Lucent Technologies, the changes in the PbO_2 scale may not have been significant enough to cause the reported capacity decline. The differences in scale morphology may be due to the maintenance history of the cells. Cell 59942, which was used as a spare, was stored primarily on open circuit since 1994. To prepare for the single cell testing at Braidwood, 59942 and another spare cell were charged and individually modified performance discharge tested. The five capacity-impaired cells examined by Argonne, which were from installed battery banks, had three or more capacity discharge/recharge cycles.

2. *The charge algorithms and float-charge procedure were inadequate to reverse this condition. In fact, the adverse scale morphology almost certainly developed during the prolonged period (>1 year) of float charging at the utilities prior to the attempted in-service discharges.*

   Review of the PVNGS Round Cell performance data does not support this conclusion (Attachment 2). Cells installed in Units 1 and 3, which have been on float for over one year, have not had a capacity loss similar to cells installed in Unit 2 and Braidwood 112.

3. *This does not mean that the adverse scale changes are irreversible, but more aggressive charging procedures would be required to convert the poorly attached outer scale and the intervening $PbSO_4$ crystals into useful active material. This alternative carries the associated risk of greater overall corrosion of the grids and a shortening of the design service life.*

   Lucent Technologies has determined that capacity losses can be limited by raising the charge voltage towards the end of charge to overcome the overvoltage associated with the diffusion impedance in the positive plate (Reference 2). PVNGS cells were recharged according to the recharge methods recommended by Lucent Technologies.

   The scale morphology of Braidwood cell 59942 may be the result of storing the cell on open circuit. Lucent Technologies has reported that extended periods of time on open circuit serve to recover capacity by permitting recystallation of the $PbSO_4$ film. Recystallation increases the porosity of the $PbSO_4$ film. The time on open circuit also allows more diffusion of ions into and out of the film, which facilitates the recharge and discharge processes (Reference 2).

6.2 Round Cell Multiple Shallow Discharge Testing

6.2.1 Test Plan

The objective of this testing, which was performed at the C&D facility in Conshohocken, PA, was to determine the charge recovery for low and high gravity Round Cells following multiple shallow discharges. As shown in the test plan (Attachment 3), an initial baseline capacity test was performed at the two hour rate to 1.75 Vpc. The high gravity Round Cells were recharged using the Lucent Technologies preferred charge method. The low gravity Round Cells were recharged similar to the method used on installed batteries at Oyster Creek. After the initial baseline test, the cells were discharged four times at a rate of 100 A for 2 hours (200 Ah). The cells were recharged at float potential for 72 hours following each 200 Ah discharge. After the fourth discharge/recharge cycle, a second two hour capacity discharge test (to 1.75 Vpc) was performed.

6.2.2 High Gravity "Used" Cells

Three cells used as spares at McGuire were sent to Conshohocken. The discharge test results of one of the three "used" cells is shown in the table below. **The high gravity "used" cell was discharge tested to only provide additional data for Duke's root cause evaluation.** The test results for this cell were never intended to be used to determine the effects of charge recovery following multiple shallow discharges on "used" high gravity Round Cells.

The other two McGuire cells were disassembled. Both cells had faulty welds (reduced weld penetration). Lucent Technologies is working with C&D (manufacturer) to determine the root cause of the faulty welds. The apparent cause for the capacity loss of the "used" cell has been attributed to shipping damage, which caused degradation of reduced weld penetrations.

6.2.3 Discharge Test Results

Testing to determine the charge recovery for low and high gravity Round Cells following multiple shallow discharges has been completed. The results (shown graphically in Attachment 4) were as follows:

Low Gravity List 1S Round Cells

Cell	Serial #	History	Initial Capacity	Final Capacity	Change
A1	78835	New (11/96)	128.4 %	117.6%	-8.4%
A2	48346	Used (8/91)	133.5%	127.4%	-4.6%

A3	48312	Used (8/91)	125.7%	119.1%	-5.3%
A4	78811	New (11/96)	127.2%	118.8%	-6.6%
A5	78786	New (11/96)	122.9%	114.3%	-7.0%

High Gravity List 1SH Round Cells

Cell	Serial #	History	Initial Capacity	Final Capacity	Change
B1	97455	Used (5/91)	87.5%	61.6%	-29.6%
B6	56051	New (3/96)	128.7%	108.4%	-15.8%
B7	55559	New (3/96)	126.3%	106.5%	-15.7%
B8	56063	New (3/96)	126.7%	98.5%	-22.3%

6.2.4 Multiple Shallow Discharge Test Conclusions

Test results indicate that recharging Round Cells at float potential following multiple shallow discharges does not fully restore battery capacity. The capacity loss for high gravity Round Cells was greater than low gravity Round Cells. The average high and low gravity Round Cell capacity loss was 17.9% and 6.4%, respectively. This result is consistent with premature capacity loss (PCL) seen in previous high gravity performance testing.

Frequent cycling at high discharge rates has been shown to be degrading to high gravity Round Cells. Current theory asserts that this effect is consistent with the PCL (Premature Capacity Loss) model for antimony-free batteries discussed in battery industry literature. PCL is an issue with low and high gravity, antimony-free cells. It is believed that the PCL effect is more predominate for high gravity cells. The effect of multiple on-line discharges at lower rates, which is more typical of normal plant DC load, appears to support the PCL model.

Considering that the maximum required capacity by design basis for the batteries is 53%, even assuming a maximum capacity loss of 22.3% (based on new high gravity Round Cell test results), there still remains considerable safety margin for Unit 2 batteries. Assuming that there is a capacity loss problem, it can be shown that due to significant safety margin, a worst case projected capacity loss would not significantly impact the PVNGS batteries ability to perform their safety function. This conclusion also applies to the Unit 1 & 3 batteries.

7.0 ROOT CAUSE DETERMINATION

To verify the failure mode(s), cells from PVNGS and Braidwood were sent to Argonne National Laboratory. Cell examinations, chemical analysis and morphological examinations ruled out contaminates and/or manufacturing defects significant enough to cause battery capacity loss. An increased number of $PbSO_4$ crystals within the positive plate material was seen. Positive grid-to-pellet interface area cracking was noted. The cracks in the corrosion layer were also populated with $PbSO_4$ crystals. Argonne concluded that these two items caused increased internal resistance, thereby reducing capacity. According to discussions with Lucent Technologies, the changes in the PbO_2 scale may not have been significant enough to cause the reported capacity decline. The scale morphology of the "good" cell (59942) was different from that of the other cells examined. These differences may be due to the maintenance history of cell 59942 (a spare cell stored on open circuit prior to one modified performance test) compared to the "bad" cells (installed cells had three or more capacity discharge/recharge cycles). The Argonne report did not specify what caused the cracking and/or the increased number of $PbSO_4$ crystals. The root cause of the capacity loss could not be determined conclusively from destructive examination analysis of the cells. Based on performance test results, the apparent cause for the AT&T (Lucent Technologies) Round Cell capacity loss, appears to be string related.

HG-18

Low individual cell and negative half cell voltage, specific gravity loss and crystal growth on the negative post (sulfation) were characteristics observed in HG-18 cells with catastrophic capacity loss. Reference electrode measurements obtained during discharge indicated the cells were positive plate limited and degraded. The cause for the positive plate degradation could not be ascertained from destructive examination analysis. Mixing a large number of cells with different discharge/recharge histories may have contributed to premature capacity loss caused by insufficient charging.

HG-14

HG-14 cells had four performance tests prior to installation. The capacity loss was consistent with PCL seen in previous high gravity performance testing. Capacity losses were probably caused by a build-up of resistance in the positive plate that resulted from deep discharge cycling.

HG-16

The capacity of nearly all HG-16 cells was greater than 100%. Mixing a large number of cells with different discharge/recharge histories may have contributed to premature capacity loss caused by insufficient charging.

STRING	APPARENT ROOT CAUSE CAPACITY LOSS
HG-14	positive plate passivation - PCL
HG-16	negative plate sulfation (crystals) - aggravated by cell mixing and borderline polarization (double platinum)
HG-18	negative plate sulfation (crystals), positive plate degradation

8.0 DETERMINATION OF OTHER SUSCEPTIBLE EQUIPMENT

8.1 Units 1 and 3 Class 1E Batteries

To date, the Unit 1 and 3 Class 1E batteries have experienced capacities expected for the Lucent Technologies Round Cell. The battery banks in Units 1 and 3 have passed their respective service and performance tests. The strings in Units 1 and 3 are mixed but have had the same discharge history. If the failure mechanism for Unit 2 capacity loss was due only to mixing strings, Units 1 and 3 batteries would have failed and/or had capacity loss prior to U2R6.

8.2 NRC/Lucent Technologies Round Cell Nuclear Utility User's Council Meeting

The Lucent Technologies Round Cell Nuclear Utility User's Council met with the NRC in Washington, DC on April 18, 1996 to discuss the use of Round Cell batteries in Nuclear Power Plants. Due to the unexpected capacity loss of the Round Cells at PVNGS Unit 2 and Braidwood Unit 1, the NRC expressed concern regarding the capability of the Round Cell to perform its intended safety-related function.

Each of the licensees presented their Round Cell operating experience. Some utilities have had no capacity loss problems. No sudden cell discharges or cell reversal have occurred during Round Cell service or performance testing. A majority of the Round Cells tested have performed well. There has been more successful tests than failures, even at utilities that have had degraded cell performance. There have been various contributing factors causing the capacity losses, all of which are being evaluated by the Utility User's Council.

The replacement battery criterion in IEEE-450 is based on the assumption that grid corrosion is the predominant failure mechanism. The corrosion product of the Round Cell pure lead plate grid is PbO_2. Consequently, the amount of active material on the cell plates tends to increase over the life of the cell. Since the replacement criterion is based on increasing deterioration due to loss of active material, it does not apply to the Round Cell. The Utility User's Council is in the process of drafting a request for an interpretation of the replacement criteria in IEEE-450. The industry consensus is as follows:

1. The Round Cells will meet operability requirements.
2. Considerable margin exists above design safety function requirements in presently installed safety-related systems.
3. Surveillance requirements are adequate to ensure degraded cells can be identified and replaced without compromising plant safety.
4. Constant potential and constant current recharge methods are capable of restoring an acceptable charge within a reasonable amount of time.
5. Recharge at constant current and high constant voltage potentials recharge cells following a deep discharge recharge at a faster rate than recharge at float potential.

The licensees participating in the User's Council agreed to provide the NRC with a summary of utility battery testing data and recharge guidance for off-line and on-line discharges (ref. RCTS 0-4-2207).

8.3 Nuclear Stations with High Gravity Round Cell Class 1E Batteries

8.3.1 Braidwood Nuclear Station

On October 30, 1995, the modified performance discharge test was performed on Braidwood safety related battery bank 1DC02E (battery 112). The tested capacity was 92%, which was below their acceptance criteria of 95%. Per discussions with Lucent Technologies, Braidwood concluded the battery performance was impacted by a 240 amp-hour discharge that had occurred 6 days prior to the modified performance test. The battery was recharged at float potential and a service test was performed on November 6, 1995. The battery bank passed the service test demonstrating that the battery was capable of performing its intended design function. To verify the battery did not have a performance problem, Braidwood planned to perform three single cell discharges. The single cell discharge testing began on March 3, 1996. The cell capacities ranged from approximately 37% to 62%. Uncertain of the reasons for the capacity loss, Braidwood Station declared 1DC02E inoperable.

Braidwood determined the battery capacity loss was caused by disintegration in the corrosion layer that normally develops between the positive plate active material and positive plate grid. The acid concentration coupled with closely spaced repetitive discharge/recharge cycling of the cells resulted in a PCL (premature capacity loss) failure.

8.3.1 McGuire Nuclear Station

In October of 1996, McGuire Nuclear Station completed the 60 month surveillance performance test for their Channel "C " battery. The tested capacity was 77.5%, which is below their acceptance criteria of 80%. Based on these test results, the battery was declared inoperable. The batteries used at McGuire are identical to the PVNGS Class 1E station batteries except that the McGuire batteries are comprised of 59 cells each.

A review of the testing history for the McGuire batteries showed that the loss of capacity for the "C" battery occurred during its third performance test. In addition, it is suspected that capacity loss may have been evident during the second performance test. Tested capacity from the second discharge test was 100%, which is low compared to historical records for the other McGuire batteries as well as PVNGS and Braidwood. Typical performance test values are normally greater than 105% for Round Cells.

Capacity loss early in the discharge test history as seen in the McGuire battery is typical of problem batteries originally installed in PVNGS Unit 2 and Braidwood (battery 112).

As shown on the graph in Attachment 5, the capacity loss on problem batteries occur early in the discharge testing history (i.e. during the second or third discharge test). In contrast, the PVNGS Units 1 & 3 batteries have had 3 - 4 discharge tests without an indication of the type of capacity loss seen on problem batteries. Based on this, we believe that the PVNGS Unit 1 & 3 batteries do not have the capacity loss problem seen at PVNGS Unit 2, McGuire or Braidwood.

In summary, testing history of PVNGS Units 1 & 3 do not indicate a loss of capacity similar to McGuire, PVNGS Unit 2 (original batteries), or Braidwood 112. All batteries that have demonstrated capacity loss have shown this loss early in testing history.

9.0 CORRECTIVE ACTIONS

9.1 Completed Corrective Actions

1. The following interim maintenance enhancements have been implemented to assess the effectiveness of the corrective actions;
   - bi-weekly half cell voltage measurements
   - monthly specific gravity measurements

2. The float range was raised. The ICV range was increased from 2.25 Vpc to 2.27 Vpc as a corrective action in case of adverse trends.

3. Procedures were modified to evaluate battery operability should an on-line battery discharge occur (battery charger not supplying bus). Instructions were added to procedure Panel B01A Alarm Responses, 4*X*AL-*X*RK1A, to check battery amperage approximately every 15 minutes until the battery charger is supplying the bus. If the battery discharge approaches 250 amps, battery operability is evaluated per procedure 40OP-9PK01, 125 Vdc Class 1E Electrical System, Appendix K.

4. The recharge maintenance instructions have been revised to use the recharge method recommended by Lucent Technologies, following a performance discharge test.

5. 2EPKAF11 and 2EPKCF13 received a high rate trickle charge to ensure equal charge states, following the battery reconfiguration.

6. The Unit 2 battery banks have been reconfigured as follows;

   2EPKAF11: HG-1
   2EPKBF12: HG-10 (new cells)
   2EPKCF13: HG-16
   2EPKDF14: Braidwood (Bryon) cells

Battery 2EPKAF11 has been reconfigured with HG-1 cells only. 2EPKAF11 received 13 cells that were performance tested under CMWO 751612. The remaining 47 cells were tested under STWOs 738776 and 738778 per 32ST-9PK04. Based on these test results, the reconfigured

battery bank capacity is greater then 100%. To preclude premature capacity due to overcycling, no additional discharge tests were performed on the battery in this final configuration.

Battery 2EPKCF13 has been reconfigured with HG-16 cells only. 2EPKCF13 received 32 cells that were performance tested under CMWO 752291. The remaining 28 cells were tested under STWOs 738776 and 738778 per 32ST-9PK04. Based on these test results, the reconfigured battery bank capacity is greater then 100%. To preclude premature capacity due to overcycling, no additional discharge tests were performed on the battery in this final configuration.

These newly reconfigured batteries, which are now the currently installed batteries, do not have the same testing history as PVNGS Unit 1 & 3. However, losses of capacity when they occur, have generally been in the 15% - 25% range. In addition, these capacity losses appear to be cycle related as opposed to time dependent. We have not seen any relationship between age and capacity loss. There has been a direct relationship between number of cycles and loss of capacity. Considering this, should the battery have a capacity loss problem, it is possible to project the Unit 2 battery capacity based on the last tested capacity and worst case estimated capacity loss.

BATTERY	TESTED CAPACITY
2EPKAF11 HG-1	**113%**
2EPKBF12 HG-10 (new cells)	**>100%**
2EPKCF13 HG-16	**103%**
2EPKDF14 Braidwood	**>100%**

Considering that the maximum required capacity by design basis for the batteries is 53%, even assuming a maximum capacity loss of 25%, there still remains considerable safety margin for the Unit 2 batteries. Assuming that there is a capacity loss problem, it can be shown that due to significant safety margin, a worst case projected capacity loss would not significantly impact the PVNGS batteries ability to perform their safety function. It should be noted that this conclusion also applies to the Unit 1 & 3 batteries as well.

BATTERY	INSTALLED CAPACITY
1EPKAF11	109%
1EPKBF12	105%
1EPKCF13	106%
1EPKDF14	107%

BATTERY	INSTALLED CAPACITY
3EPKAF11	106%
3EPKBF12	110%
3EPKCF13	109%
3EPKDF14	113%

9.2 Recommended Corrective Action

Lucent Technologies submitted a memorandum dated July 26, 1996 (Attachment 6) to the AT&T Round Cell Nuclear Utility User's Council. The memorandum stated Lucent Technologies Inc., Microelectronics Group - Power Systems Division had decided to discontinue manufacturing high gravity Round Cells. Lucent Technologies also decided to discontinue "marketing and sales activities of all power products into the nuclear utility market." This decision was based on several key issues: past and current customer concerns about long term battery performance, premature capacity loss of high gravity cells, amount of technical support required and Lucent Technologies' business decision to focus on their more profitable telecommunications market.

Since the high gravity Round Cell battery may not deliver the long term performance results that we require, the installed Round Cells will be replaced with qualified batteries that have had a proven history of reliable performance. Design and implementation will be tracked in CATS under CRDR 2-6-0050.

10.0 MAINTENANCE RULE GOAL

2EPKCF13 and 2EPKDF14 were declared inoperable because the capacity of both batteries was below the Technical Specification Surveillance Requirement 4.8.2.1.e limit of 90%. The degradation experienced by the Unit 2 batteries had resulted in capacities that were still in excess of

that required for the batteries to perform their safety-related function. Calculations performed demonstrated that the projected capacities provided greater than 200% margin above that required for safety related loads. Each train of the class 1E battery had sufficient capacity to independently supply the required loads for 2 hours. Therefore, the capacity loss of the Unit 2 Lucent Technologies Round Cells was not sufficient to cause a functional failure of the PK System.

11.0 REFERENCES

1. George Wood Vinal, *Storage Batteries*, 4th edition, 1955.

2. F. C. Laman, M. C. Weeks, K. R. Bullock, "Cause and Effect of Premature Capacity Loss in High Specific Gravity Round Cell Batteries During Repetitive Deep Discharge Cycling," August 26, 1996.

3. AT&T Lineage® 2000 Round Cell Battery Product Manual, Issue 1, August 1990.

4. Argonne National Laboratory Destructive Analysis of Lead-Acid AT&T Round Cells Report, December 20, 1996.

5. IEEE Std 450-1995, IEEE Recommended Practice for Maintenance, Testing, and Replacement of Vented Lead-Acid Batteries for Stationary Applications.

6. IEEE Std 450-1980, IEEE Recommended Practice for Maintenance, Testing, and Replacement of Large Lead Storage Batteries for Generating Stations and Substations.

7. Braidwood Nuclear Station, Battery Bank 112 - 1DC02E Root Cause Evaluation Report, Rev. 0, January 15, 1997.

12.0 ATTACHMENTS

1. Argonne National Laboratory Destructive Analysis of Lead-Acid AT&T Round Cells Report
2. PVNGS Discharge Test Tables
3. Round Cell Charging Methods Test Plan
4. Round Cell Multiple On-Line Shallow Discharge Curves
5. Industry Performance Test Examples High-Gravity Round Cells
6. Memorandum of Record - Nuclear Utility Market Sales

ATTACHMENT 1

ARGONNE NATIONAL LABORATORY
DESTRUCTIVE ANALYSIS OF LEAD-ACID AT&T ROUND CELLS REPORT

DESTRUCTIVE ANALYSIS OF LEAD-ACID AT&T ROUND CELLS

December 20, 1996

Performed under
Contract No. P-96102

Prepared by:

J. A. Smaga
J. J. Marr
D. R. Simon

Table of Contents

DESTRUCTIVE ANALYSIS OF LEAD-ACID AT&T ROUND CELLS

Prepared by:
J. A. Smaga
J. J. Marr
D. R. Simon

1.0 Summary

The cause of capacity loss in cells used for backup power generation was determined through detailed examinations of representative cells. The examinations were conducted by personnel from the Electrochemical Technology Department and the Analytical Chemistry Laboratory of the Chemical Technology Division at Argonne National Laboratory (ANL). The cells were made by a common manufacturer, Lucent Technologies (formerly a division of AT&T), but used at two different nuclear power stations, the Braidwood Station of Commonwealth Edison and the Palo Verde Station of Arizona Public Service.

Six high-gravity, lead-acid AT&T Round Cells were disassembled, and the components were evaluated following appropriate analytical procedures. The specific gravity and inorganic impurities in the electrolyte were determined from multiple samples from each cell. Microscopy studies were conducted on positive and negative electrodes from each cell. Interpretation of the electrode morphologies was augmented by intrusion porosimetry measurements. The microscopy studies also included examination of corrosion of the positive electrode grid for these cells.

Our data synthesis focused on similarities and differences between cell 59942, the spare Braidwood cell, which showed no capacity loss, and the remaining cells from Braidwood and Palo Verde, which demonstrated the capacity loss phenomenon. In most respects, the cells proved to be very comparable. The positive electrodes retained a fine particulate structure from the PbO_2 scale to the surface. The presence of $PbSO_4$ crystals was minimal. All of the negative electrodes retained an open network of interconnected, high-surface-area lead particles. Sulfation of these electrodes was limited to their surfaces and was related to the time spent off charge in the laboratory. Electrolyte stratification was not significant while the cells were on float charge. The levels of electrolyte impurities did not vary significantly from cell to cell. Some small differences were noted in the final positive electrode dimensions. These differences, however, were discernible between cell groupings from the two utilities and can be explained on the basis of differences in service life.

One clear difference was the structure of the grid corrosion scale. The PbO_2 scale on the 59942 positive grids was fairly dense, averaging 40 μm in thickness with no major breaks parallel to the underlying lead substrate. Positive grids from other cells developed scales that were comparable in total thickness; however, 10-μm to 15-μm thick sections of the outer scale spalled off and left a virtually continuous 3-μm gap within the scale running parallel to the grid interface. In some instances, two separations developed in the outer half of the PbO_2 scale. High concentrations of $PbSO_4$ crystals were present in these gaps. In the plane parallel to the gap, these crystals reached 30 μm in size, but perpendicular to the gap the crystal thickness averaged 2 μm or less. No evidence of a similar sulfation effect was found in the vicinity of 59942 grids.

The capacity loss was best explained by adverse changes in the PbO_2 scale formed on the positive grids. The extended lateral separations in the outer scale region and the presence of $PbSO_4$ crystals in these gaps formed a highly resistive barrier that impeded electron transfer, especially under high-rate conditions.

2.0 Examination Procedure

Six AT&T high-gravity Round Cells arrived before the contract execution date. Periodic float charging insured that the cells were maintained at a comparable state-of-charge (~100% SOC) prior to cell teardown. Initially, the cells were divided into two strings, and charging was switched between the two strings. Charging was performed at a constant voltage of 2.25 V per cell. Typically, the current response of these cells decayed below 500 mA within the first 3 hours. The current continued to decay for the first 25 hours until it reached a relatively constant value of ~100 mA, which was maintained for the duration of a float-charge period. Periodic charging continued as cells were removed for examination and the strings were reconfigured. The current response under constant-voltage charging never varied significantly from the initial behavior. Table 1 summarizes the charging history at ANL for each cell. On average, each cell was charged for ~35% of the time during a 5- to 7-week period. The time between the final float charge and the teardown procedure ranged between 0 and 4 days.

Table 1. Float-Charge Histories at ANL

Cell Serial Number	Dates on Float Charge (1996)	Accumulated Charging Time (Hours)	Date of Teardown
59941	6/27-28; 7/2-3; 7/11-17; 7/22-29	295	7/31/96
59942	6/27-28; 7/2-3; 7/11-17; 7/22-29	295	8/2/96
76712	7/1-2; 7/8-11; 7/17-22; 7/29-8/5	340	8/7/96
74975	7/1-2; 7/8-11; 7/17-22; 7/29-8/5; 8/7-12	435	8/12/96
77773	7/1-2; 7/8-11; 7/17-22; 7/29-8/5; 8/7-12	435	8/14/96
59936	6/27-28; 7/2-3; 7/11-17; 7/22-29; 8/7-12	407.5	8/16/96

Prior to removal of a cell from its last charge, a small hole was drilled in the cell lid and 50-mL electrolyte samples were extracted via an inserted length of tubing. In each cell, the first sample was extracted ~3 cm below the electrolyte level. The tubing was then lowered to ~3 cm from the cell bottom, and after waiting ~30 minutes, a second sample was extracted. These samples were analyzed for specific gravity and trace elements. The bulk of the trace element analysis was performed by the System Material Analysis Department of Commonwealth Edison.

Each cell teardown followed the same steps. The electrolyte was pumped out of the cell and the cell interior was purged briefly with nitrogen. The cell lid was removed and the electrode assembly was lifted free of the container. The perimeter bonds between positive lugs were severed with a reciprocating saw. The negative electrodes were separated from the

central post by severing the radial grid elements adjacent to the post. All electrodes were removed and inspected, but electrode samples were taken only from four preselected electrodes: the uppermost positive electrode (P1), the second negative from the top (N2), the lowest positive electrode (P18), and the second negative from the bottom (N18). The sediment at the bottom of each cell was also collected.

The subsequent electrode studies included intrusion porisimetry, limited X-ray diffraction, and optical and scanning electron microscopy. Samples of electrodes were prepared in the following manner. The preselected electrodes underwent repeated immersions in water over several days to remove sulfuric acid. Sections were then removed from the neutralized electrodes, and these sections were vacuum dried for over a day. Standard metallographic procedures were employed to prepare four different microscopy samples from each electrode. These samples were cross sections near the inner and outer perimeters of these circular electrodes and surface sections from the same general areas.

3.0 Teardown Observations

No serious defects were noticed in the construction of these six cells. All welded connections were sound; the various insulating and sealing components were intact; and the electrodes were relatively free of serious imperfections. Cell-specific comments can be found on the cell worksheets attached as Appendix 1. Generalized comments on the condition of the electrodes are provided in the remainder of this section.

3.1 Positive Electrodes

The positive electrodes retained a number of earmarks from the pasting and formation processes. The top surfaces were highly textured, while the bottom surfaces were relatively smooth. The top-surface texture consisted of deep grooves and high ridges, with some finer structure overlaid on this alternating pattern (Fig. 1). The texture was evidently imparted to the electrodes by a coarse fabric shortly after the pasting operation; thus, we used the term "burlap" to describe it. The smoother undersides had little surface texture other than minor pasting flaws. The slight bowing of the axial grid elements in the direction of pasting were clearly discernible on this side of the electrodes (Fig. 2).

The positive paste-to-grid adhesion was deemed good. Pellet loss was minor in most cells and was represented by the loss of individual pellets or pellet fragments, usually at the outer perimeter (Fig. 3). The worst incidence of pellet loss involved cell 59941. Two sizable indentations were found on the outer perimeter rims. One extended from the third positive electrode to the sixth positive electrode, and the other extended from the twelfth positive electrode to the fifteenth positive electrode. Apparently, the welded electrode stack was hit twice before insertion in the cell jar. As a consequence, several perimeter pellets were dislodged in the immediate area of impact, and hairline gaps were opened between the grid and paste several centimeters in from the impact zone (Fig. 4).

The only consistent difference noted between the 5xxxx-series cells and the 7xxxx-series cells pertained to the physical dimensions of the positive electrodes. Dimensional data for all electrodes are presented in Table 2. The average of the mean diameters was 317.3 mm for the 5xxxx-series positive electrodes but 316.5 mm for the 7xxxx-series counterparts. The trend in thickness measurements was the opposite. The average thicknesses for the 5xxxx-

Table 2. Final Positive and Negative Electrode Dimensions

Cell Serial Number	Electrode	Thickness (mm)	Diameter (mm)
59941	P1	6.0	317.2
	P18	6.0	317.2
59942	P1	6.6	317.8
	P18	6.5	318.0
59936	P1	6.5	316.7
	P18	6.6	317.0
76712	P1	6.5	315.7
	P18	6.6	317.5
74975	P1	6.9	316.2
	P18	6.6	316.7
77773	P1	6.7	316.3
	P18	6.8	316.7
59941	N2	5.0	292.6
	N18	4.6	292.6
59942	N2	4.7	292.4
	N18	4.6	292.6
59936	N2	4.6	293.8
	N18	4.6	293.3
76712	N2	4.9	292.4
	N18	4.7	292.4
74975	N2	4.5	292.6
	N18	4.5	292.1
77773	N2	4.6	293.7
	N18	4.7	294.1

and 7xxxx-series positive electrodes were 6.4 and 6.7, respectively. Both of these trends were interpreted as outcomes of a difference in service time. The larger diameters for the 5xxxx-series electrodes reflected greater positive-electrode expansion, a time-related corrosion phenomenon. The reduced thicknesses of 5xxxx-series electrodes was a consequence of positive active-material shedding, also a usage-dependent degradation process. Sediment, which is a measure of active-material shedding, corroborated this premise. The sediment found in the bottoms of the 5xxxx-series cells weighed 250% more on average than the sediment from the 7xxxx-series cells. Performance differences related to these dimensional differences would be expected to be second-order effects and have little impact on usable capacity.

3.2. Negative Electrodes

The negative paste-to-grid adhesion was adequate, but the type and quantity of minor imperfections was greater than for the positive electrodes. These imperfections were again traceable to electrode fabrication, especially the pasting process. For the negative electrodes, the burlap texture was evident on the bottom surfaces, and the top surfaces were relatively smooth, in a sense a mirror reversal of the positive electrodes (Fig. 5). The grooves and ridges of the burlap pattern were not as pronounced for the negative electrodes. The presence of this

pattern on both electrodes suggested that a common coarse separator was used during a common formation process.

The most consist pasting flaw for the negative electrodes was a mild tendency to underpaste. Once the paste was applied, it was not completely worked into contact with the grid elements. The end result was intermittent areas with surface gaps along the grid interface. On the top surfaces, these interfacial gaps ranged from fairly broad, shallow separations to slight hairline breaks (Fig. 6). On the electrode undersides, the gaps tended to be wider and deeper and were commonly found near either the outer or inner perimeter (Fig. 7). These separations generally occurred at only one or two interfaces of a given pellet, and the pellets remained in place. The only loose negative pellet was found in cell 59941, and it was dislodged from one of the areas where the electrode assembly had been struck and dented.

Other pasting flaws were less prevalent. Areas of overpasting due to the application of too much paste or due to intentional patching were found on the undersides of a few electrodes (Fig. 8). Drops of excess paste were also inadvertently bonded to the top surfaces of other electrodes (Fig. 9). Doctor-blade marks were also discernible. Breaks in the leveling action left slight ridges on individual pellets, and incomplete blade travel across the electrode left larger raised ridges along the outer perimeter (Fig. 10).

Two other flaws, blistering and "dimpling," were observed on the negative electrodes (Fig. 11). Examples of blisters were found in every cell. They commonly develop during formation when hydrogen gas is entrapped in localized pockets just beneath the surface. In some, but not all cells, individual pellets had shallow indentations. These dimpled pellets were often found in a series of consecutive pellets along an electrode perimeter and were an apparent artifact of pasting or handling.

4.0 Electrolyte Analyses

The electrolyte in each cell proved to be on specification in terms of quantity and composition. In each cell, the electrolyte meniscus fell between the level lines marked on the sidewall of the container. The specific-gravity measurements are summarized in Table 3. The average of the two measurements made for each cell ranged from the design density of 1.300 g/cc to 1.307 g/cc. The slightly higher gravities probably reflected water loss due to electrolysis.

The results of the sample submissions for impurity analysis are presented in Appendix 2. No trace element was present in concentrations greater than 15 ppm. Typical concentrations were 12 ppm Ca, and ~5 ppm for Al, Fe, and Mg, with all other reported contaminants (Ba, Cd, Cl, Cu, Mn, Ni, Pt, and Zn) present in concentrations of 2 ppm or less. Cadium levels showed the greatest variability, ranging from below detectable limits to under 2 ppm, but these results were consistent for duplicate samples submitted to both analytical services. None of these impurities were found in concentrations high enough to impair cell performance.

Table 3. Electrolyte Specific Gravity Measurements

Cell Serial Number	Specific Gravity (g/cc)		
	At Top	At Bottom	Cell Average
59941	1.298	1.302	1.300
59942	1.295	1.305	1.300
59936	1.307	1.307	1.307
76712	1.304	1.308	1.306
74975	1.304	1.306	1.305
77773	1.303	1.304	1.304
Averages	1.302	1.305	1.304

By design, each electrode rises ~10° above horizontal from the outer perimeter to the inner perimeter. The truncated conical geometry serves to direct movement of gas bubbles first inward along the undersides of the electrodes and then upward through the open central channels around the negative terminal post. The result of the directed gas bubble movement is forced electrolyte circulation. Our electrolyte samples, which were collected under float charge, did show a slight location dependence in specific gravity. As shown in Table 3, the electrolyte samples collected near cell bottoms averaged 0.003 g/cc more in density than the average for the samples collected near the tops. This density gradient, as later studies in sections 5.0 and 6.0 proved, was insufficient to induce discernible differences in the electrodes. The electrode design was thus deemed adequate to avoid electrolyte stratification and the consequent impairment of cell capacity.

5.0 Electrode Assessment

Scanning electron microscopy (SEM) was the primary tool used to evaluate the condition of both the negative and positive electrodes. Interpretation of the electrode microstructures by this method is qualitative, but comparisons made across common electrode samples from the different cells revealed some distinctive differences, especially concerning the morphology of the corrosion scale formed on the positive-electrode grids. The intrusion porosimetry performed on selected samples was less comprehensive, but it did provide a more quantitative view of the pore structure available for transport of sulfate ions.

5.1 Negative Electrodes

The microstructure of the negative electrodes was consistent from cell to cell. In the interior, these electrodes consisted of a sintered network of 2- to 5-μm lead particles (Fig. 12). The sintered connections between particles were well formed, but the lead particles still possessed high surface area. The void volume was ample and essentially free of $PbSO_4$ crystals. The upper half of Table 4 summarizes the intrusion porosimetry results for three pairs of electrodes from three of these cells. The findings for pore volume, pore area, pore diameter, and bulk density are very comparable, especially for full-capacity cell 59942 and low-capacity

cell 76712. The data for low-capacity cell 59941 suggested that its electrodes were slightly more porous and had more internal surface area. If these limited samplings truly represent these electrodes, the enhanced porosity and area would be beneficial, not detrimental, to electrode performance.

Differences in appearance were limited to the surfaces of the negative electrodes. A common characteristic was coarsening of the surface particles (Fig. 13). The surface morphology was better described as partial aggregates with a characteristic dimension of ~10 μm. The only cell-to-cell difference for the negative electrodes was the degree of surface sulfation. This condition was directly related to the time between termination of float charging and cell disassembly. When a cell was examined immediately after charging termination, no $PbSO_4$ was evident (Fig. 13). When a multi-day period elapsed, small needles and platelets of $PbSO_4$ grew in both size and concentration (Fig. 14). After four days, the $PbSO_4$ particles averaged 5 μm along their major growth axis. True sulfation results when large (>100 μm), difficult-to-reconvert crystals develop within as well as on the negative electrodes. Weeks of inactivity are generally required to develop this type of microstructure.

Table 4. Porosimetry Data for Negative and Positive Electrodes

Cell-Electrode Identification	Pore Volume (cc/g)	Pore Area (m^2/g)	Pore Diameter (μm)	Bulk Density (g/cc)
59941-N2	0.179	2.06	0.346	3.68
59941-N18	0.178	2.19	0.337	3.71
59942-N2	0.156	1.88	0.330	3.89
59942-N18	0.151	1.67	0.362	3.88
76712-N2	0.145	1.64	0.353	3.99
76712-N18	0.157	1.82	0.345	3.85
Averages	0.161	1.88	0.346	3.83
59941-P1	0.108	3.24	0.134	4.64
59941-P18	0.118	2.51	0.188	4.30
59942-P1	0.111	2.44	0.182	4.40
59942-P18	0.116	3.52	0.132	4.32
76712-P1	0.121	3.54	0.137	4.21
76712-P18	0.117	2.39	0.196	4.20
Averages	0.115	2.94	0.162	4.35

In each of these cells, the critical grid interface showed good contact between the negative active material and the grid. Physically, the negative-electrode paste maintained close proximity to the grid elements except where underpasting resulted in areas of broad, V-shaped gaps (Fig. 15). Adherence was promoted by the formation of a sintered metallurgical bond

between the grid and adjacent lead particles (Fig. 16). The good conductivity of the grid to the active material, coupled with the open structure of interconnected, high-interfacial-area lead particles, made the negative electrodes a most unlikely source of capacity-loss problems.

5.2 Positive Active Material

The microstructure of the positive active material also proved to be very consistent from cell to cell. Lead dioxide was essentially the sole constituent. Within the core of an electrode pellet, these particles typically ranged from 2 to 5 μm in dimension and were identifiable as discrete particles, but still appeared to form good particle-to-particle contact between adjoining particles (Fig. 17). At the surface, the morphology differed. Finer particles with greater surface area tended to merge into larger 20- to 30-μm aggregates (Fig. 18). This change in structure was evident in every cell and was discernible not only for the fresh surfaces exposed by breaking pellets, but also for polished cross sections (Fig. 19).

Intrusion porosimetry also found no significant differences in the positive electrodes from different cells. These results are summarized in the lower half of Table 4. Given the variation for electrodes from the same cell, the values for pore volume, pore area, and mean pore diameter were virtually indistinguishable for full-capacity cell 59942 and low-capacity cells 59941 and 76712. The bulk density of the last cell appeared to be 5 to 10% less than that of the other two cells. In essence, the porosimetry results confirmed the qualitative impression from the microscopic studies. None of the physical changes in the positive active material were deemed great enough to cause the reported capacity decline.

5.3 Corrosion of Positive-Electrode Grid

Corrosion of the positive-electrode grids is an expected (and undesired) reaction in lead-acid cells. Prolonged conversion of metallic lead to more PbO_2 weakens the structural integrity of the grid as it simultaneously increases the stresses imparted by the expanding mass of active material. None of these cells experienced sufficient corrosion to fail because of grid growth. The modest growth reported in Section 3.1 supported this premise. Our microscopy studies, however, found differences in scale morphology and composition that clearly delineated the high-capacity cell from the low-capacity cells.

The PbO_2 scale formed on the positive grids of high-capacity cell 59942 followed the expected stages of growth and development. A dense scale formed and thickened over time. A limiting thickness of 30 to 40 μm was reached as the outermost scale broke up under normal service and formed particle masses that were indistinguishable from original active material. The PbO_2 scale remained adhered to the lead substrate for all examined samples. No separations were evident in the dense scale; only a few occasional hairline cracks developed in the outer scale regions (Fig. 20). When separated from the active material, the exterior surface of the scale was highly textured and particle-like, and when the scale was removed, it cleaved very clearly at the substrate, revealing the lead substrate (Fig. 21).

In every capacity-impaired cell, the structure of the scale was altered. The monolithic nature of the scale was destroyed by the development of extended separations within the PbO_2 scale. These separations presumably started as fine hairline cracks that propagated laterally to the grid interface. The separations were offset from this interface and were most pronounced in the outer half of the once-intact scale (Fig. 22). In some instances, multiple lateral separations

were evident. The gaps between scale sections consistently ranged between 2 and 5 μm. The new scale morphology was not the result of increased scale thickness; the combined thickness of the scale sections was still in the range of 30 to 40 μm, which was the same thickness range found for the 59942 grids. Cracks in the scale do not have a severe impact on cell performance if they are perpendicular to the grid interface. A relatively uniform electron flux can then be maintained in all radial directions. The lateral separations in these scales, however, severely inhibited electron transfer between grid and active material by forcing electrons to channel along sparse bridges across semicontinous gaps.

Further examination of these scale separations revealed that $PbSO_4$ crystals had formed within them. On occasion, these crystals could be discerned by looking down into scale separations (Fig. 23). They could be seen much more clearly after sections of the outer scale were removed (Fig. 24). The removal process was relatively easy because in the affected cells, the scale would preferentially cleave along the existing lateral separations rather than at the grid interface. All of these crystals were relatively flat (1 to 3 μm) because of the geometric constraints imposed by the narrow gaps. In the plane of the separation, however, some crystals reached 30 μm in major dimension. The planar growth was variable and resulted in crystals with distinct shapes. Most often, simpler and much thinner disc-shaped crystals formed, such as those shown in Fig. 23. On occasion, these crystals developed in pairs and bore a resemblance to ears, such as those shown in Fig. 24. In other instances, both rounded crystals and intersecting acicular platelets were observed for grid samples from the same cell (Fig. 25).

The $PbSO_4$ crystals illustrated the severity of the lateral scale separations in two ways. First, their virtually exclusive presence in these restricted regions attested to the localized impairment in electrochemistry. The bulk of the positive electrodes, including those from the capacity-impaired cells, were nearly free of these crystals. Second, their occupation of the scale separations physically reinforced the stability of the defective scale structure. With active cycling, the outer scale region would be expected to convert into a mass of PbO_2 particles. Effective electrical continuity would require intimate contact of these new particles with the remaining grid scale. However, as the outer scale breaks down, the blocking action of the $PbSO_4$ crystals would impede inward movement of the newly formed PbO_2 particles to create new contacts. Chemical conversion of the insulating $PbSO_4$ into conductive PbO_2 would occur only when the outer scale is completely converted and sufficient electrolytic pathways opened. The critical scale-to-active-material interface would be restored only after this last conversion process has occurred.

6.0 Correlation of Performance Data with Examination Findings

Discharges employing current interruptions or discrete changes in current level can be analyzed in detail to deduce changes in IR-free potential and internal impedance over time. Operation under a constant load does not generate the same level of data and limits interpretation to general observations upon the discharge voltage curve. The available curves, (Appendix 3) provided by the utilities for the five cells that suffered capacity losses were reviewed for indications of changes in cell impedance. These curves showed an increase in the pure resistance component of impedance for the discharges where the capacity was lost. While other sources of ohmic loss cannot be ruled out through this type of "black box" analysis, the findings were definitely consistent with the development of resistance-enhancing changes in the structure and composition of corrosion scale present on the positive-electrode grids.

Our interpretation was based on load currents of 600 A and 714 A for the 5xxxx-series cells and 7xxxx-series cells, respectively. The initial resistance at the start of charge was calculated to be ~250 μΩ for unimpaired AT&T Round Cells. For subsequent discharges where the capacity loss became evident, the voltage curves began depressed from earlier discharges and showed progressively greater voltage depression as the discharges progressed. At 15 minutes into the discharge, which was the first common time provided for all five cells, the voltage depression ranged from 15 to 45 mV, a 8% to 25% increase in resistance. Internally, the suppressed voltage meant that the potential between the electrodes was reduced. With a reduced potential to drive ionic transport, polarization of the reactions occurring at the electrodes became more difficult to overcome and caused a further decline in the effective potential. In effect, a negative feedback loop was established that accelerated the voltage decline with depth of discharge. After 60 minutes, voltage suppression ranged from 35 to 115 mV, depending on the particular cell.

This scenario appeared to be valid for all five cells, although further interpretation was needed to bring the voltage curves for cell 74975 into compliance. Instead of overlaying, the early discharges trended upwards with successive discharges, rising ~30 mV from the first to fourth cycle. The voltage improvement very likely occurred because formation of this cell was incomplete and continued during early cycling. The fourth discharge was still consistently lower in voltage for a given time than the early discharges of the other cells. When this added complexity is considered, the fifth voltage curve showing the loss of capacity in cell 74975 is seen to be consistent with the other discharges showing capacity losses and similar to the last discharge of cell 76712.

In our estimation, capacity impairment would persist on subsequent discharges as long as the detrimental scale condition existed. The charge algorithms and float-charge procedure were inadequate to reverse this condition. In fact, the adverse scale morphology almost certainly developed during the prolonged period (>1 year) of float charging at the utilities prior to the attempted in-service discharges. This does not mean that the adverse scale changes are irreversible, but more aggressive charging procedures would be required to convert the poorly attached outer scale and the intervening lead sulfate crystals into useful active material. This alternative carries the associated risk of greater overall corrosion of the grids and a shortening of the design service life.

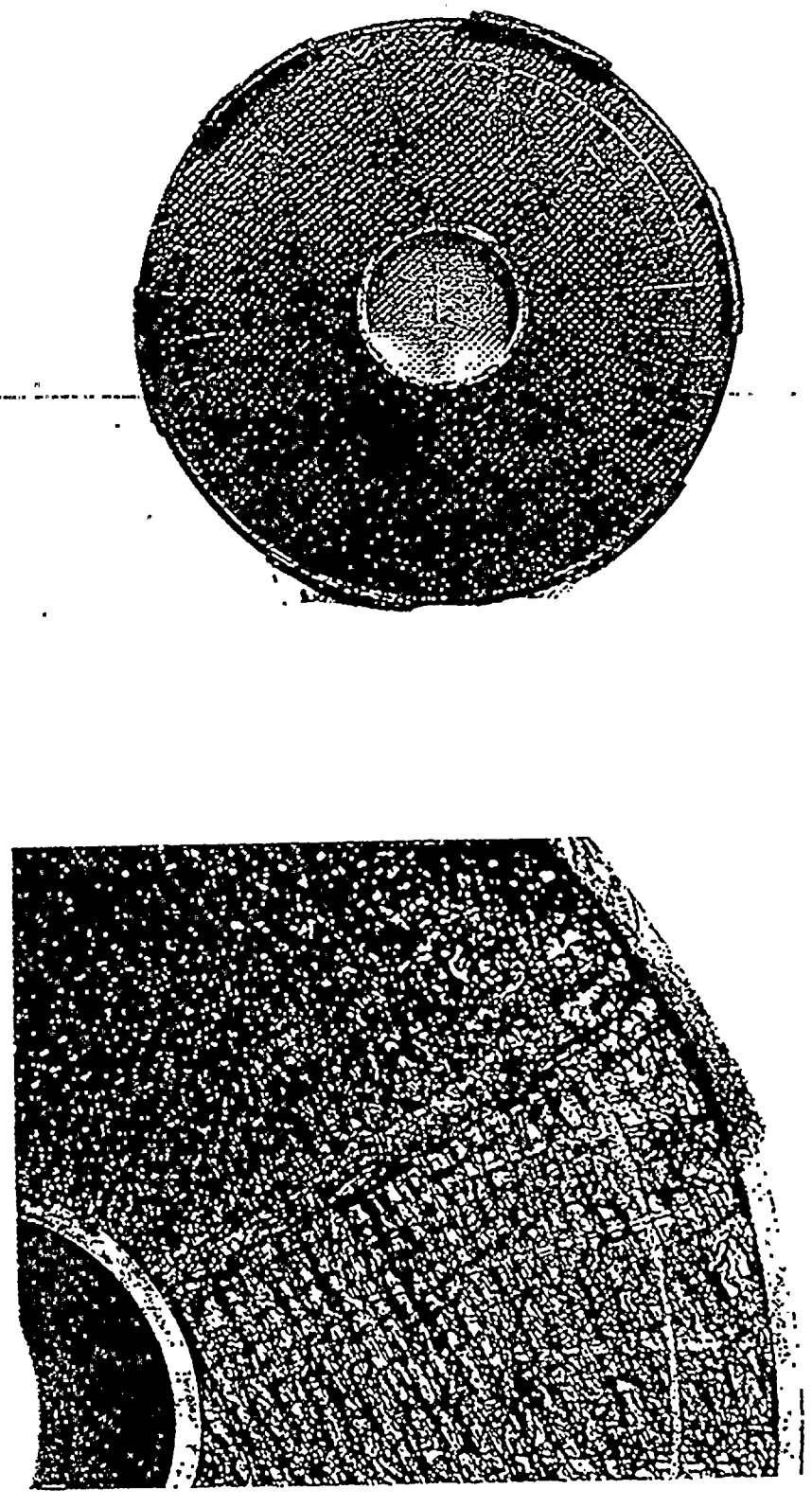

Fig. 1. Positive-Electrode Top Surface (upper, cell 59936; lower, cell 78712)

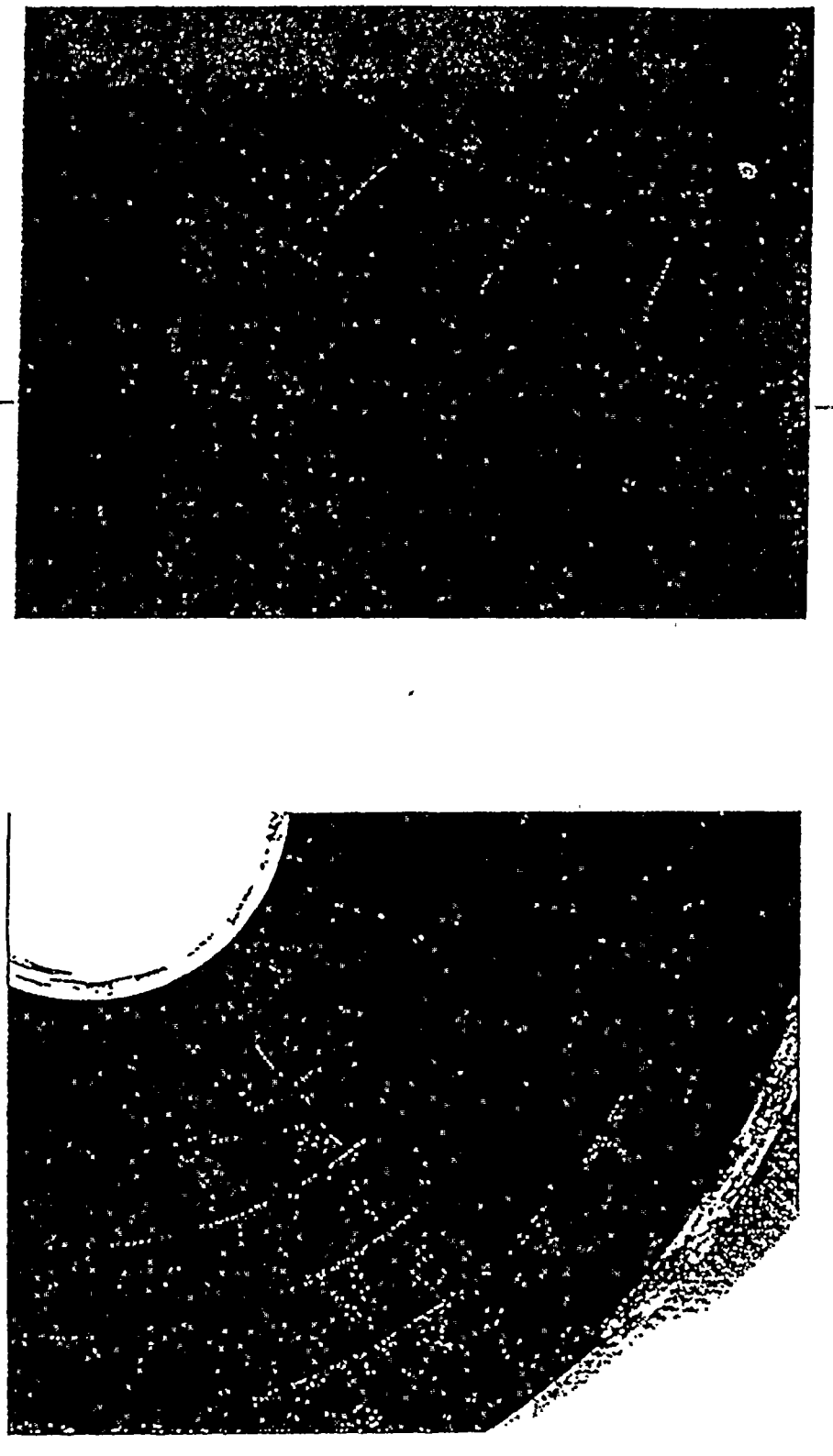

Fig. 2. Positive-Electrode Bottom Surface (upper, cell 59942; lower, cell 76712)

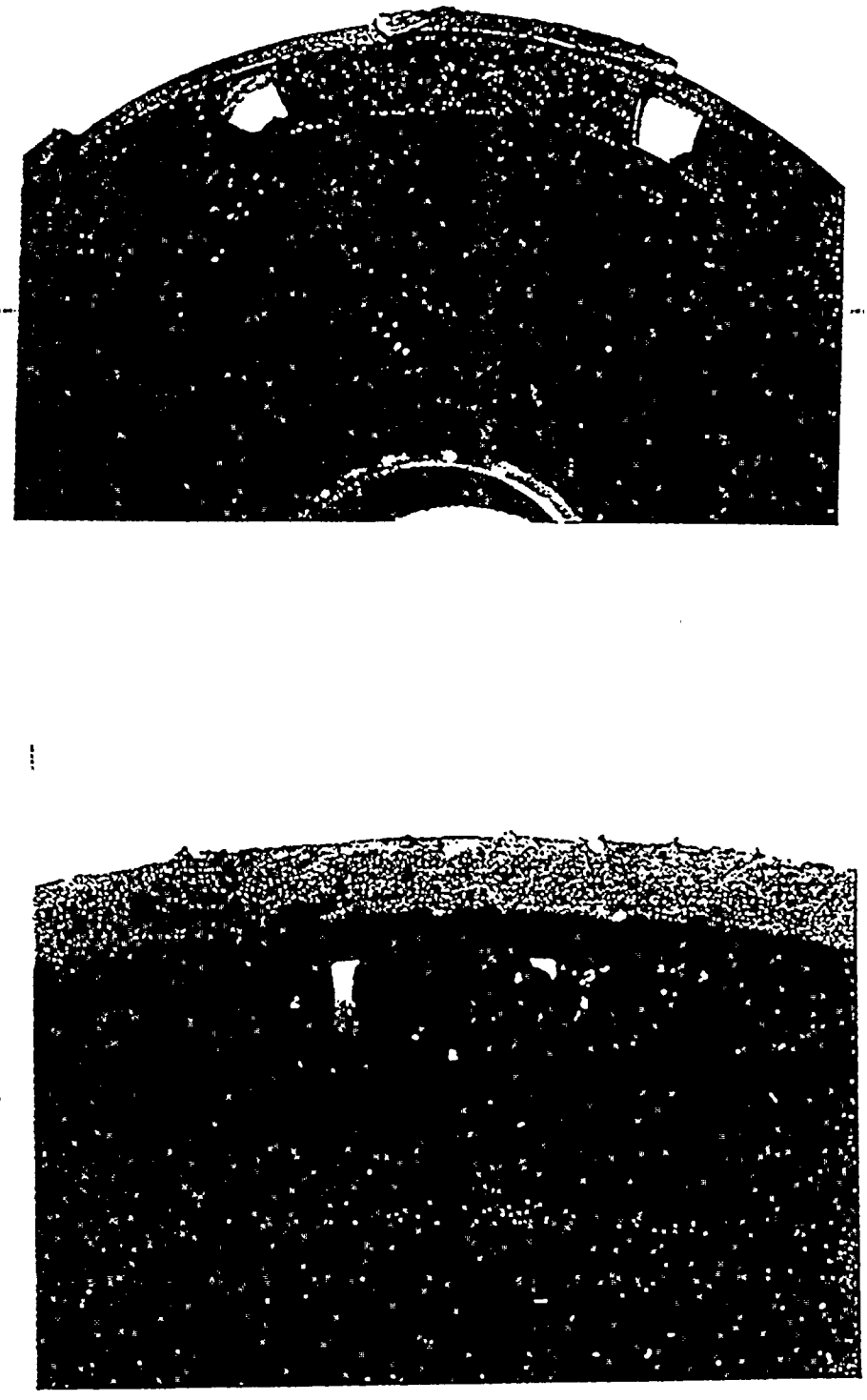

Fig. 3. Missing Positive-Electrode Pellets (upper, cell 77773; lower, cell 74975

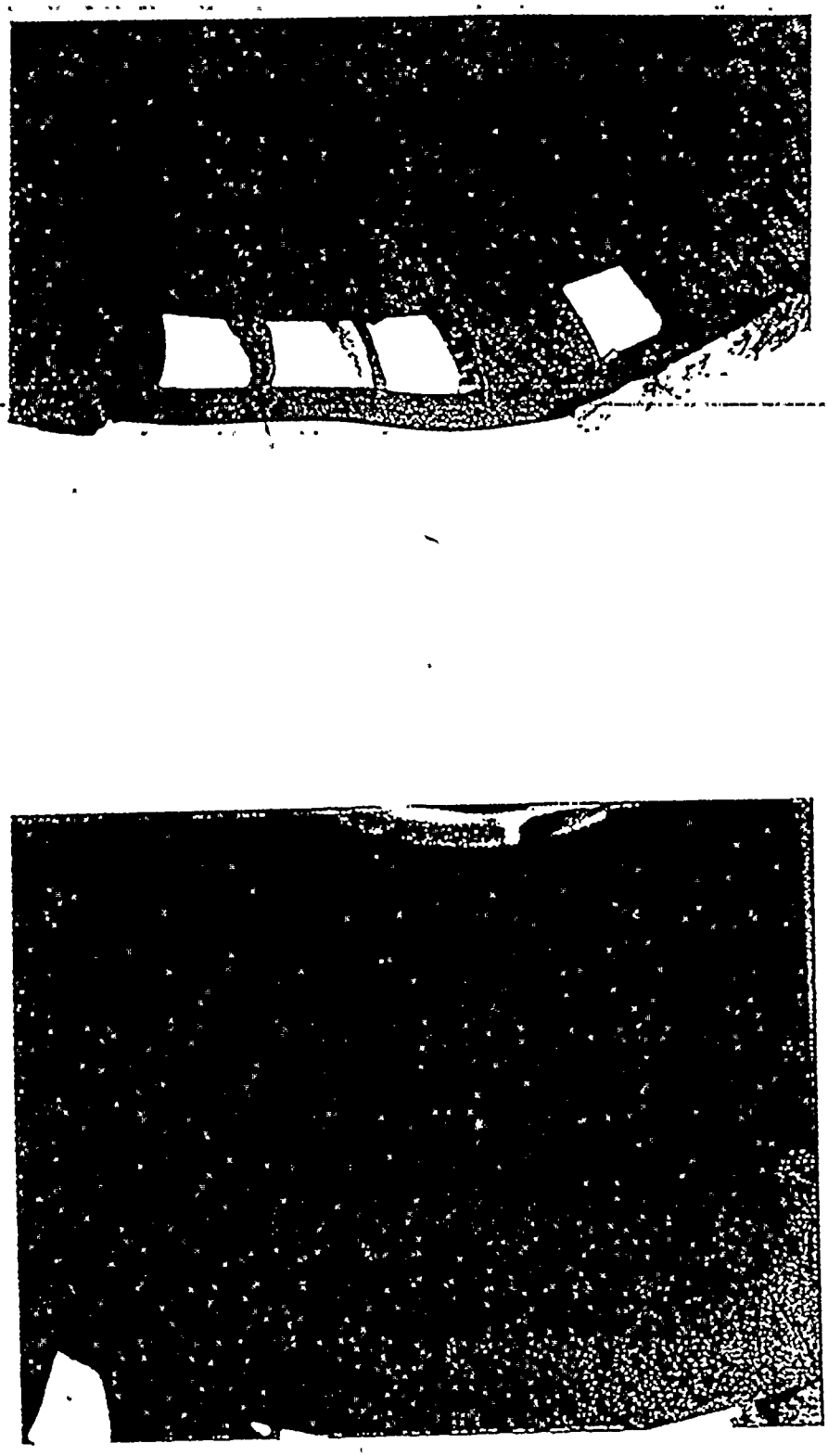

Fig. 4. Multiple Pellet Loss (upper) and Fine Pellet-to-Grid Separations (lower) in an Impact Area on a Positive Electrode from Cell 59941

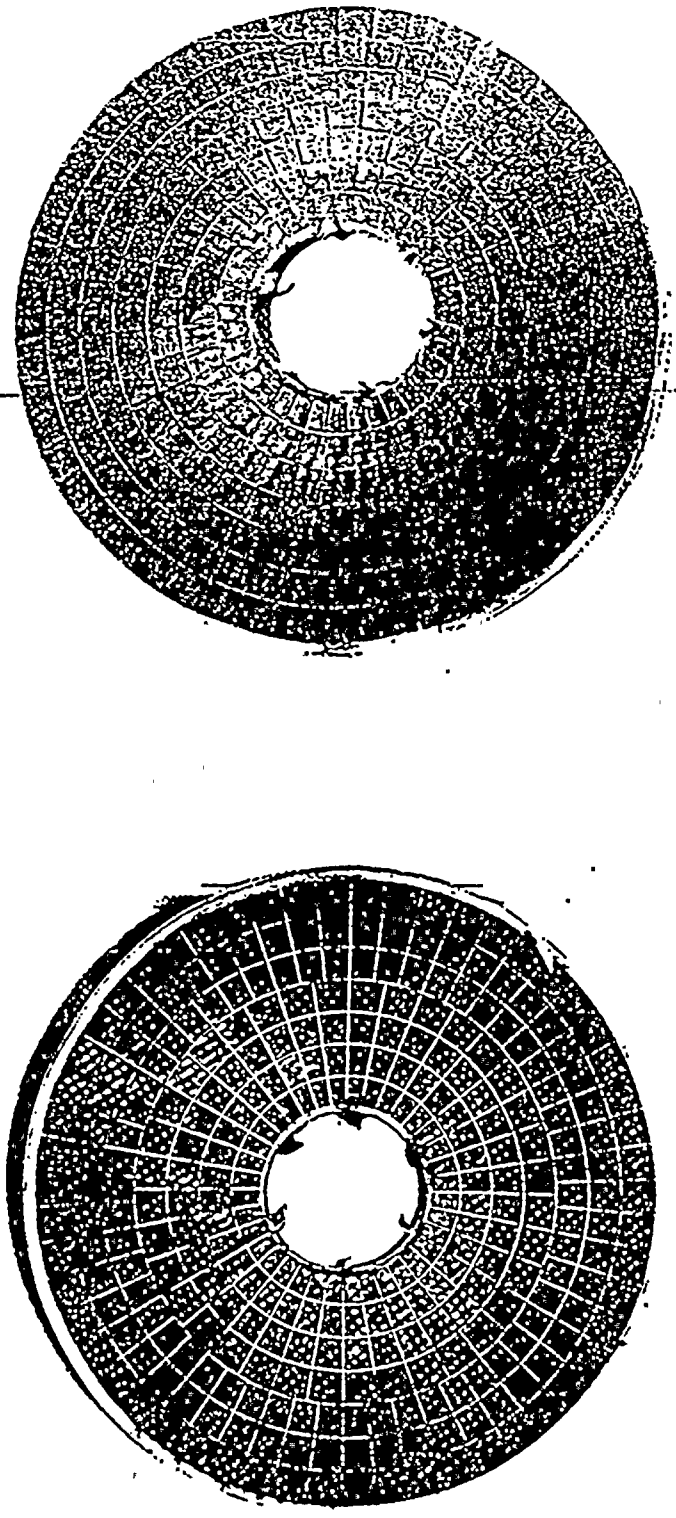

Fig. 5. Top (upper, cell 59941) and Bottom (lower, cell 59942) Surfaces of the Negative Electrode

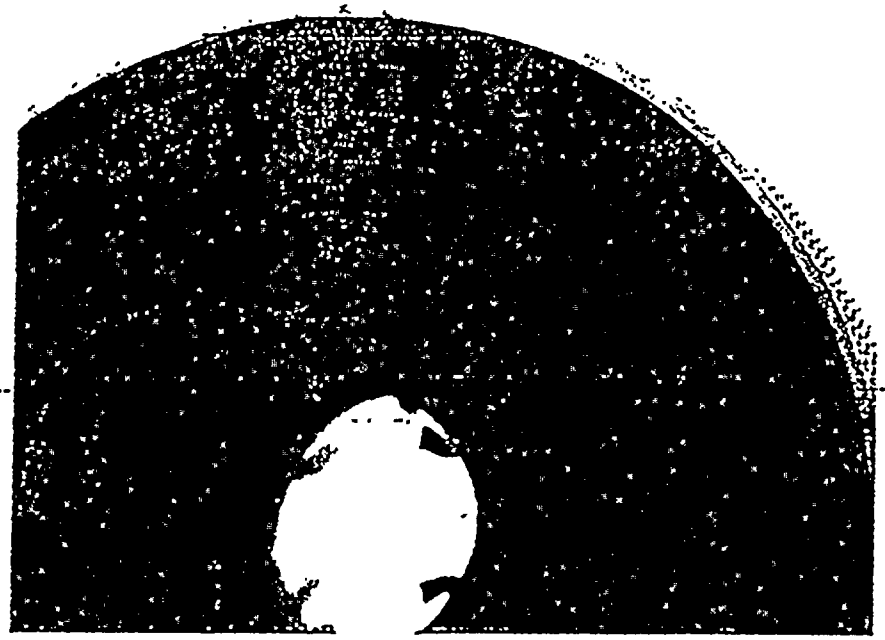

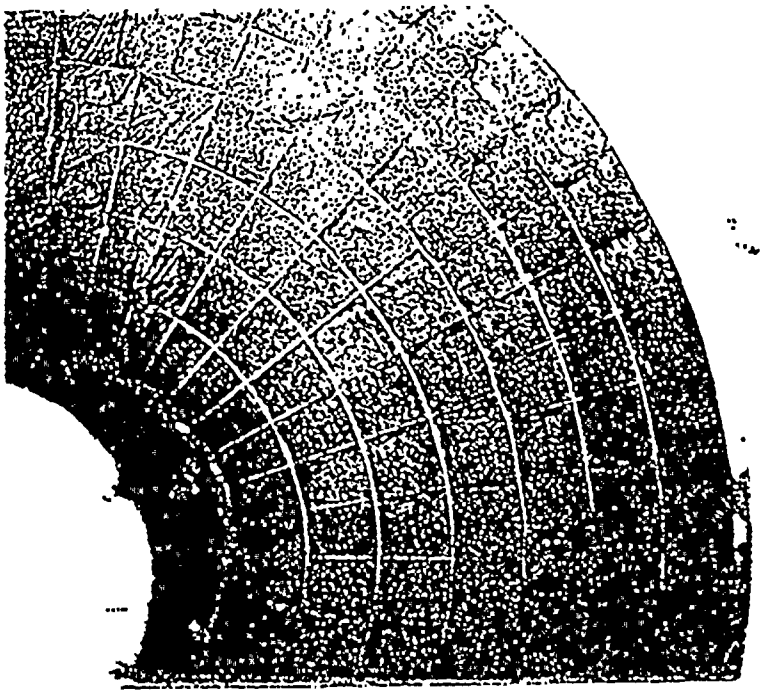

Fig. 6. Mild Underpasting of the Negative Electrode on the Top Surface (upper, cell 74975; lower, cell 76712)

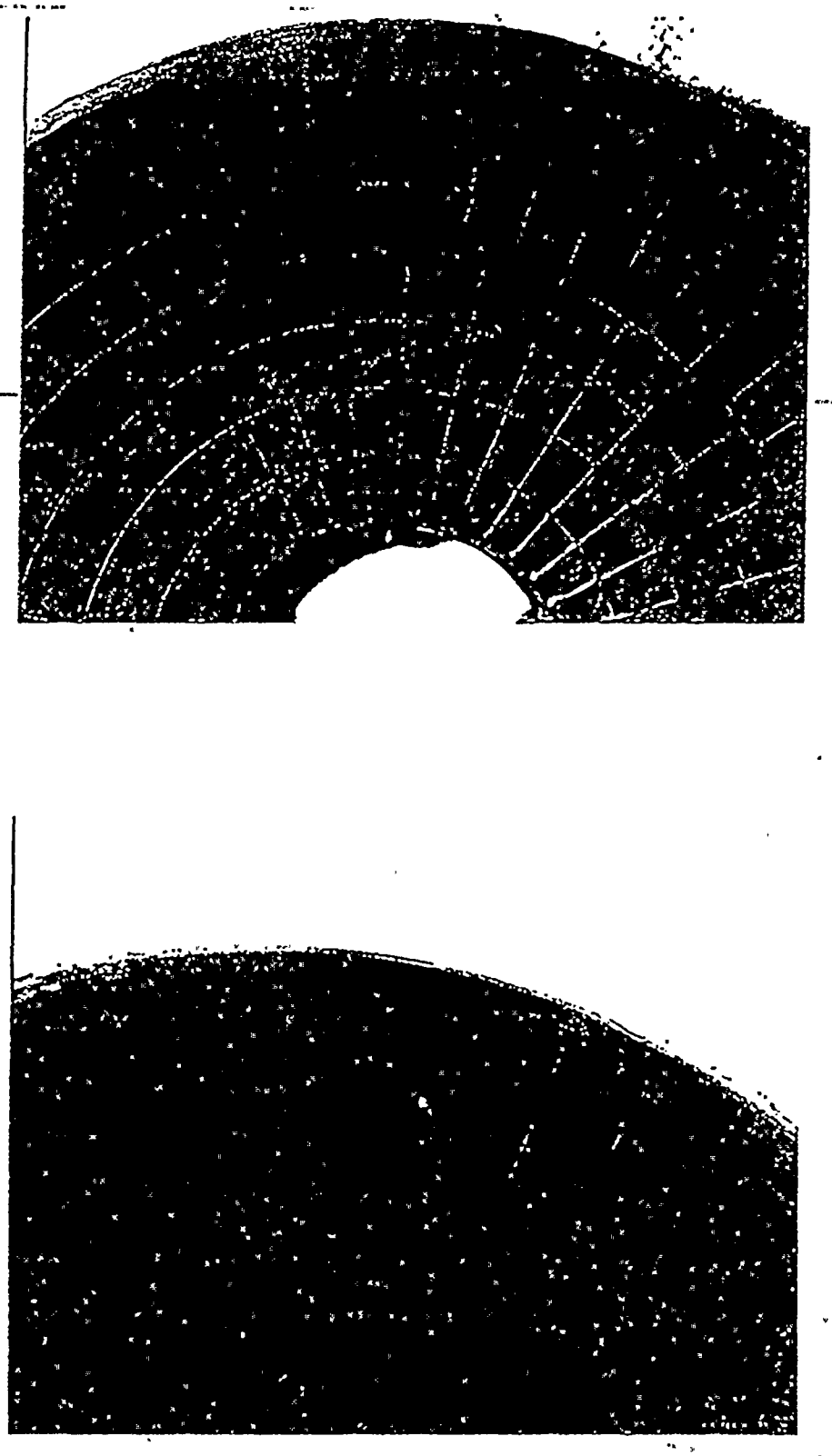

Fig. 7. Mild Underpasting of the Negative Electrode on the Bottom Surface (upper, cell 59942; lower, cell 74975)

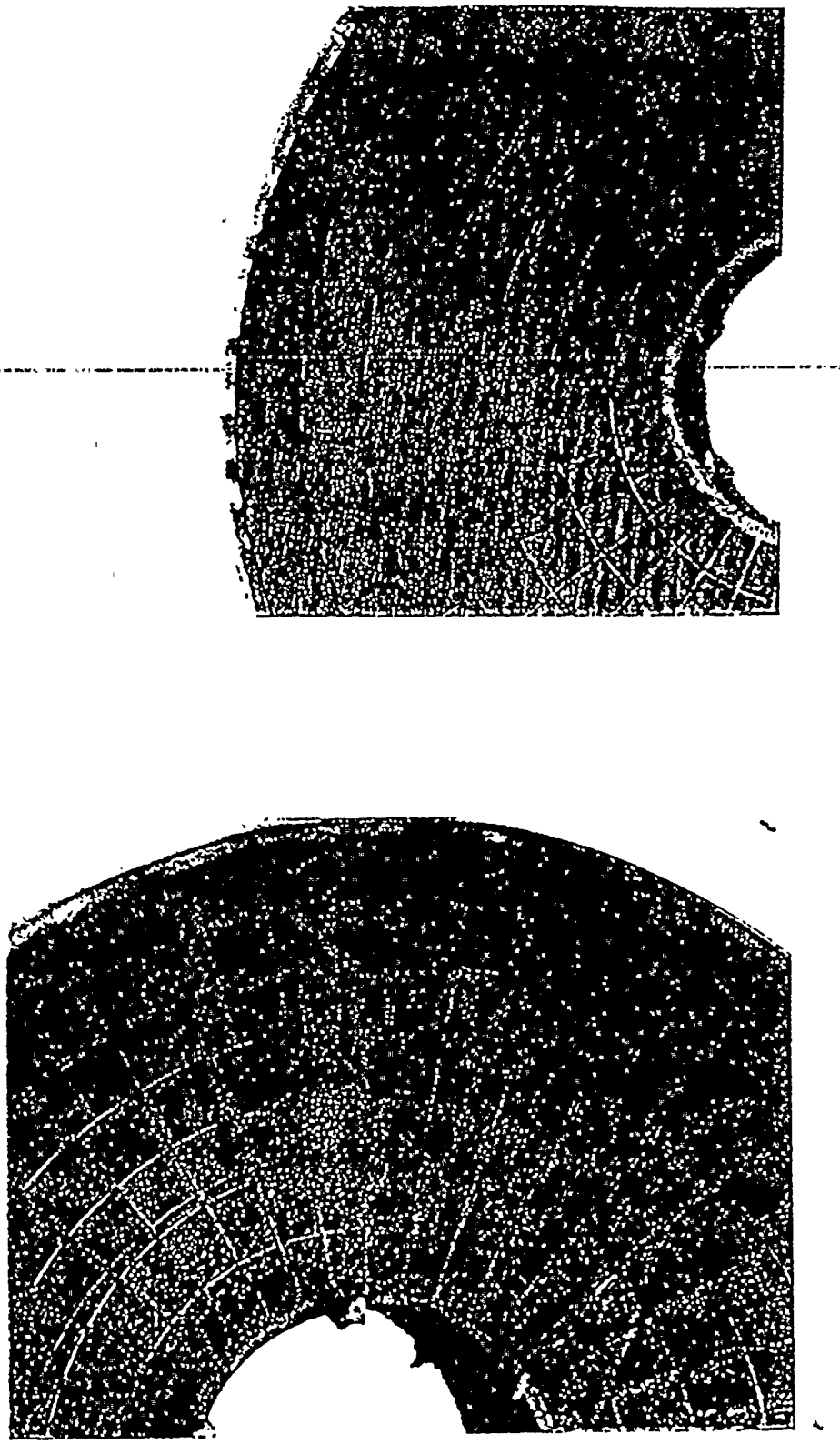

Fig. 8. Area of Operpasting (upper) and an Intentional Patch (lower) in Negative Electrodes from Cell 76712

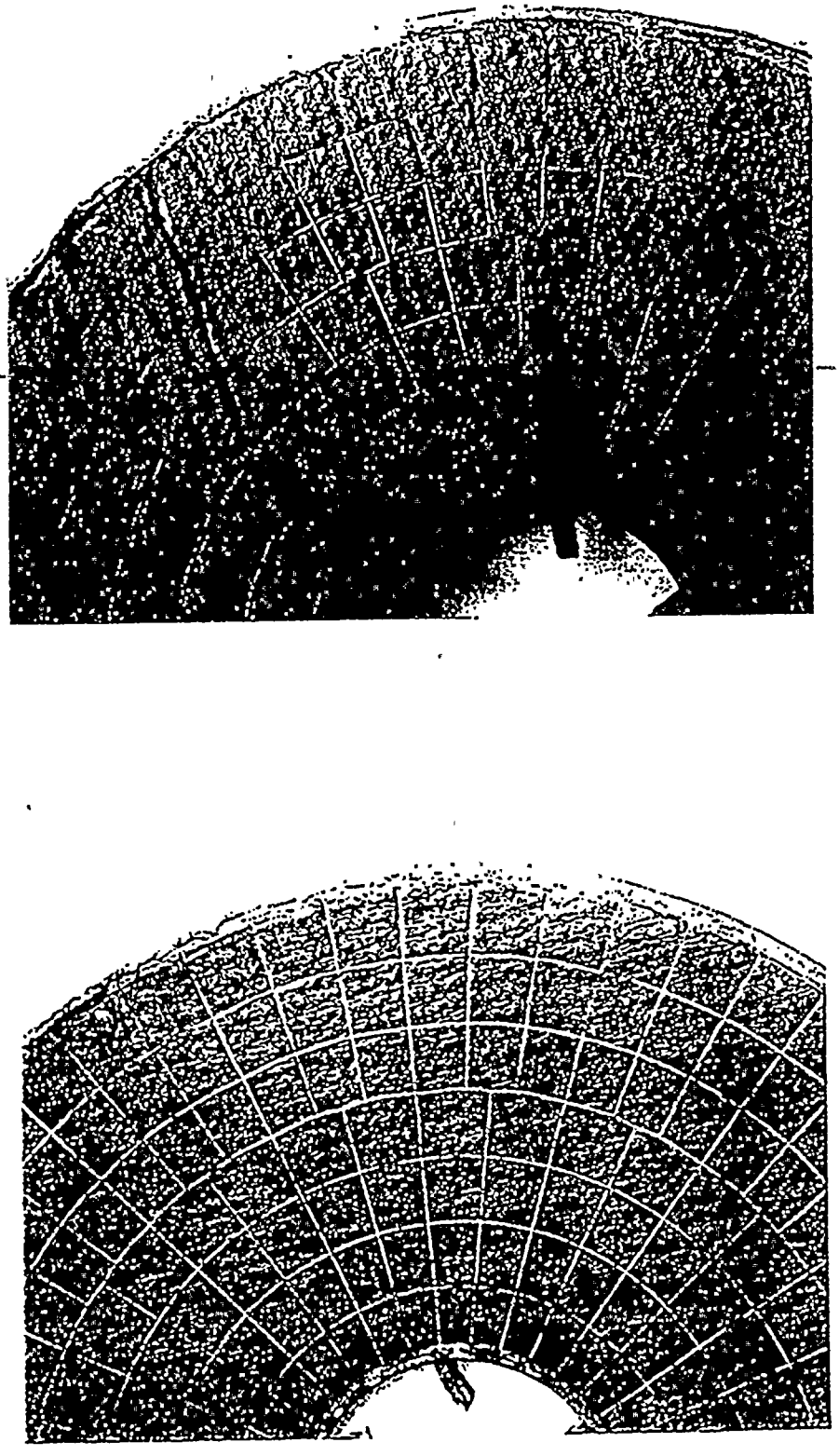

Fig. 9. Inadvertently Bonded Drops of Negative-Electrode Paste (upper, cell 59936; lower, cell 77773)

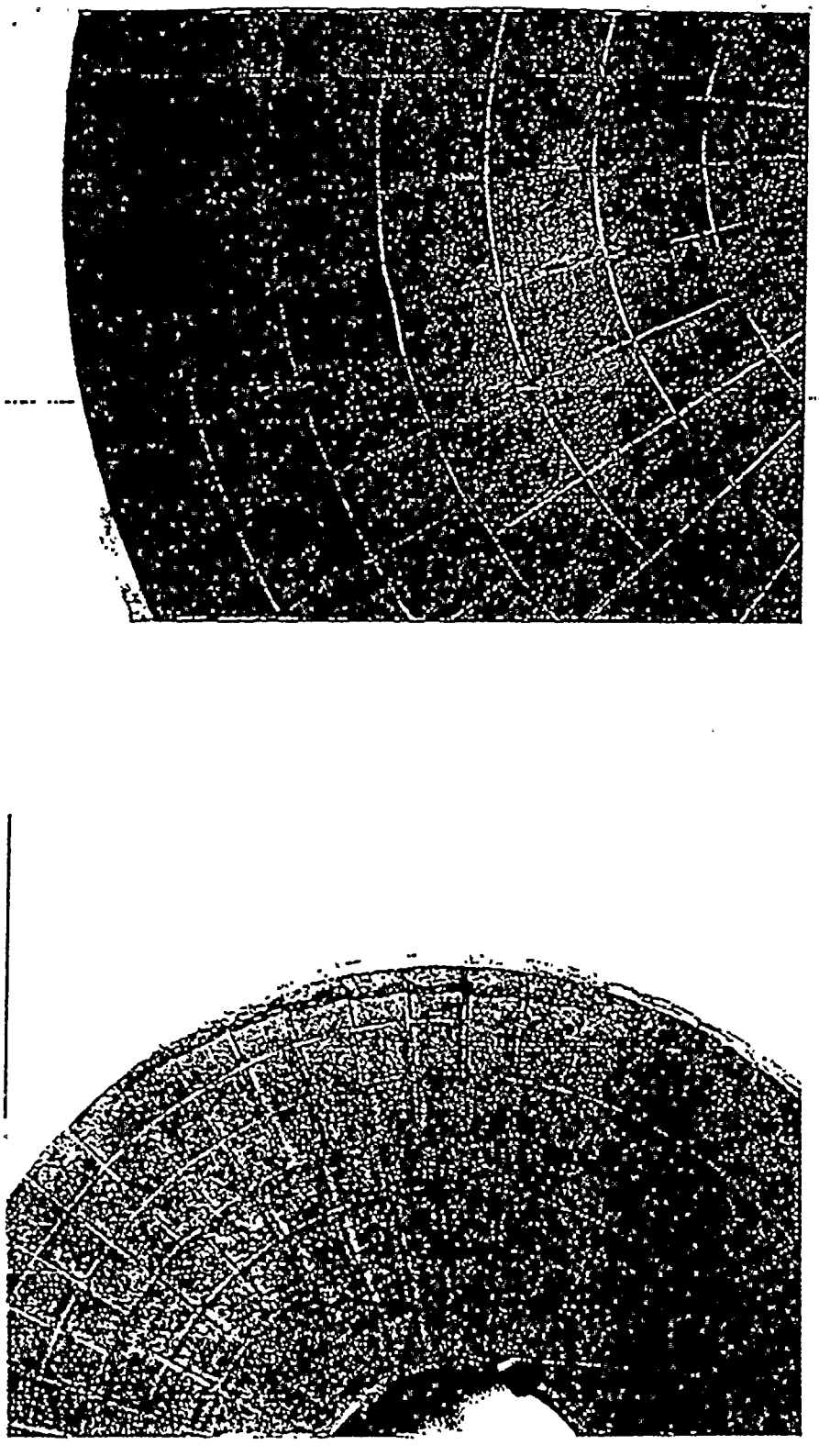

Fig. 10. Slight Ridges (upper, cell 59941) and an Extended Perimeter Ridge (lower, cell 77773) Due to Breaks in Negative-Electrode Pasting

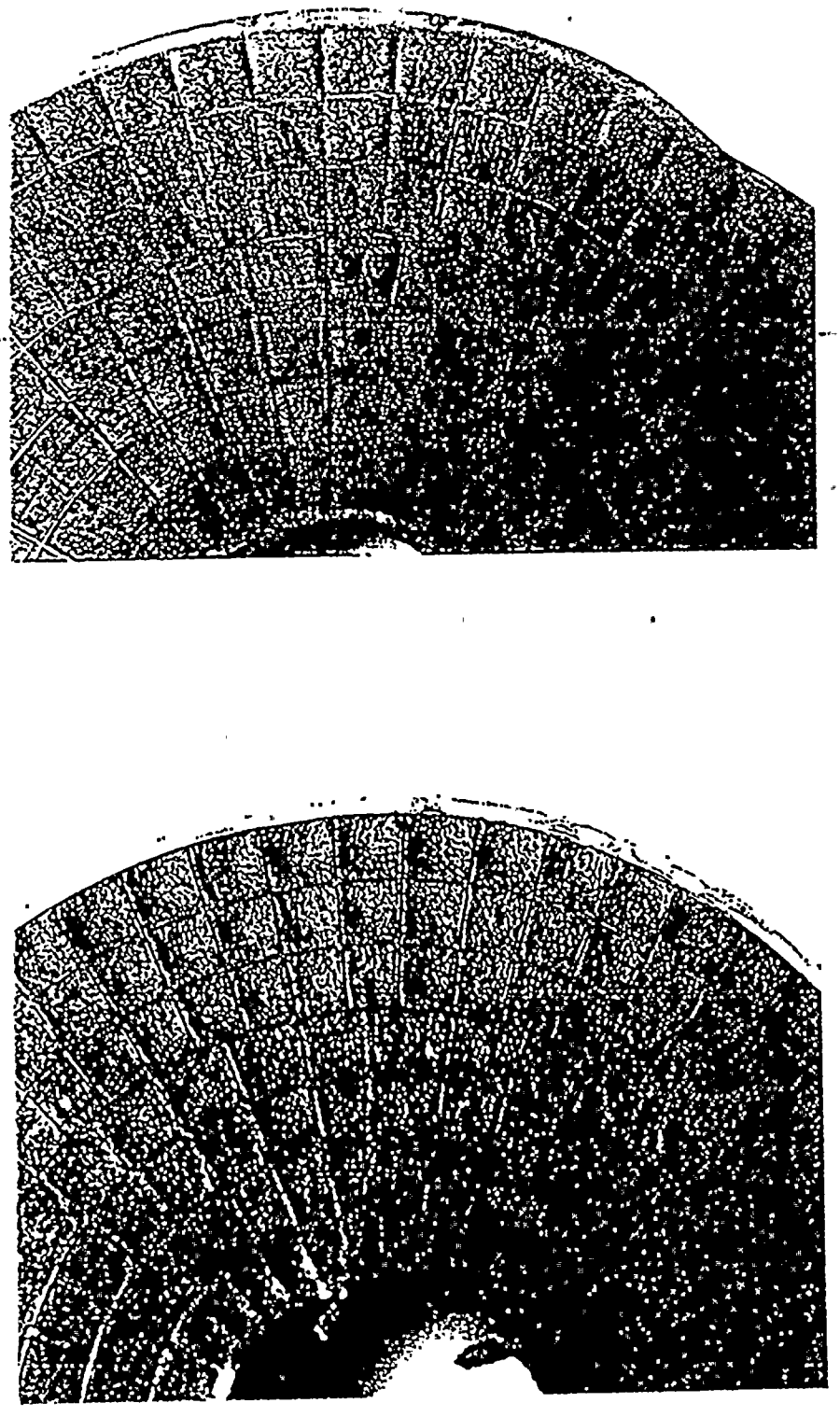

Fig. 11. Blisters (upper, cell 77773) and "Dimpled" Pellets (lower, cell 59936) on the Top Surfaces of Negative Electrodes

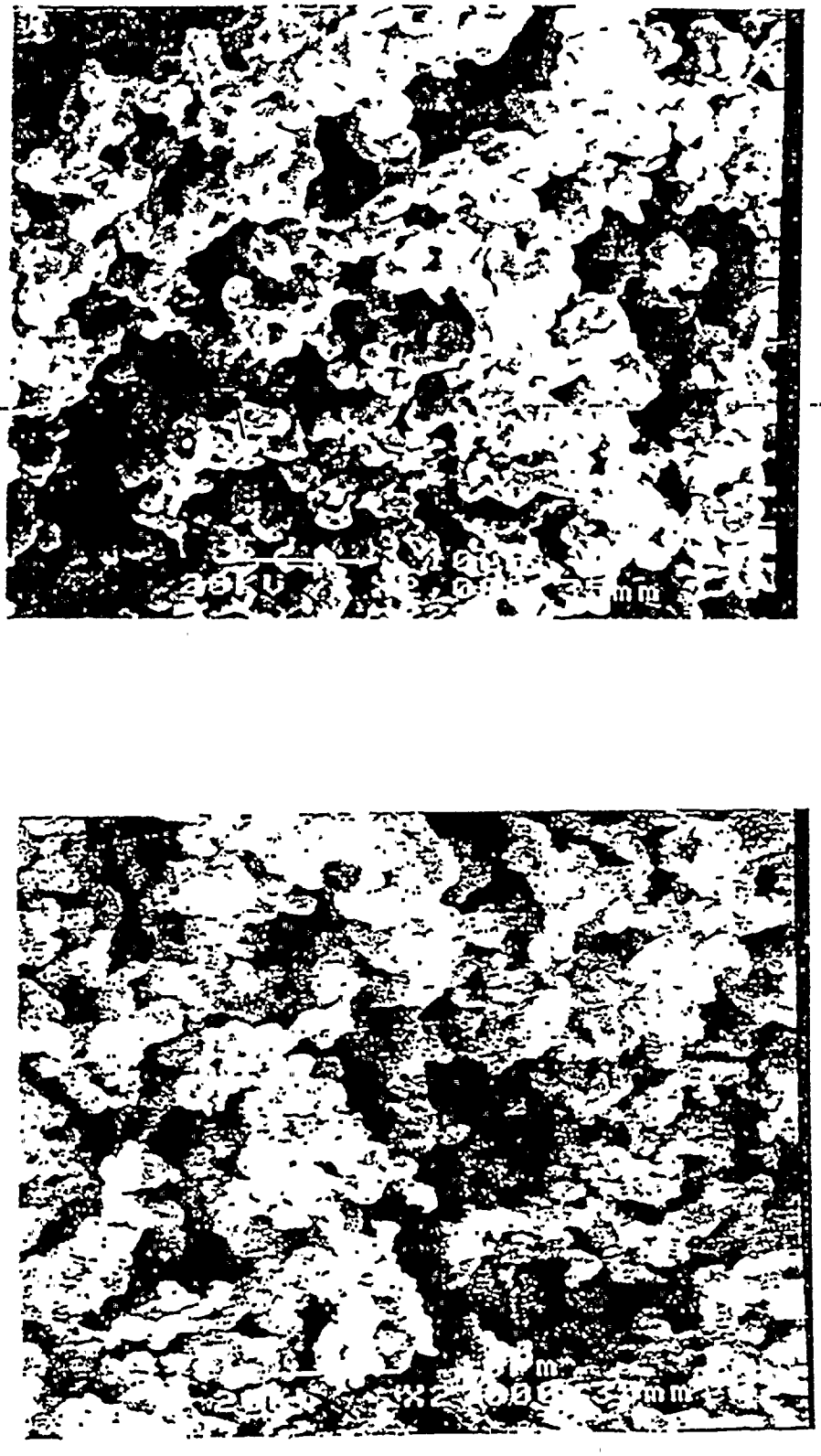

Fig. 12. Typical Microstructures of Negative-Electrode Interiors (upper, cell 59941; lower, cell 77773)

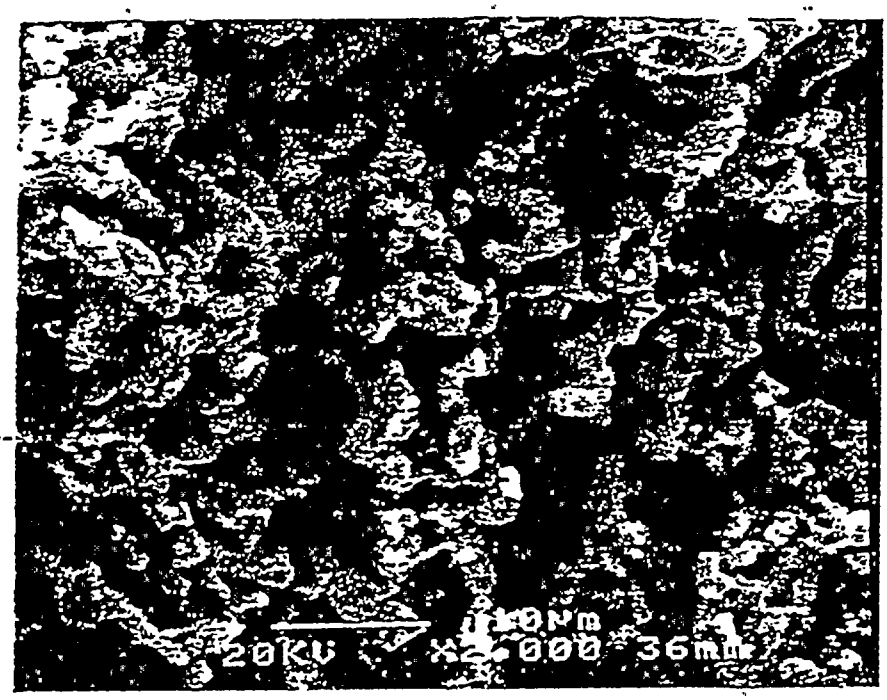

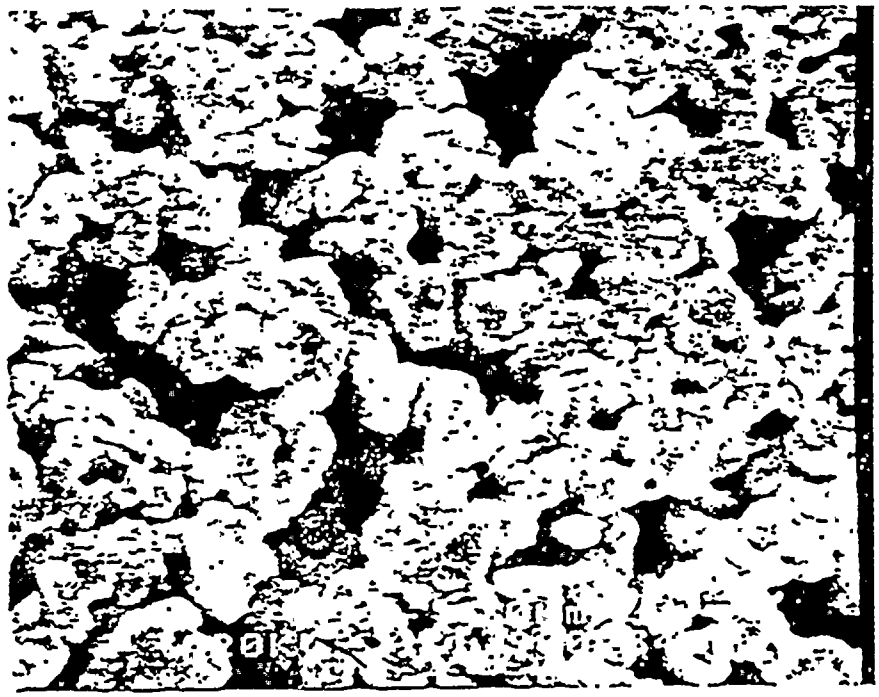

Fig. 13. Comparison of Interior (upper) and Surface (lower) Microstructures for Negative Electrodes from Cell 74975

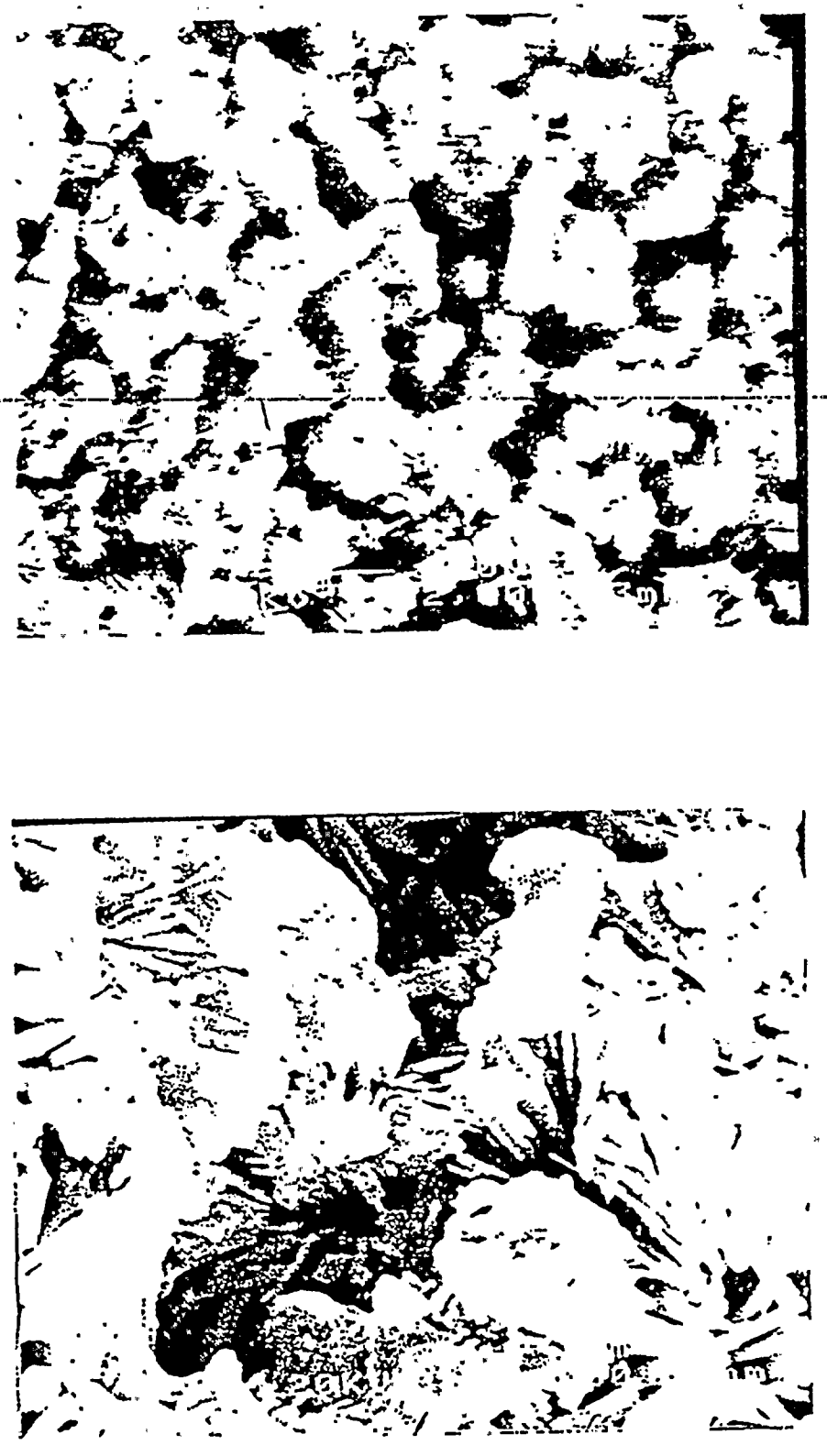

Fig. 14. Fine $PbSO_4$ Platelets on Negative Electrodes after 2 Days (upper, cell 76712) and 4 Days (lower, cell 59936) without Float Charging

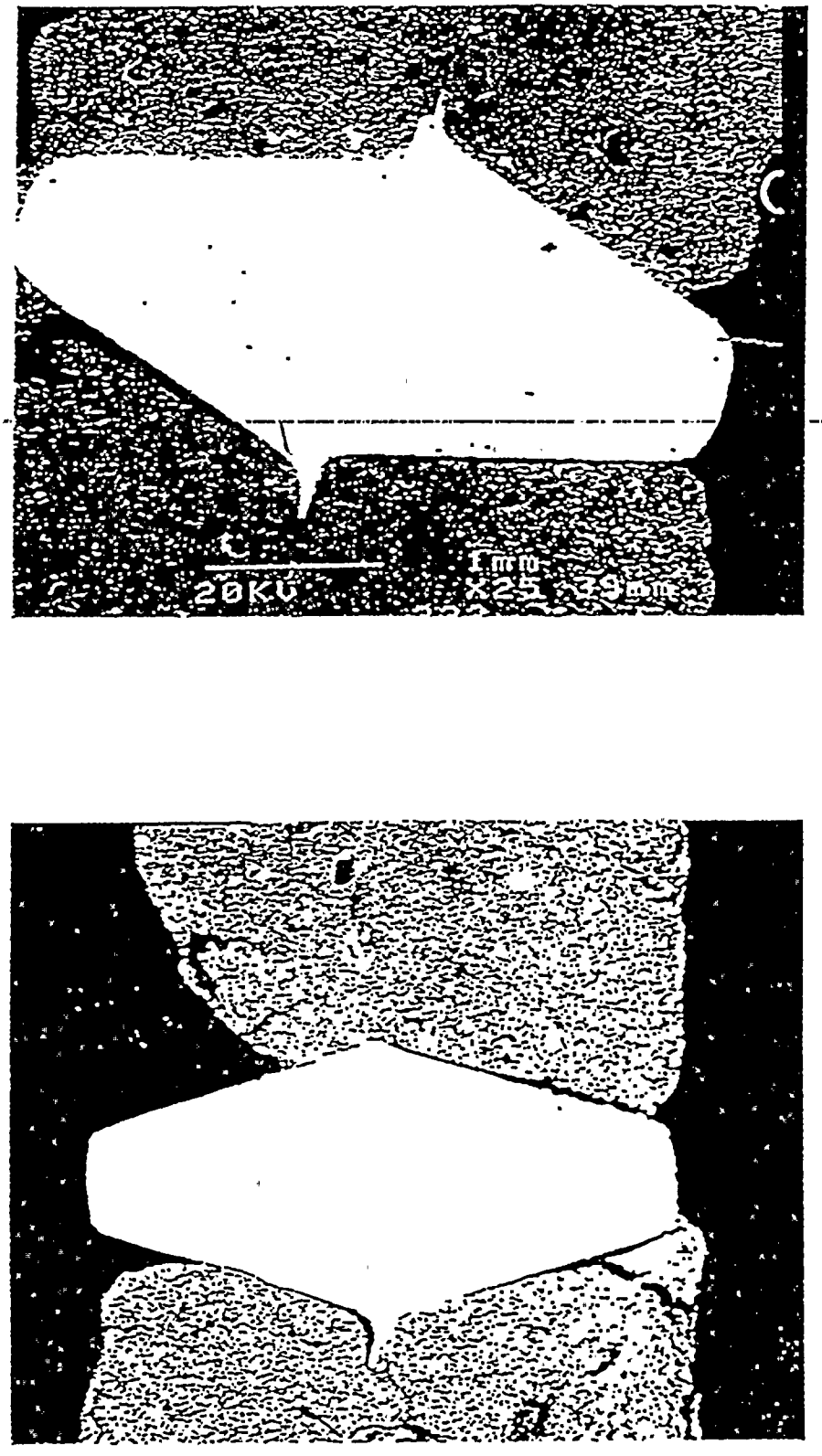

Fig. 15. Grid-to-Active-Material Contact for Properly Pasted (upper, cell 59942) and Underpasted (lower, cell 76712) Negative Electrodes

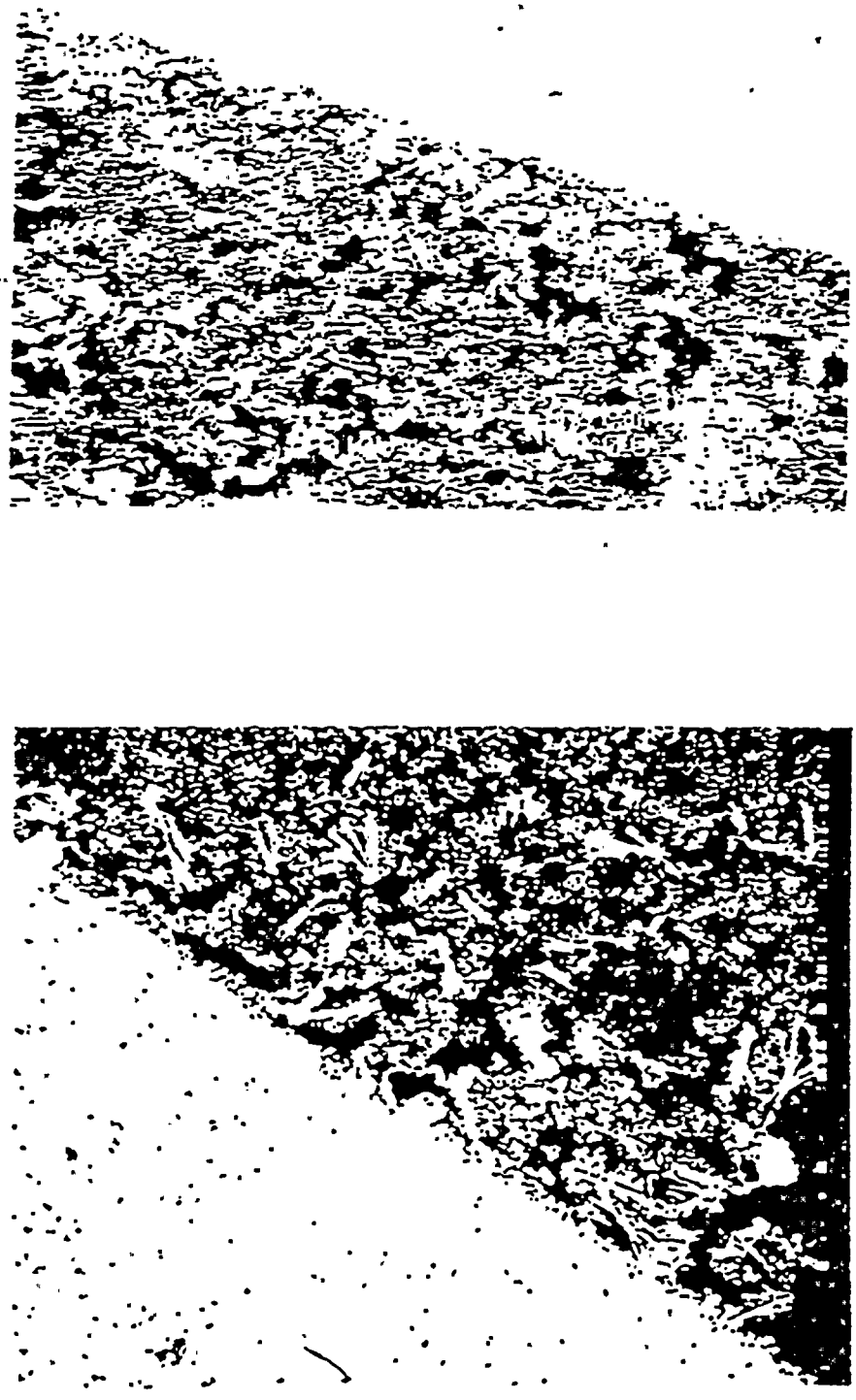

Fig. 16 Metallurgical Bond between the Negative Grid and Active Material (upper, cell 59936; lower, cell 59942)

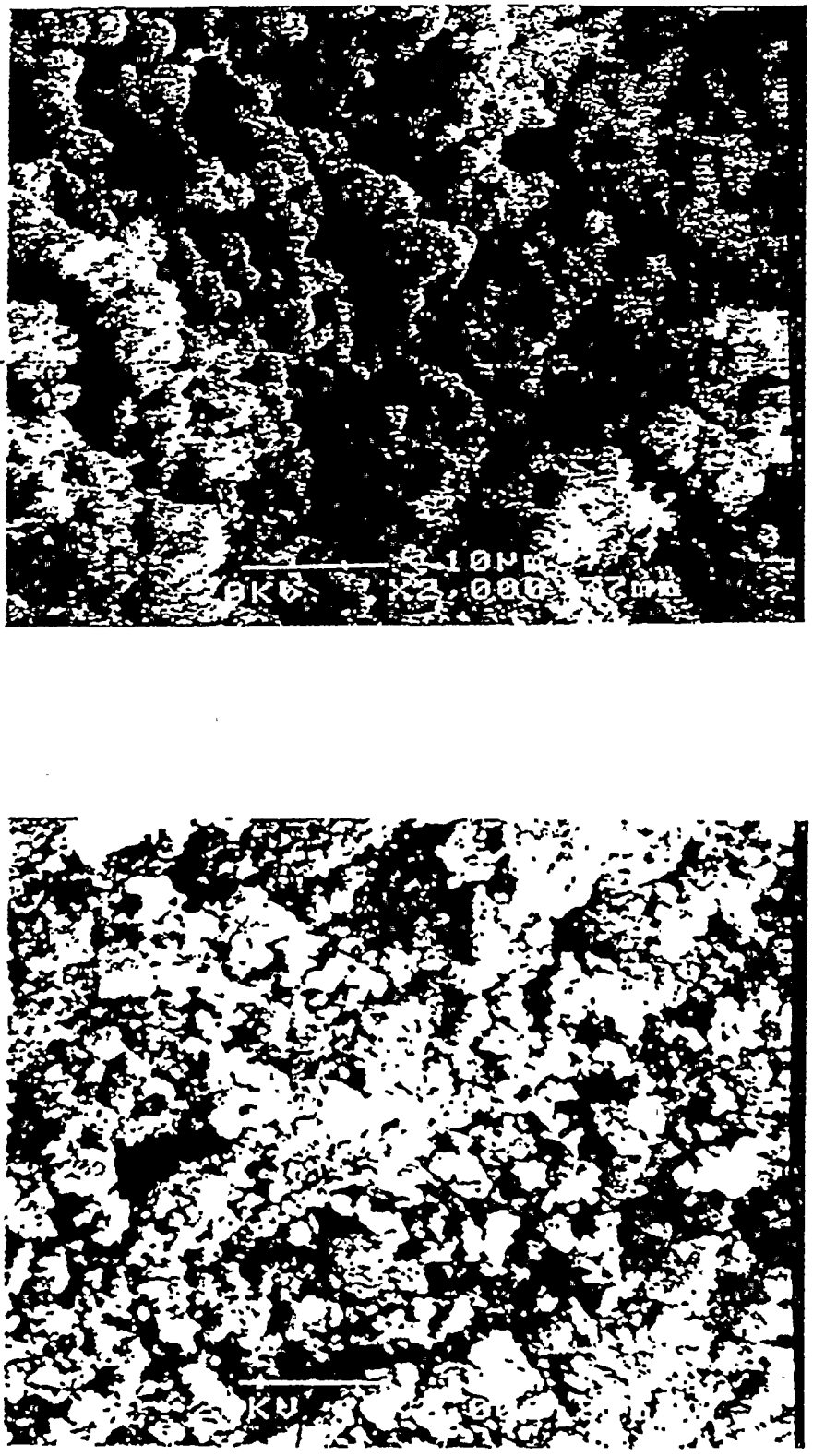

Fig. 17. Typical Microstructures of Positive-Electrode Interiors (upper, cell 74975; lower, cell 77773)

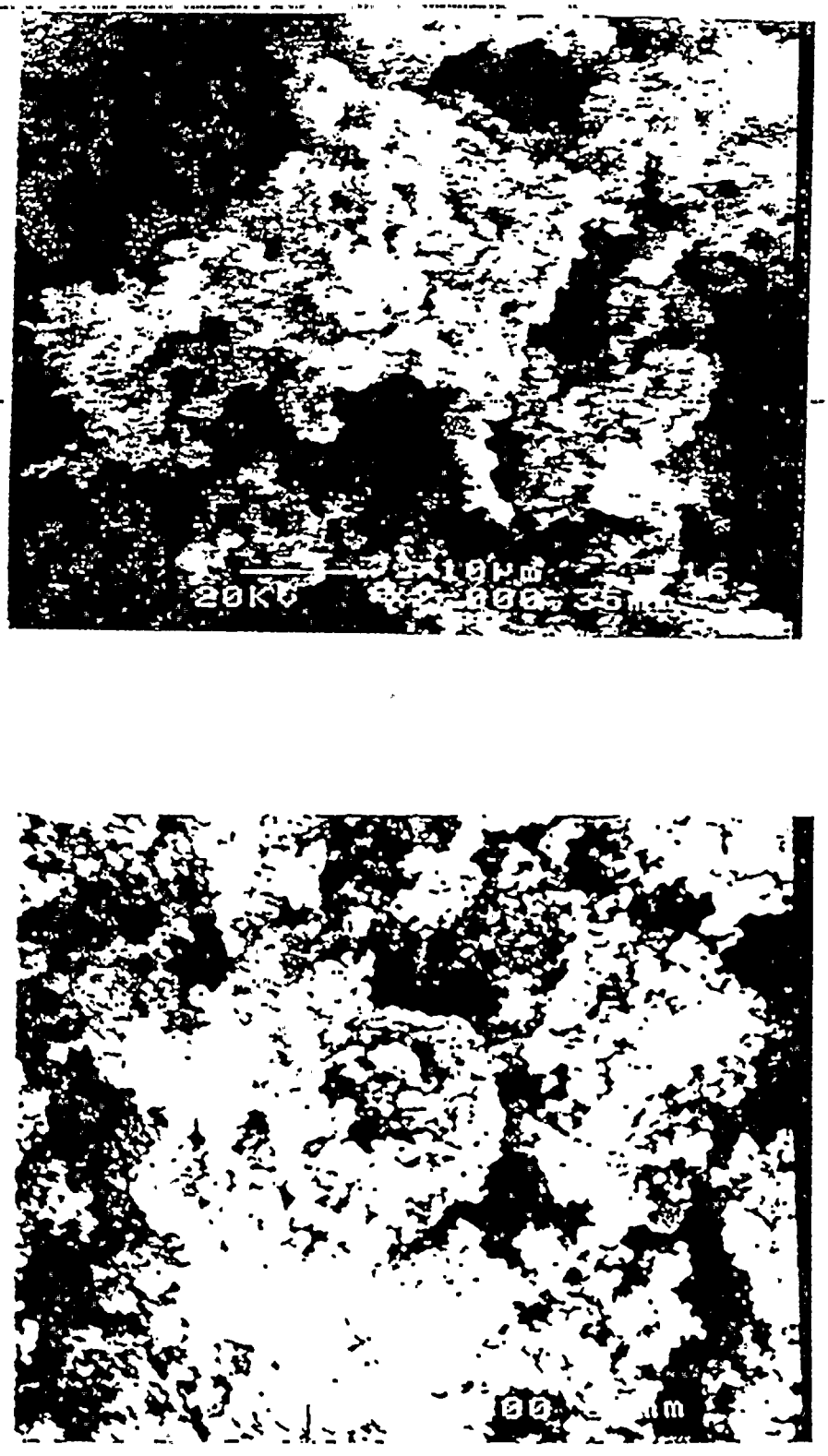

Fig. 18. Typical Microstructures of Positive-Electrode Surfaces (upper, cell 74975; lower, cell 77773)

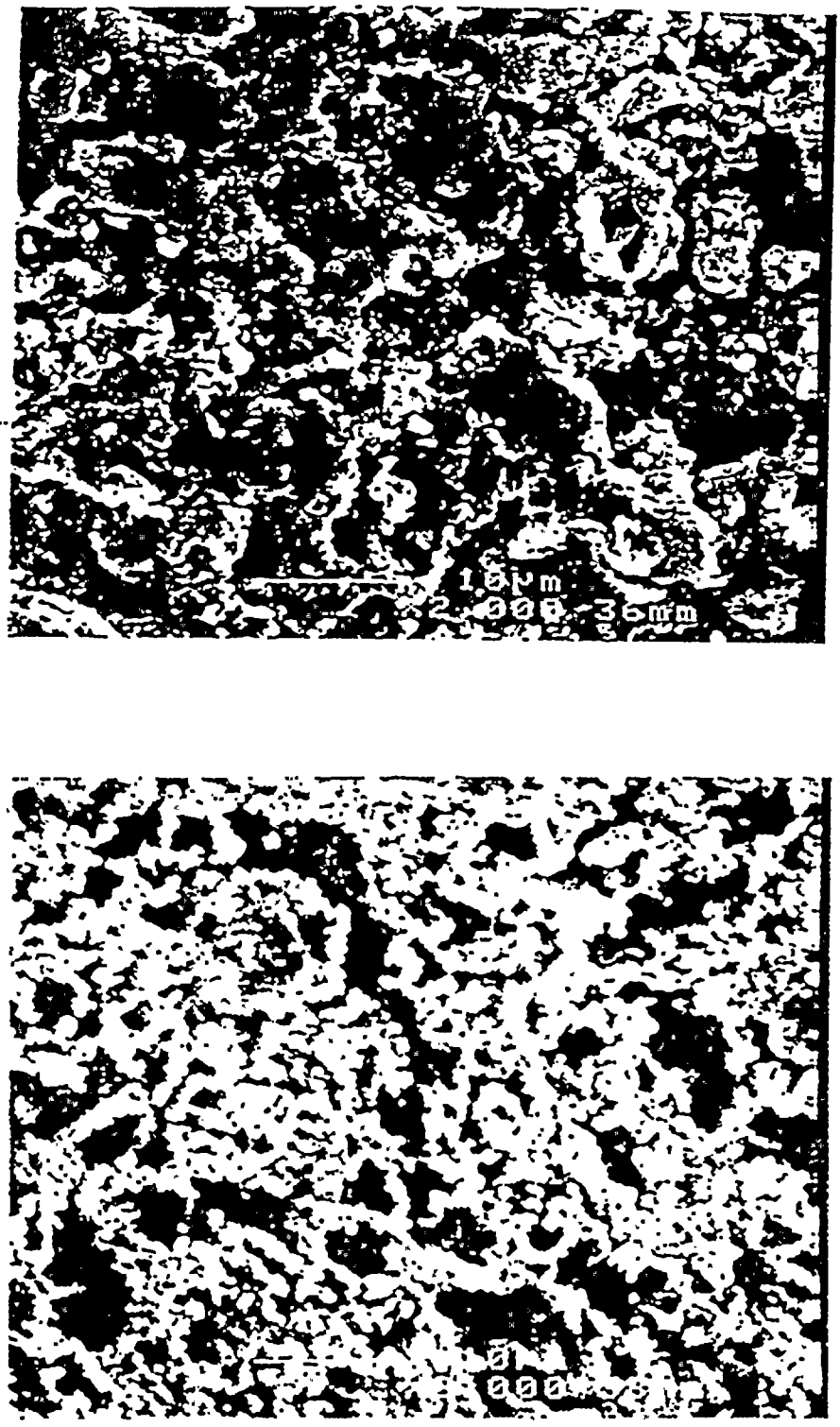

Fig. 15. Cross Sections for Cell 59941 Showing the Difference between Interior (upper) and Surface (lower) Morphology of Positive-Electrodes

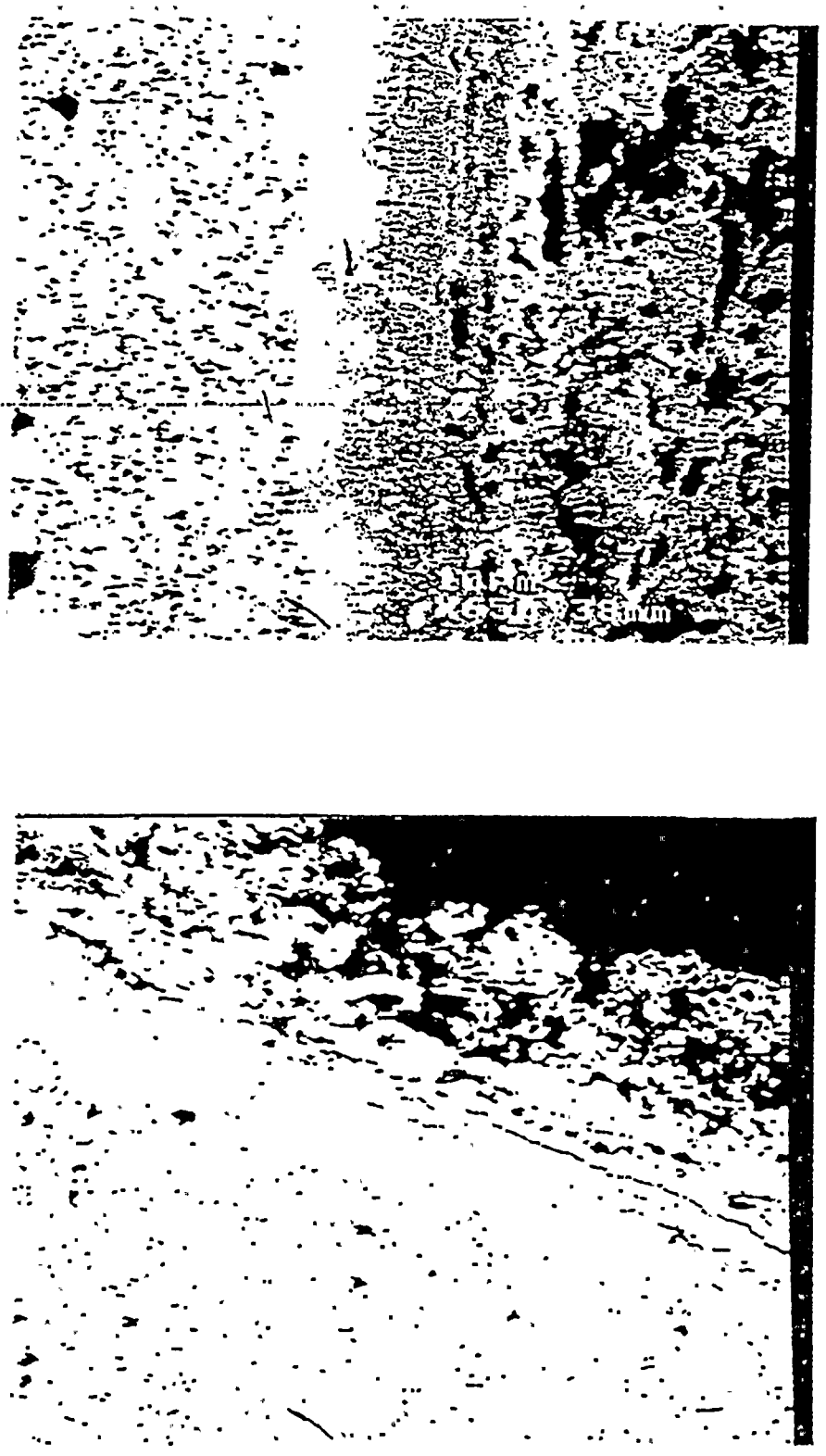

Fig. 20. Cross Sections from Cell 59942 Showing Dense PbO_2 Scale Formed on the Positive Grids

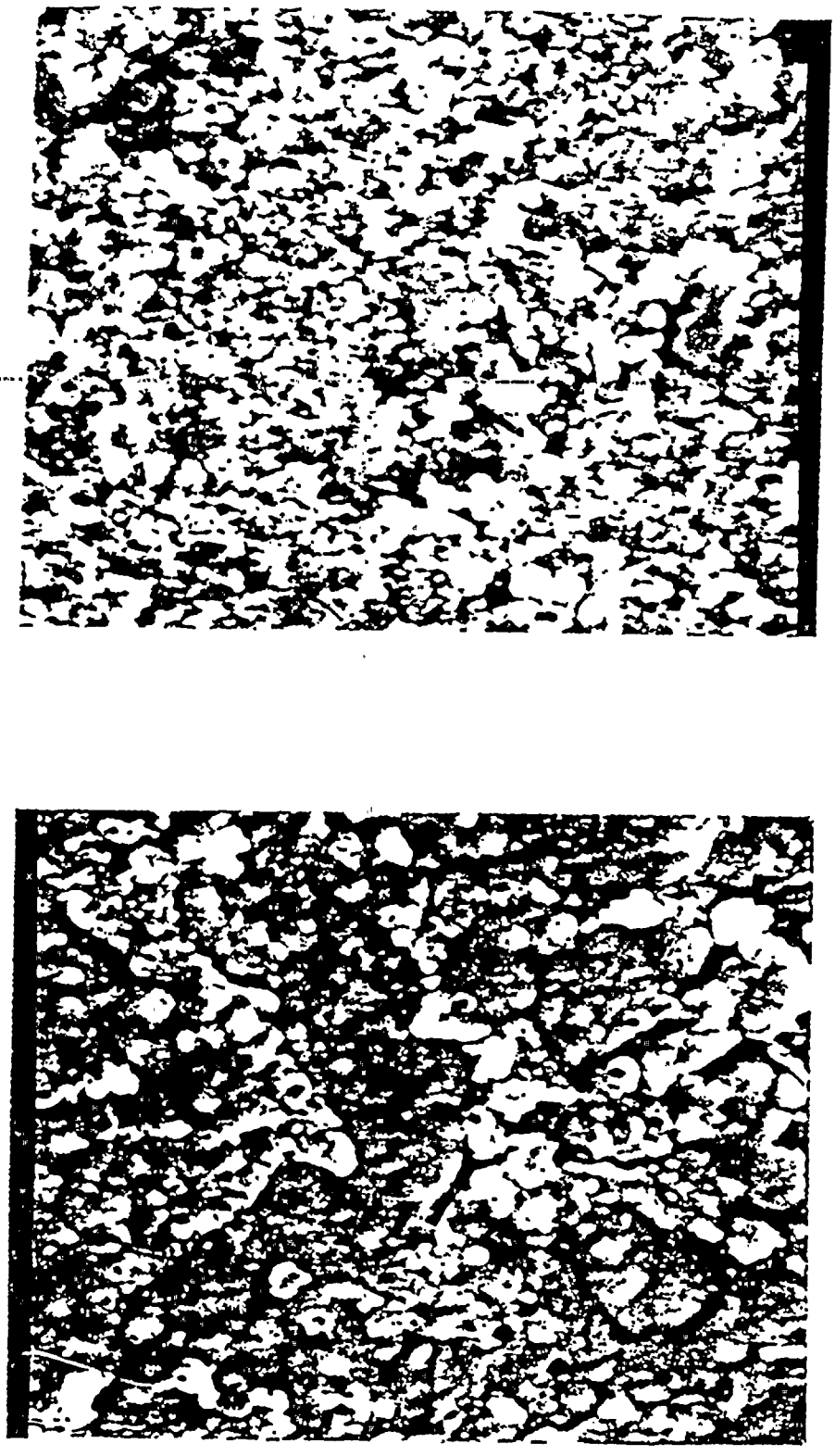

Fig. 21. Exterior Scale Surface (upper) and Exposed Substrate (lower) after Scale Removal for 59942 Grid Samples

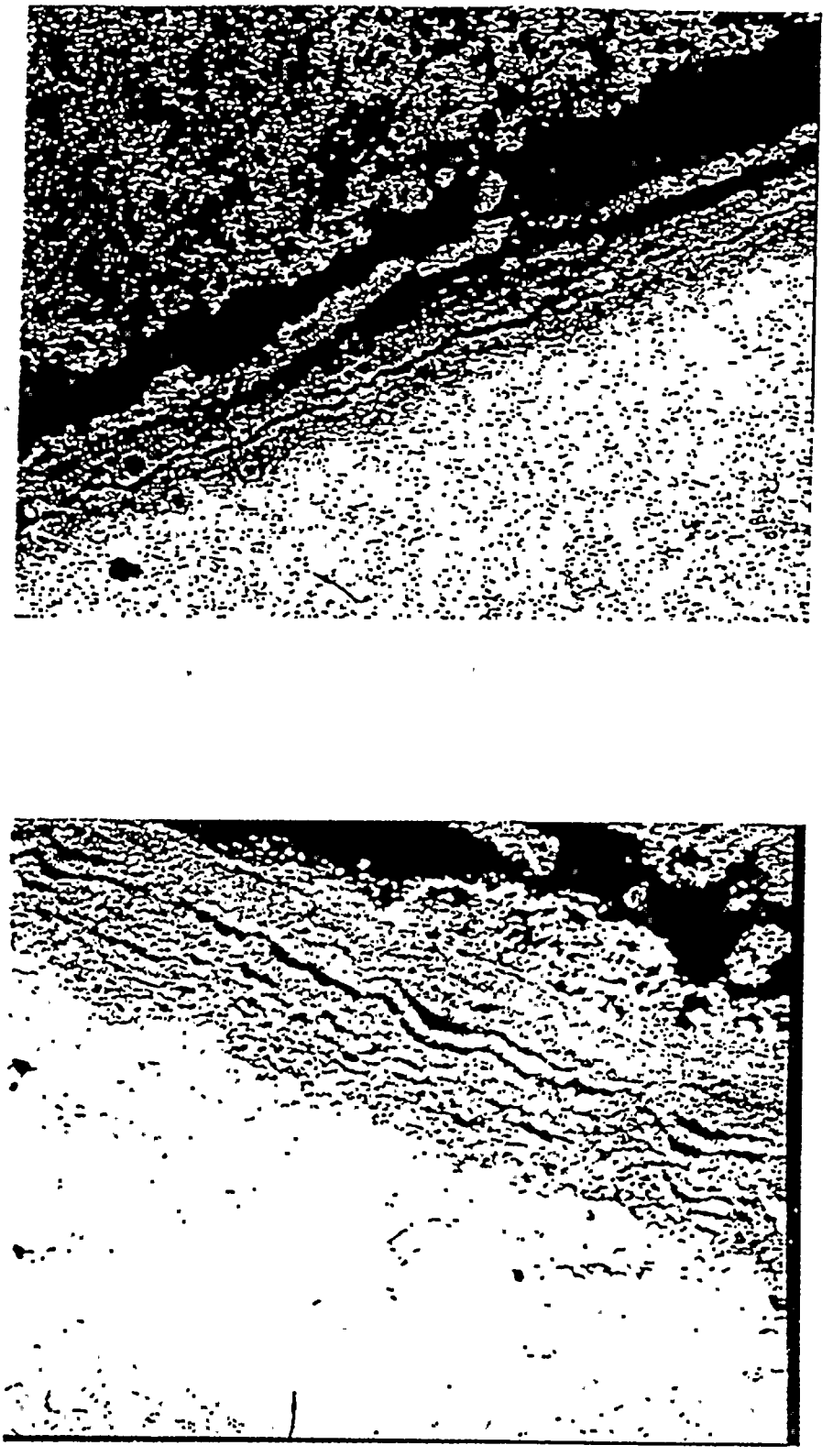

Fig. 22. Lateral Separations in the PbO_2 Scale for Positive Grids from Capacity-Loss Cells (upper, cell 59941; lower, cell 74975)

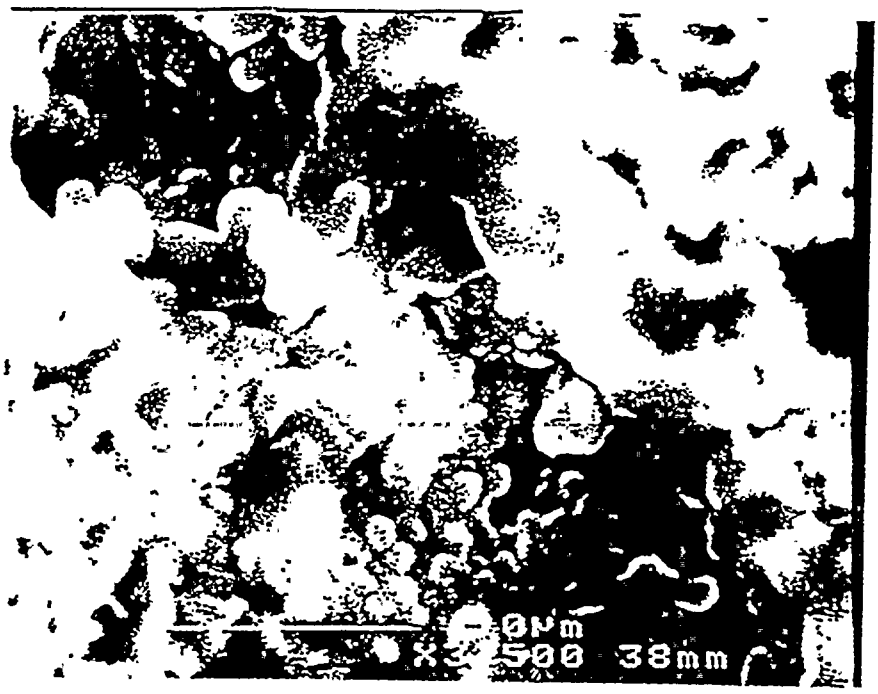

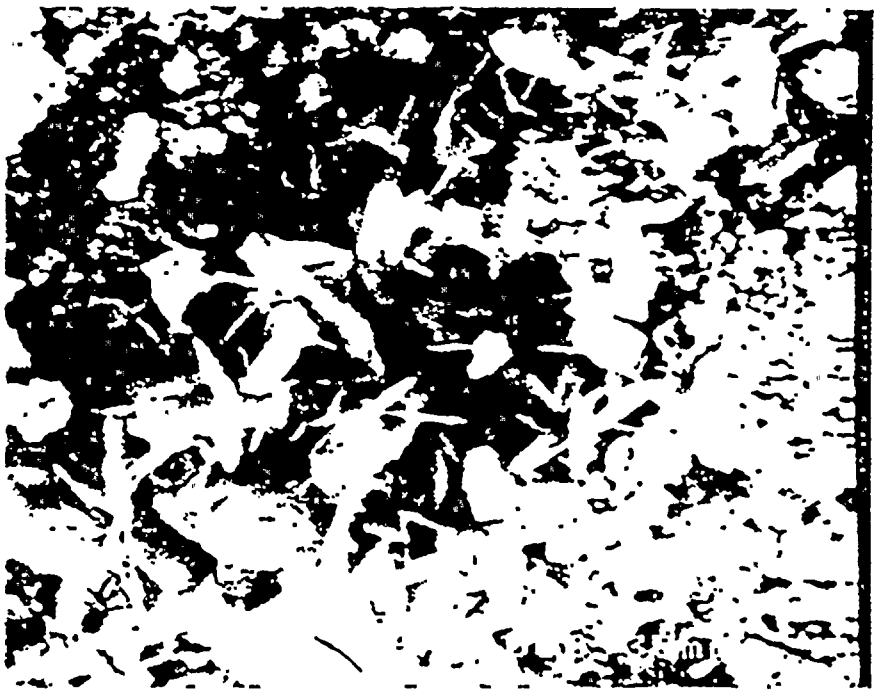

Fig. 23. Small, Disc-Shaped Crystals of $PbSO_4$ as Viewed within the Scale Separation (upper, cell 59941; lower, cell 76712)

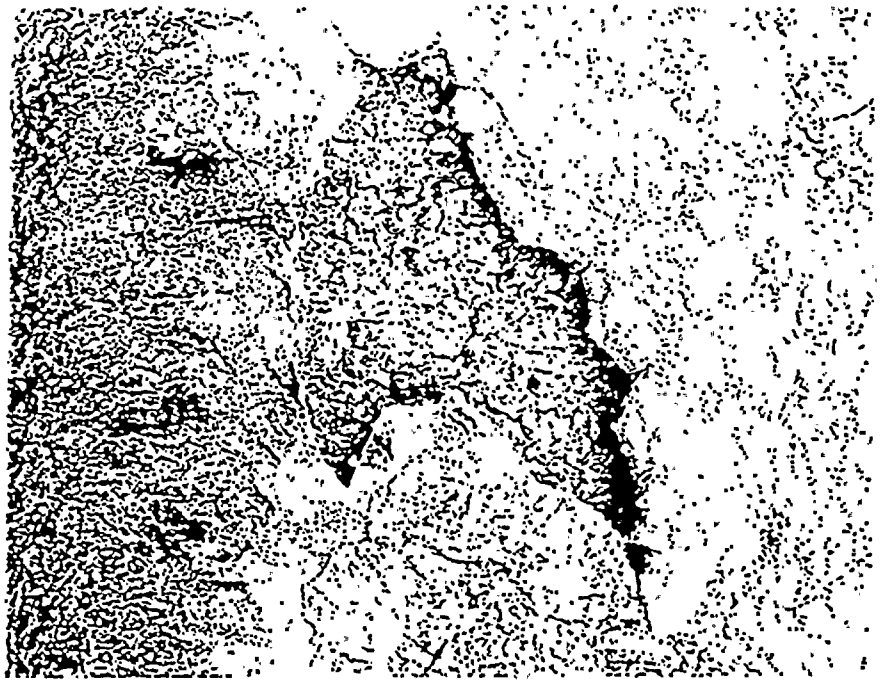

24. Exterior Surface of Scale (upper) with the Outer Scale Section Removal to Reveal $PbSO_4$ Crystals (lower) Embedded in Scale Separation of Cell 77773

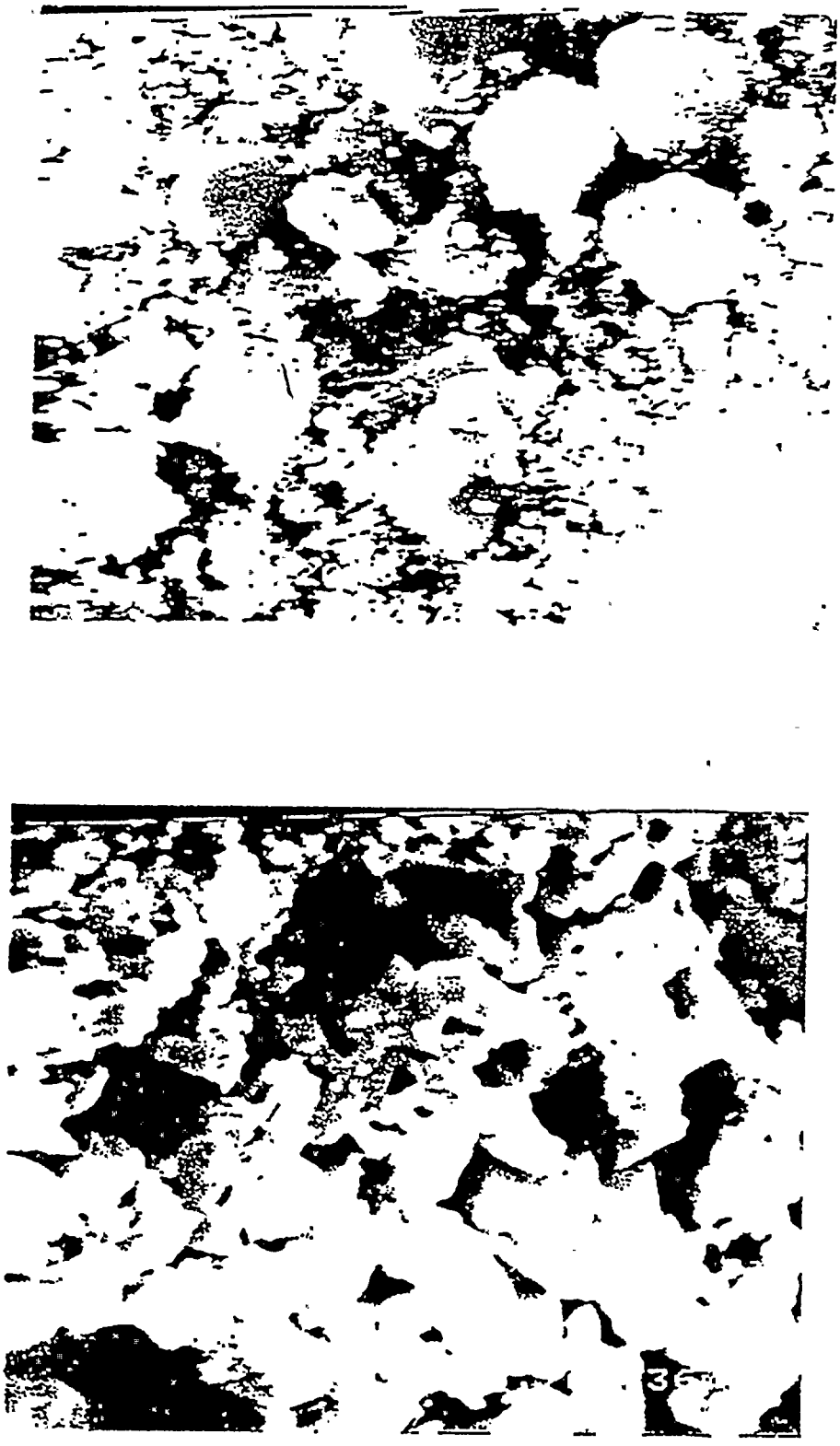

Fig. 25. Rounded (upper) and Plate-like $PbSO_4$ Crystals in the Scale Separation of Cell 59936

APPENDIX 1

POST-TEST ANALYSIS WORKSHEETS

POST-TEST ANALYSIS OF AT&T ROUND LEAD-ACID BATTERY

DATE: 12/19/96

CELL ID: 59941	TOTAL HOURS ON CHARGE: 295	TEARDOWN DATE: 7/31/96

GENERAL OBSERVATIONS:

Electrolyte: 3.5 gallons free electrolyte

Specific Gravity: Top : 1.298 Bottom : 1.302

Appearance: Top: Clear Bottom: Some black suspended particles

Positive Electrodes: Total 18 electrodes.

Dimension: Diameter (mm): #1 -- 317.2, 322.6 (with connector)
#18 -- 317.2, 323.3 (with connector)

Thickness (mm): #1 -- 6.0
#18 -- 6.0

Appearance: Black. Loose positive active-material was found on the electrode next to the connector. Surface active material washed away easily. #5 electrode had one pellet missing. More pellets fell off after the electrodes had been washed.

Negative Electrodes: Total 19 electrodes.

Dimension: Diameter (mm): #2 -- 292.6
#18 -- 292.6

Thickness (mm): #2 -- 5.0
#18 -- 4.6

Appearance: Gray. #6 electrode had one pellet missing. Blisters were found on the negative electrodes.

Separators: Excellent condition

Others:
1. Two dented areas (4 cm X 6.5 cm) were observed on the side of the cell. One located on the top half of the cell next to the positive connector, from 3rd positive to 6th positive electrode. The other located on the bottom half of the cell, from 12th electrode to 15th electrode.
2. Considerable amount of sediment was found on the bottom of the cell.
3. Burlap patterns were observed on face-up side of the positive electrodes and face-down side of negative electrodes.

POST-TEST ANALYSIS OF AT&T ROUND LEAD-ACID BATTERY

DATE: 12/19/96

CELL ID: 59941

ANALYTICAL SUBMISSIONS:

Electrolyte:

Top and bottom samples to SMAD
Bottom sample to ACL

Mercury Porosimetry:

4 samples to IGT

Others:

X-ray diffraction

SEM RESULTS:

Positive Electrodes: Samples collected from electrodes #1 and #18

1. Morphology change in the positive active material was found on the surface of the electrode.
2. All of the positive grids had an oxidized layer with cracks in the layer.
3. Small $PbSO_4$ crystals formed at grid/active material interface.

Negative Electrodes: Samples collected from electrodes #2 and #18

1. Minor oxidation of the active material occurred on the surface of the electrode. The particle morphology for the active material located in the center of the electrodes was normal.
2. The interface between the grid and the active material was in excellent condition. Neither corrosion layer nor gap could be found.

POST-TEST ANALYSIS OF AT&T ROUND LEAD-ACID BATTERY

DATE: 12/19/96

CELL ID: 59942	TOTAL HOURS ON CHARGE: 295	TEARDOWN DATE: 8/2/96

GENERAL OBSERVATIONS:

Electrolyte: 3.5 gallons free electrolyte

Specific Gravity Top : 1.295 Bottom : 1.305

Appearance: Top: Clear Bottom: Clear

Positive Electrodes: Total 18 electrodes.

Dimension: Diameter (mm): #1 -- 317.8, 323.3 (with connector)
#18 -- 318.0, 324.1 (with connector)

Thickness (mm): #1 -- 6.6
#18 -- 6.5

Appearance: Black. Bent radial grid elements and loss of contact between the pellets and the grid were found on all the electrodes. Loss of active material was also found on the outer edge of some of the plates.

Negative Electrodes: Total 19 electrodes.

Dimension: Diameter (mm): # 2 -- 292.4
#18 -- 292.6

Thickness (mm): # 2 -- 4.7
#18 -- 4.6

Appearance: Gray. Missing active material was observed on the surface of the electrodes next to the grid. Large blisters were also found on the surface of the electrodes.

Separators: Excellent condition

Others:
1. Burlap pattern existed on the face-up side of positive electrodes and face-down side of negative electrodes (for all the electrodes).
2. Large flakes of positive active material were found in the sediment.
   The amount of sediment = 150.0 g.

POST-TEST ANALYSIS OF AT&T ROUNDE LEAD-ACID BATTERY

DATE: 12/19/96

CELL ID: 59942

ANALYTICAL SUBMISSIONS:

Electrolyte:

Top and bottom samples to SMAD
Bottom sample to ACL

Mercury Porosimetry:

4 samples to IGT

Others:

None

SEM RESULTS:

Positive Electrodes: Samples collected from electrodes #1 and #18

1. No noticeable change in particle morphology was observed
2. The oxidized layer around the grid was intact. In general, the adherence between the oxidized layer and the active mass was reasonably good. However, some weak connections between the grid and the active pellets were observed.

Negative Electrode: Samples collected from electrodes #2 and #18

1. No $PbSO_4$ exists in the negative active material.
2. The interface between the grid and the active-material was in excellent condition. Neither corrosion layer nor gap could be observed.

POST-TEST ANALYSIS OF AT&T ROUND LEAD-ACID BATTERY

DATE: 12/19/96

CELL ID: 76712	TOTAL HOURS ON CHARGE: 340	TEARDOWN DATE: 8/7/96

GENERAL OBSERVATIONS:

Electrolyte: 3.5 gallons free electrolyte

Specific Gravity Top : 1.304 Bottom : 1.308

Appearance: Top: Clear Bottom: Clear

Positive Electrodes: Total 18 electrodes.

Dimension: Diameter (mm): #1 -- 315.7, 323.3 (with connector)
#18 -- 317.5, 324.1 (with connector)

Thickness (mm): #1 -- 6.5
#18 -- 6.6

Appearance: Black. Pasting marks and missing pellets were found on some of the positive electrodes. Bent radial grid elements were also found on the electrode.

Negative Electrodes: Total 19 electrodes.

Dimension: Diameter (mm): # 2 -- 292.4
#18 -- 292.4

Thickness (mm): # 2 -- 4.9
#18 -- 4.7

Appearance: Gray. Negative electrodes had a rough surface. Pasting marks and large blisters were observed on some of the negative electrodes.

Separators: Excellent condition

Others:
1. Burlap pattern existed on the face-up side of positive electrodes and face-down side of negative electrodes (for all the electrodes).
2. 32 g of sediment was collected from the bottom of the cell.

POST-TEST ANALYSIS OF AT&T ROUND LEAD-ACID BATTERY

DATE: 12/19/96

CELL ID: 76712

ANALYTICAL SUBMISSIONS:

Electrolyte:

Top and bottom samples to SMAD

Mercury Porosimetry:

4 samples to IGT

Others:

None

SEM RESULTS:

Positive Electrode: Samples collected from electrodes #1 and #18

1. Small $PbSO_4$ crystals existed in the grid/active material interface.
2. Thick oxidized layer with cracks existed on the surface of all of the positive grids.
3. Change of active-material morphology occurred on the surface of the plates.

Negative Electrode: Samples collected from electrodes #2 and #18

SEM results indicated that the negative electrodes were in reasonably good condition. Grids were intact. The connections between the grid and the active-material were excellent. The morphology of the negative active material was normal.

POST-TEST ANALYSIS OF AT&T ROUND LEAD-ACID BATTERY

DATE: 12/19/96

CELL ID: 74975	TOTAL HOURS ON CHARGE: 435	TEARDOWN DATE: 8/12/96

GENERAL OBSERVATIONS:

Electrolyte: 3.5 gallons free electrolyte

Specific Gravity: Top : 1.304 Bottom : 1.306

Appearance: Top: Clear Bottom: Clear

Positive Electrodes: Total 18 electrodes.

Dimension: Diameter (mm): #1 -- 316.2, 324.6 (with connector)
#18 -- 316.7, 323.8 (with connector)

Thickness (mm): #1 -- 6.9
#18 -- 6.6

Appearance: Black. Cracks and loose active material were observed for these electrodes. Bent radial grid elements were also found on the outer edge of the plates.

Negative Electrodes: Total 19 electrodes

Dimension: Diameter (mm): # 2 -- 292.6
#18 -- 292.1

Thickness (mm): # 2 -- 4.5
#18 -- 4.5

Appearance: Gray. Negative electrodes had pasting marks and some rough surface areas. Missing active material was observed on the surface of the electrode next to the grid. Loose particles were found on #3 electrode

Separators: Excellent condition

Others:

1. Approximately 34 g of sediment was collected from the bottom of the cell.
2. All electrodes had burlap patterns on face-up side of the positive electrodes and face-down side of the negative electrodes.

POST-TEST ANALYSIS OF AT&T ROUND LEAD-ACID BATTERY

DATE: 12/19/96

CELL ID: 74975

ANALYTICAL SUBMISSIONS:

Electrolyte:

Top and bottom samples to SMAD

Mercury Porosimetry:

None

Others:

None

SEM RESULTS:

Positive Electrodes: Samples collected from electrodes #1 and #18

1. Small $PbSO_4$ crystals existed in the grid and active-material interface.
2. All of the positive grids had an oxidized layer with cracks.
3. Change of active-material morphology occurred on the surface of the plates.

Negative Electrodes: Samples collected from electrodes #2 and #18

1. Oxidization was found on the rough surface areas.
2. Rod-shaped crystals (binding material?) were observed in the center of the electrode.

POST-TEST ANALYSIS OF AT&T ROUND LEAD-ACID BATTERY

DATE: 12/19/96

CELL ID: 77773	TOTAL HOURS ON CHARGE: 435	TEARDOWN DATE: 8/14/96

GENERAL OBSERVATIONS:

Electrolyte: 3.5 gallons free electrolyte

Specific Gravity: Top : 1.303 Bottom : 1.304

Appearance: Top: Clear Bottom: Clear

Positive Electrodes: Total 18 electrodes.

Dimension: Diameter (mm): #1 -- 316.3, 323.3 (with connector)
#18 -- 316.7, 323.0 (with connector)

Thickness (mm): #1 -- 6.7
#18 -- 6.8

Appearance: Black. Positive electrodes had rough surfaces. Missing pellets were also observed on the outer edge of the plates

Negative Electrodes: Total 19 electrodes.

Dimension: Diameter (mm): #2 -- 293.7
#18 -- 294.1

Thickness (mm): #2 -- 4.6
#18 -- 4.7

Appearance: Gray. Blisters and dimples were found on the surface of most negative electrodes. Missing active material was observed on the surface of the electrode next to the grid. Two dents were also found on the side of the electrodes.

Separators: Excellent condition

Others:

1. 82.8 g of sediment was collected from the bottom of the cell.
2. All electrodes had burlap patterns on face-up side of the positive electrodes and face-down side of the negative electrodes.

POST-TEST ANALYSIS OF AT&T ROUND LEAD-ACID BATTERY

DATE: 12/19/96

CELL ID: 77773

ANALYTICAL SUBMISSIONS:

Electrolyte:

Top and bottom samples to SMAD
Bottom sample to ACL

Mercury Porosimetry:

None

Others:

None

SEM RESULTS:

Positive Electrodes: Samples collected from electrodes #1 and #18

1. Large $PbSO_4$ crystals existed in the grid and active-material interface.
2. All of the positive grids had an oxidized layer with cracks in the layers.
3. Change of active-material morphology occurred on the surface of the plates.

Negative Electrodes: Samples collected from electrodes #2 and #18

SEM results indicated that the negative electrodes were in reasonably good condition. Grids were intact. The connections between the grid and the active material were excellent. The morphology of the negative active material was normal

POST-TEST ANALYSIS OF AT&T ROUND LEAD-ACID BATTERY

DATE: 12/19/96

CELL ID: 59936	TOTAL HOURS ON CHARGE: 407.5	TEARDOWN DATE: 8/16/96

GENERAL OBSERVATIONS:

Electrolyte : 3.5 gallons free electrolyte

Specific Gravity: Top : 1.307 Bottom : 1.307

Appearance: Top: Clear Bottom: Clear

Positive Electrodes: Total 18 electrodes.

Dimension: Diameter (mm): #1 -- 316.7, 322.0 (with connector)
#18 -- 317.0, 324.0 (with connector)

Thickness (mm): #1 -- 6.5
#18 -- 6.6

Appearance: Black. Missing active material was observed on the face-down side of the electrodes (near the connector).

Negative Electrodes: Total 19 electrodes.

Dimension: Diameter (mm): #2 -- 293.8
#18 -- 293.3

Thickness (mm): #2 -- 4.6
#18 -- 4.6

Appearance: Gray. Blisters, dimples, and loss of active material were observed on the face-up side of the electrodes. Cracks were found on the face-down side of the electrodes.

Separators: Excellent condition

Others:

1. 104.3 g of sediment was collected from the bottom of the cell.
2. All electrodes had burlap patterns on face-up side of the positive electrodes and face-down side of the negative electrodes.

POST-TEST ANALYSIS OF AT&T ROUND LEAD-ACID BATTERY

DATE: 12/19/96

CELL ID: 59936

ANALYTICAL SUBMISSIONS:

Electrolyte:

... Top and Bottom samples to SMAD

Mercury Porosimetry:

None

Others:

None

SEM RESULTS:

Positive Electrode: Samples collected from electrodes #1 and #18

1. Thick oxidized layer with cracks existed on the surface of all of the positive grids.
2. Large $PbSO_4$ crystals existed in the grid/active material interface.
3. $PbSO_4$ crystal imprints were observed on the grid inner oxidized layer.
4. Change of active-material morphology occurred on the surface of the plates.

Negative Electrode: Samples collected from electrodes #2 and #18

SEM results indicated that the negative electrodes were in reasonably good condition. Grids were intact. The connections between the grid and the active material were excellent. The morphology of the negative active material was normal.

APPENDIX 2

IMPURITY ANALYSES FOR ELECTROLYTE SAMPLES

ANALYTICAL CHEMISTRY LABORATORY
Argonne National Laboratory
Argonne, IL 60439

ICP-AES Analysis Report

Spec. No.: 58527

Sample Material: Sulfuric Acid Solution (30-40%)

Submitted by: Jane Marr CMT/200 Date Received:09-10-96

Reporting Units: ug/mL Date Reported:09-18-96

ACL Number	Your Number	Al1	Ba	Ca2	Cd	Fe1	Mg2	Zn		
96-1053-01	59941-B	5.41	<0.02	13.6	0.05	5.18	4.91	0.72		
96-1053-02	59942-B	5.57	<0.02	13.0	0.12	5.29	4.92	0.69		
96-1053-03	77773-B	4.99	<0.02	11.8	1.43	6.22	4.35	0.31		

NOTE: Samples will be discarded one (1) month after date of report unless otherwise arranged. When making future inquiries regarding this work, you must reference OUR number(s) above. For further information about the results reported here, please call E. A. Huff at extension 2-3633.
Reference Number:

Estimated Accuracy:+/-10%

Copies To: J. Marr
D. Green
ACL Office

Analyst(s): E. Huff
D. Huff

Remarks: 1:5 dilutions were analyzed.

TABLE
BATTERY ELECTROLYTE
BRAIDWOOD STATION
AUGUST, 1996

	All results are listed as micrograms per gram (μg/g).						
Parameter	#59936 Top	#59936 Bottom	#59941 Top	#59941 Bottom	#59942 Top	#59942 Bottom	Fed. Specs. * O-S-801E CL. 3
Cadmium, Cd	<0.04	<0.04	<0.04	<0.04	0.08	0.08	Not Specified
Calcium, Ca	11.7	12.1	11.7	11.8	11.6	11.7	Not Specified
Chloride, Cl	1	<1	2	<1	2	<1	4
Copper, Cu	<0.02	<0.02	<0.02	<0.02	<0.02	<0.02	20
Iron, Fe	4.24	4.18	4.22	4.19	4.12	4.35	20
Manganese, Mn	<0.06	<0.06	<0.06	<0.06	<0.06	<0.06	0.08
Nickel, Ni	<0.2	<0.2	<0.2	<0.2	<0.2	<0.2	0.4
Platinum, Pt	<2	<2	<2	<2	<2	<2	Not Specified
Zinc, Zn	0.49	0.51	0.46	0.46	0.47	0.61	16
Parameter	#74975 Top	#74975 Bottom	#76712 Top	#76712 Bottom	#77773 Top	#77773 Bottom	Fed. Specs. * O-S-801E CL. 3
Cadmium, Cd	<0.04	<0.04	0.56	0.57	1.2	1.2	Not Specified
Calcium, Ca	10.9	11.1	10.9	10.5	10.2	10.1	Not Specified
Chloride, Cl	<1	<1	1	<1	<1	<1	4
Copper, Cu	<0.02	<0.02	<0.02	<0.02	<0.02	<0.02	20
Iron, Fe	5.65	5.66	5.15	5.22	5.21	5.40	20
Manganese, Mn	<0.06	<0.06	0.06	0.06	<0.06	<0.06	0.08
Nickel, Ni	<0.2	<0.2	<0.2	<0.2	<0.2	<0.2	0.4
Platinum, Pt	<2	<2	<2	<2	<2	<2	Not Specified
Zinc, Zn	0.36	0.27	0.83	0.29	0.24	0.24	16

* For new electrolyte.

APPENDIX 3

DISCHARGE CURVES FOR THE AT&T ROUND CELLS

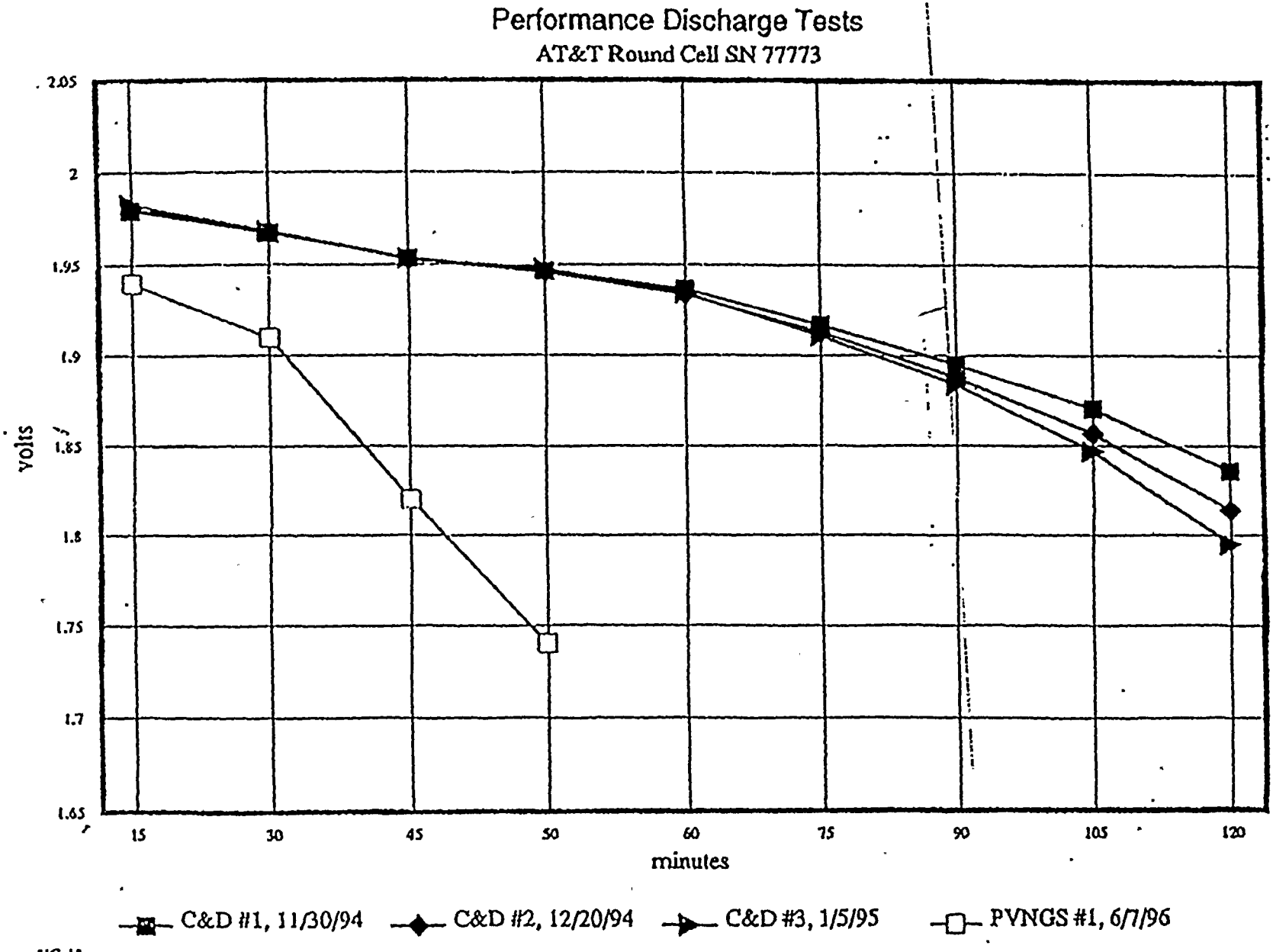
Performance Discharge Tests
AT&T Round Cell SN 77773
2.05
2
1.95
1.9
1.85
1.8
1.75
1.7
1.65
volts
15
30
45
50
60
75
90
105
120
minutes
C&D #1, 11/30/94
C&D #2, 12/20/94
C&D #3, 1/5/95
PVNGS #1, 6/7/96

HO-18

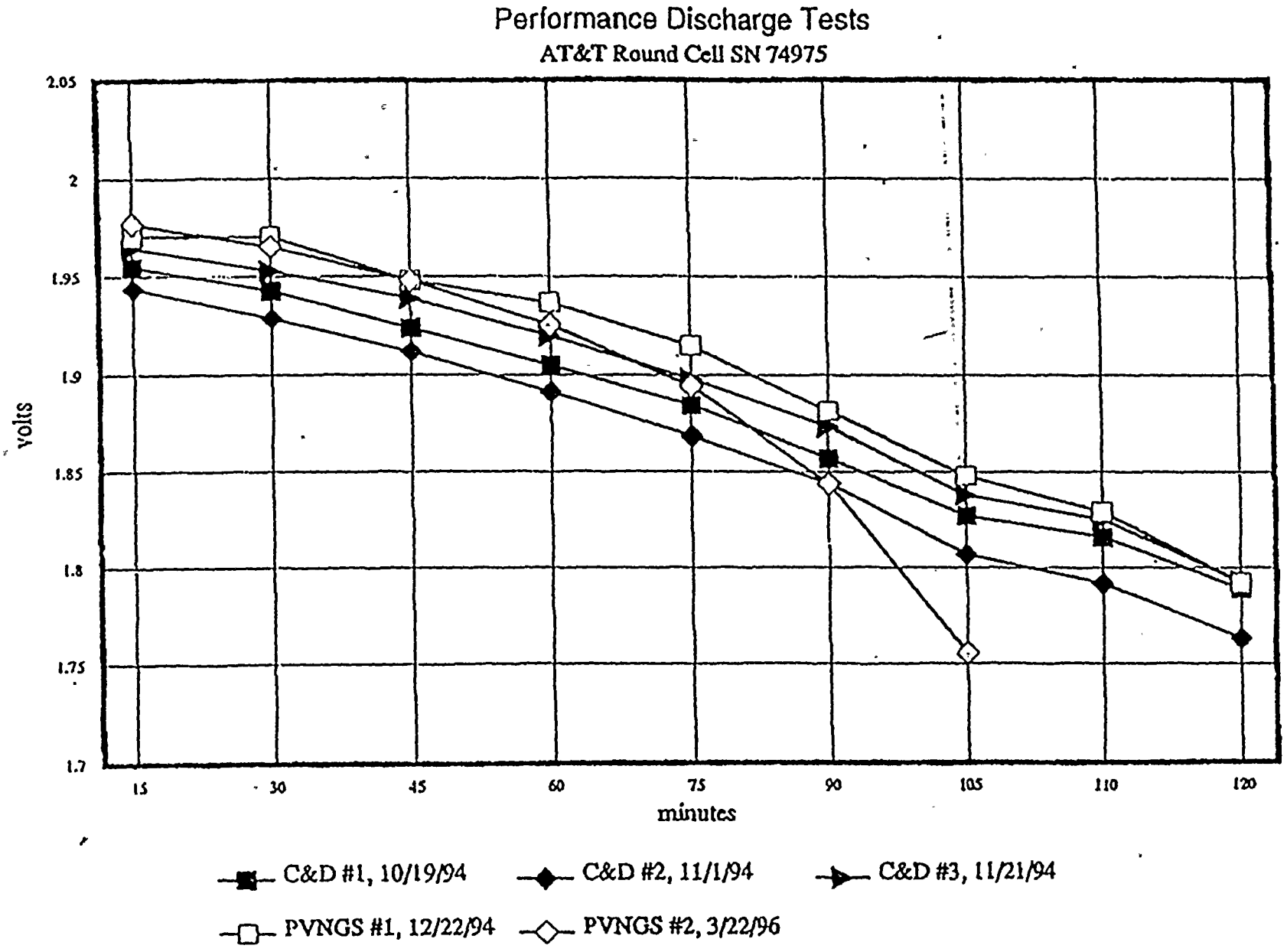
Performance Discharge Tests
AT&T Round Cell SN 74975
2.05
2
1.95
1.9
1.85
1.8
1.75
1.7
volts
15
30
45
60
75
90
105
110
120
minutes
C&D #1, 10/19/94
C&D #2, 11/1/94
C&D #3, 11/21/94
PVNGS #1, 12/22/94
PVNGS #2, 3/22/96

HG-14

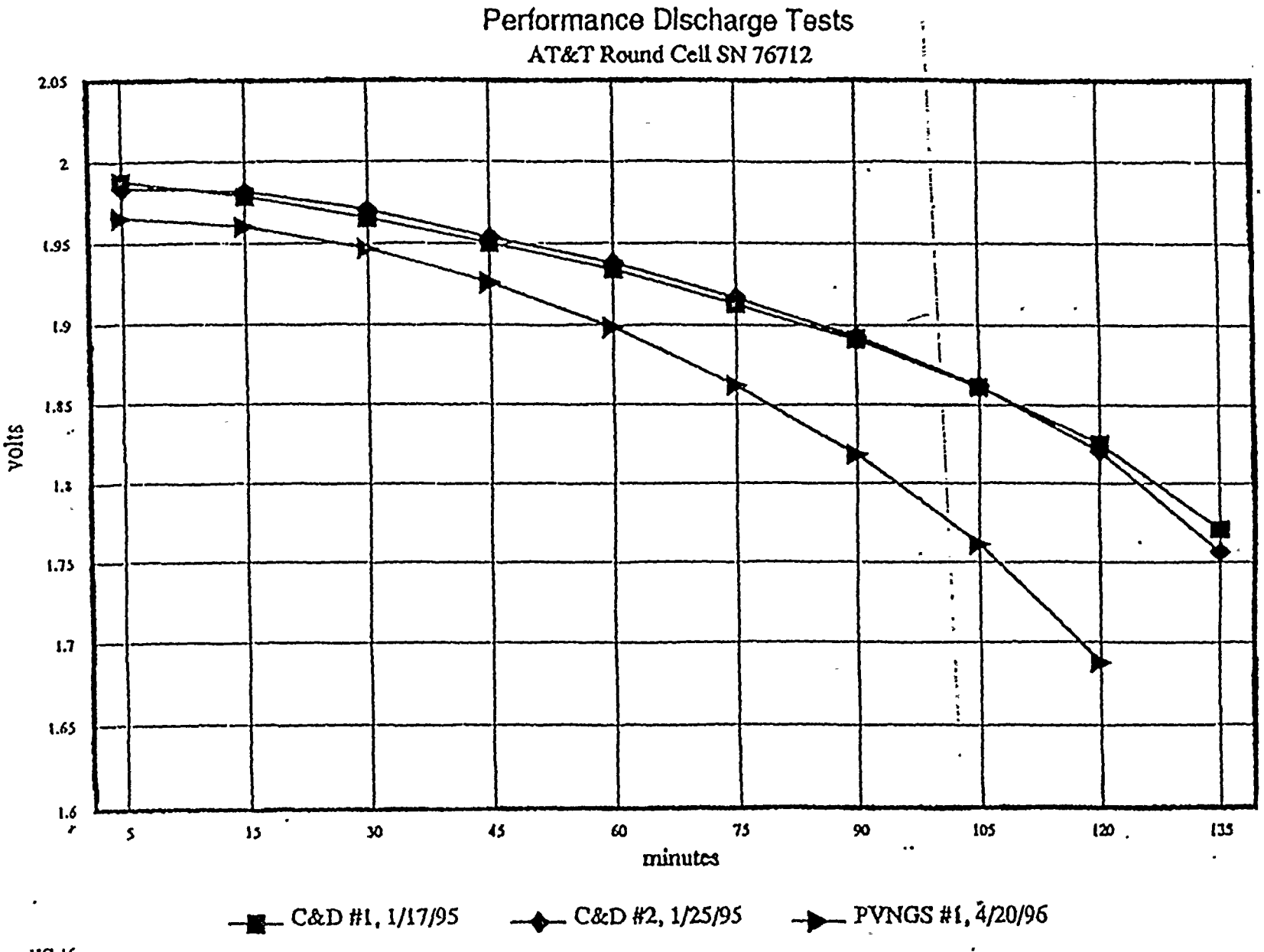
Performance Discharge Tests
AT&T Round Cell SN 76712
2.05
2
1.95
1.9
1.85
1.8
1.75
1.7
1.65
1.6
volts
5
15
30
45
60
75
90
105
120
135
minutes
C&D #1, 1/17/95
C&D #2, 1/25/95
PVNGS #1, 4/20/96

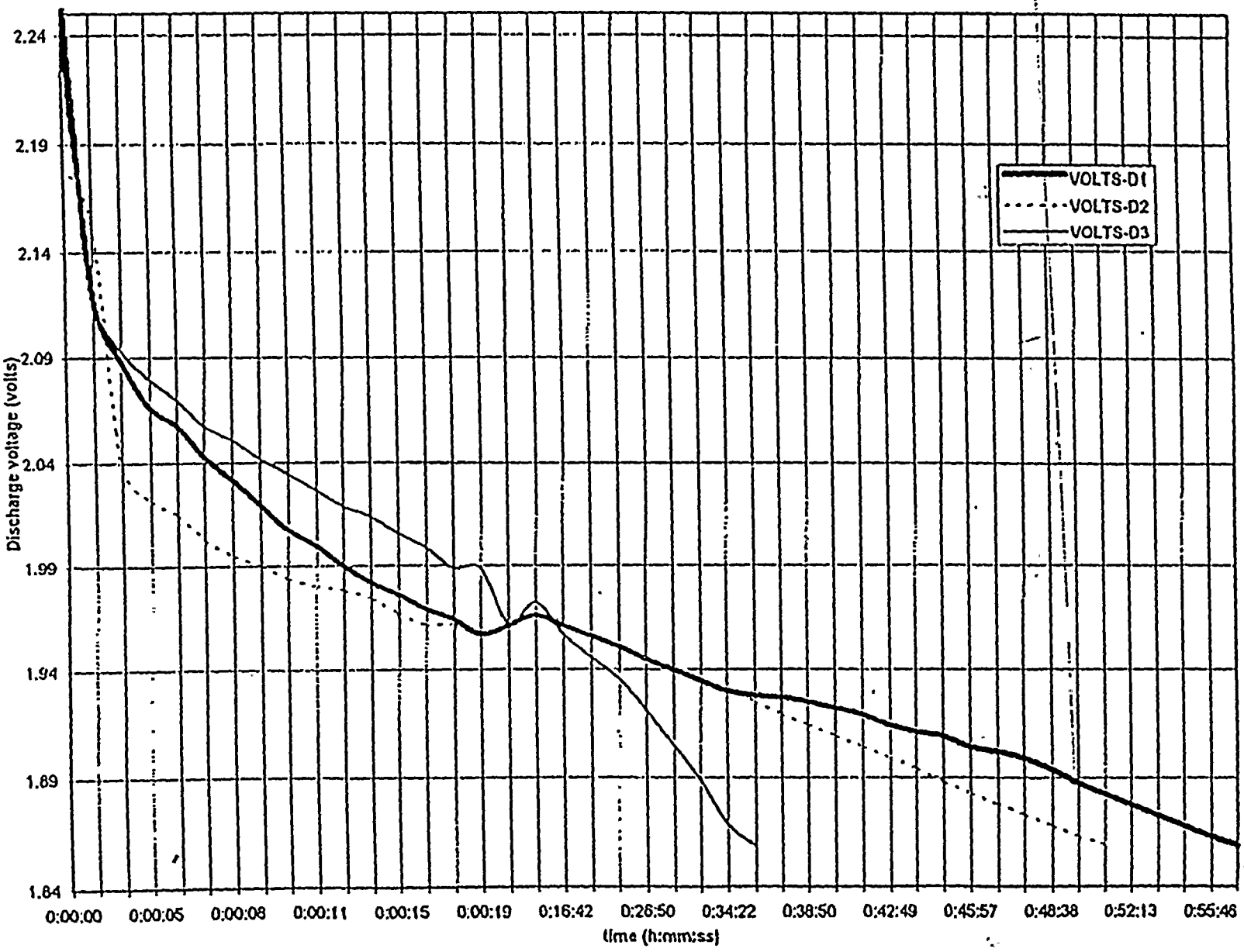
2.24
2.19
2.14
2.09
2.04
1.99
1.94
1.89
1.84
Discharge voltage (volts)
VOLTS-D1
VOLTS-D2
VOLTS-D3
0:00:00
0:00:05
0:00:08
0:00:11
0:00:15
0:00:19
0:16:42
0:26:50
0:34:22
0:38:50
0:42:49
0:45:57
0:48:38
0:52:13
0:55:46
time (h:mm:ss)

Sheet1 Chart 2

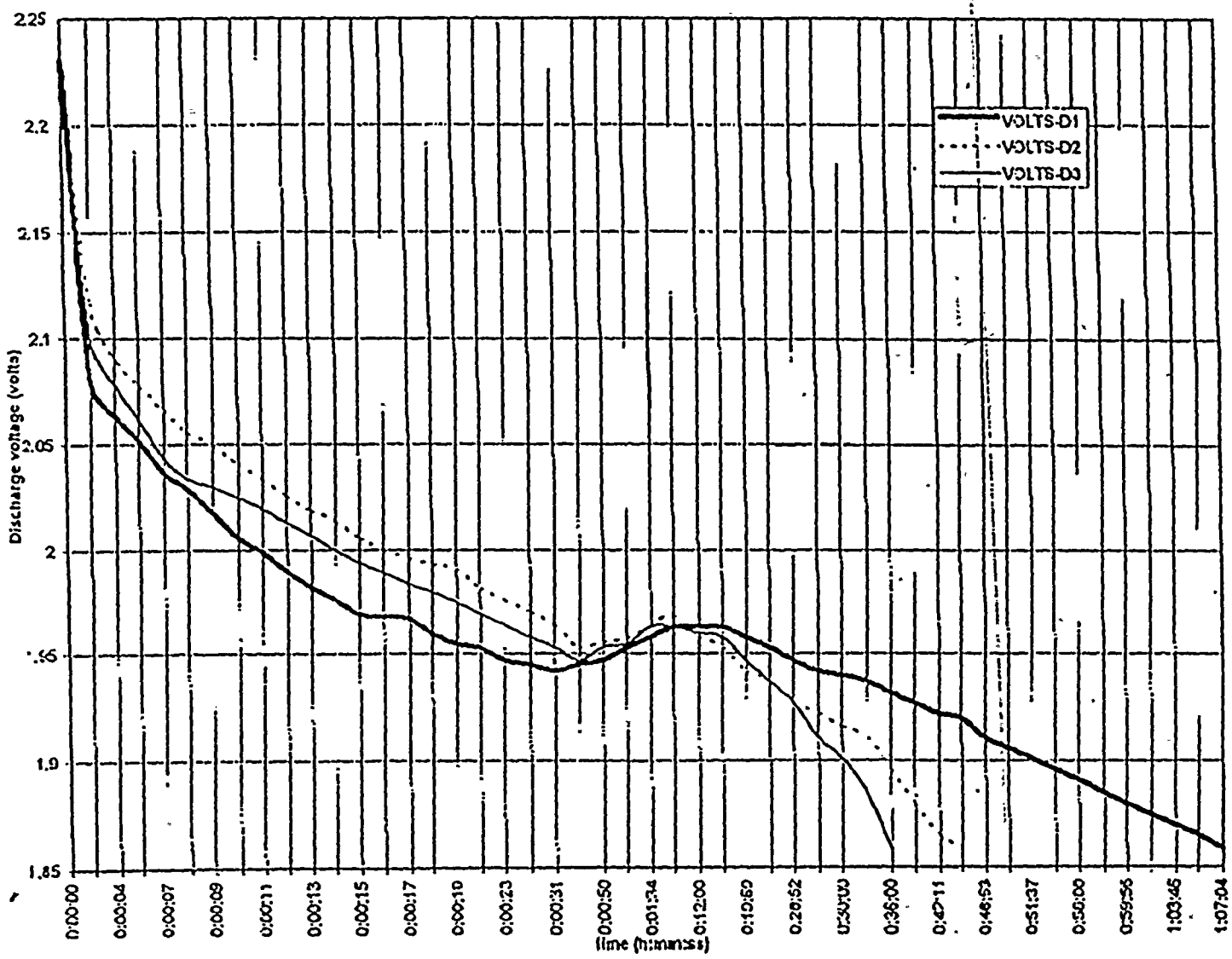

ATTACHMENT 2

PVNGS DISCHARGE TEST TABLES

UNIT 1

	C&D	C&D	PVNGS	PVNGS	PVNGS	PVNGS	# Service Tests	# Performance Tests
A	**104%** 1/7/92	Service Test 1/15/92	Service Test 3/92	**108.6%** 9/93 **(+4.4%)**	Service Test 4/95	Service Test 9/96	4	2
B	Service Test 2/5/92	**108%** 2/21/92 2nd Test	Service Test 4/92	**105.4%** 10/93 **(-2.4%)**	Service Test 4/95	Service Test 10/96	4	3
C	**103%** 1/7/92	Service Test 1/15/92	Service Test 3/92	**106%** 9/93 **(+2.9%)**	Service Test 4/95	Service Test 9/96	4	2
D	Service Test 2/5/92	**102.5%** 2/21/92 2nd Test **109.2%** (514A rate)	Service Test 4/92	**106.6%** 10/93 **113.6%** (514A rate) **(+4.0%)**	**107.4%** (514A rate) 4/95 **(-5.5%)**	Service Test 10/96	3	4

UNIT 3

	C&D	PVNGS	PVNGS	PVNGS	PVNGS	# Service Tests	# Perf. Tests
A	**107.5%** 9/92	Service Test 10/92	**105.6%** 4/94 **(-1.8%)**	Service Test 10/95	Service Test 3/97	3	2
B	**108.3%** 9/92	Service Test 10/92	**110.0%** 3/94 **(+1.6%)**	Service Test 10/95	Service Test 2/97	3	2
C	**106.7%** 9/92	Service Test 10/92	**109.2%** 4/94 **(+2.3%)**	Service Test 10/95	Service Test 3/97	3	2
D	**107.5%** 9/92	Service Test 10/92	**112.9%** 3/94 **(+5.0%)**	Service Test 10/95	Service Test 2/97	3	2

SPARES

	C&D		PVNGS	PVNGS	PVNGS	PVNGS	PVNGS	# Serv Tests	# Perf Tests
1-1	~104% 1/92	C&D Service Test 1/92	Service Test 3/92	106.0% 9/93 (+2)	108.8% 10/94 (+2.6)	Service Test 4/95	Service Test 9/96	4	3
1-2	~104% 1/92	C&D Service Test 1/92 .	Service Test 3/92	108.0% 9/93 (+4)	107.1% 10/94 (-.8)	Service Test 4/95	Service Test 9/96	4	3
1-3	~104% 1/92	C&D Service Test 1/92	Service Test 3/92	108.0% 9/93 (+4)	106.7% 10/94 (-1.2)	Service Test 4/95	Service Test 9/96	4	3
1-4	~104% 1/92	C&D Service Test 1/92	Service Test 3/92	107.5% 9/93 (+3.0)	107.1% 10/94 (-.4)	Service Test 4/95	Service Test 9/96	4	3
3-1	~108% 9/92	PV Service Test 10/92	104.2% 4/94 (-4.0)	107.9% 10/94 (+3.6)	Service Test 10/95	Service Test 3/97		3	3
3-2	~108% 9/92	PV Service Test 10/92	104.2% 4/94 (-4.0)	116.7% 10/94 (+12.0)	Service Test 10/95	Service Test 3/97		3	3
3-3	~108% 9/92	PV Service Test 10/92	104.2% 4/94 (-4.0)	108.7% 10/94 (+4.3)	Service Test 10/95	Service Test 3/97		3	3
3-4	~108% 9/92	PV Service Test 10/92	104.2% 4/94 (-4.0)	103.7% 9/94 (-.5)	Service Test 10/95	Service Test 3/97		3	3

Round Cell Charging Methods
Test Plan

Objectives:

After an inadvertent discharge on-line a question has been raised concerning the ability of the round cell to restore charge at float potential. This question was primarily raised due to C&D testing at Conshohocken where 100% return of charge could not be accomplished at float potential. In addition, events at Braidwood also seem to infer that full charge cannot be returned at float potential. After an inadvertent discharge on line at Braidwood of approximately 250Ahr's, full charge could not be achieved after an extended period of time on float.

Three possible operating scenarios have to be evaluated for on-line discharges.

1. **Amp-hours discharged are less than DBA margin.** For this case it has been shown that as long as sufficient capacities exist for the DBA profile, there is no safety significance to the discharge. Plants should assure that procedures are in-place for Operators to monitor discharge amps so that Engineers can determine remaining capacity of the battery.

2. **Amp-hours discharged are greater than DBA margin.** Battery will be declared inoperable and recharged using higher potential off-line methods.

3. **Multiple on-line shallow discharges.** Frequent cycling at high discharge rates has been shown to be degrading to high gravity round cells. Current theory asserts that this effect is consistent with the PCL (Premature Capacity Loss) model for antimony free batteries discussed in battery industry literature. The effect of multiple on-line discharges at lower rates more typical of normal plant DC load is not known. This is an issue with low and high gravity cells. It is believed that the PCL effect is more predominate for high gravity cells. Current testing seems to also support this. However testing that has been performed on cycling used a boost charge subsequent to each performance test. The effect of this boost charge may have been to recover capacity for low gravity cells. In any case, a boost charge could not be done on line at any plant. Engineers need to know charge return following normal on-line float charging techniques.

Hence the objective of the following test plan will be to determine charge recovery for low and high gravity cells following multiple shallow discharges. The purpose of this testing will be to assist the battery engineer in making operability determinations for the plant Class 1E batteries.

Test Details

Charge return at float after multiple inadvertent discharges. List 1S & 1SH cells

a) Test 10 cells at C&D -- Conshohocken
   Two low gravity old (production date 1991 or sooner) "good" cells
   Three high gravity new cells
   Three low gravity new cells
   Two high gravity cells from McGuire
b) Separate cells into 2 groups
   1 low gravity, 1 high gravity
c) Measure intercell connections (post to post)
   Acceptance criteria: ≤ 0.019 milliohms
d) Boost 24 hours @ 2.50 vpc
e) Float 7 days (minimum) 1/29/97
   High gravity - 2.25 vpc
   Low gravity - 2.20 vpc
f) Measure specific gravity and electrolyte level
   Temperature correct specific gravity and electrolyte level
   Specific gravity acceptance criteria:
      High gravity - 1.300 ± .005
      Low gravity - 1.215 ± .005
g) Performance test to establish baseline **2/19/97**
   Prior to discharge
      torque intercell and terminal connections
      measure specific gravity and electrolyte level
   High gravity - discharge @ 514 amps (temp corrected) to 1.75 vpc (2 hr rate)
   Verify discharge current (@ shunt) and string voltage (@ battery bank terminals) with DMM
   Measure intercell connections (post to post)
h) Performance test to establish baseline 2/12/97
   Low gravity - discharge @ 435 amps (temp corrected) to 1.75 vpc (2 hr rate)
   Verify discharge current (@ shunt) and string voltage (@ battery bank terminals) with DMM

i) Charge - constant potential (300 amp charger) 2/12/97(low gravity), **2/19/97(high gravity)**
High Gravity - 2.33 vpc, <10 amps / 2.7 vpc to 120%
Low Gravity - 2.29 vpc for 54 hours after the current stabilizes for three consecutive hourly readings

j) Measure specific gravity and electrolyte level 2/14/97(low gravity), **2/21/97(high gravity)**
Temperature correct specific gravity and electrolyte level

k) Float 7 days (minimum) 2/14/97(low gravity), **2/21/97(high gravity)**
High Gravity - 2.25 vpc
Low Gravity - 2.20 vpc

l) Measure specific gravity and electrolyte level 2/28/97
Temperature correct specific gravity and electrolyte level
Specific gravity acceptance criteria:
High gravity - 1.300 ± .005
Low gravity - 1.215 ± .005

m) Discharge 200 AHR's (2 hours @ 100 amps) **2/28/97 low and high gravity**
Strings may be combined for discharge
Measure intercell connections (post to post)
Acceptance criteria: ≤ 0.019 milliohms
Verify discharge current (@ shunt) and string voltage (@ battery bank terminals) with DMM

n) Place on float charge for 72 hours 2/28/97

o) Repeat steps m and n **three additional** times 3/3/97, 3/6/97, 3/9/97

p) Measure specific gravity and electrolyte level 3/12/97
Temperature correct specific gravity and electrolyte level

q) Measure intercell connections (post to post) 3/12/97
Acceptance criteria: ≤ 0.019 milliohms

r) Performance test 3/12/97
High gravity - discharge @ 514 amps (temp corrected) to 1.75 vpc (2 hr rate)
Verify discharge current (@ shunt) and string voltage (@ battery bank terminals) with DMM

s) Performance test 3/12/97
Low gravity - discharge @ 435 amps (temp corrected) to 1.75 vpc (2 hr rate)
Verify discharge current (@ shunt) and string voltage (@ battery bank terminals) with DMM

t) Charge - constant potential (300 amp charger) 3/12/97
High Gravity - 2.33 vpc, <10 amps / 2.7 vpc to 120%
Low Gravity - 2.29 vpc for 54 hours after the current stabilizes for three consecutive hourly readings

u) Place cells on float charge 3/14/97

Round Cell Multiple C[illegible]e Shallow Discharges

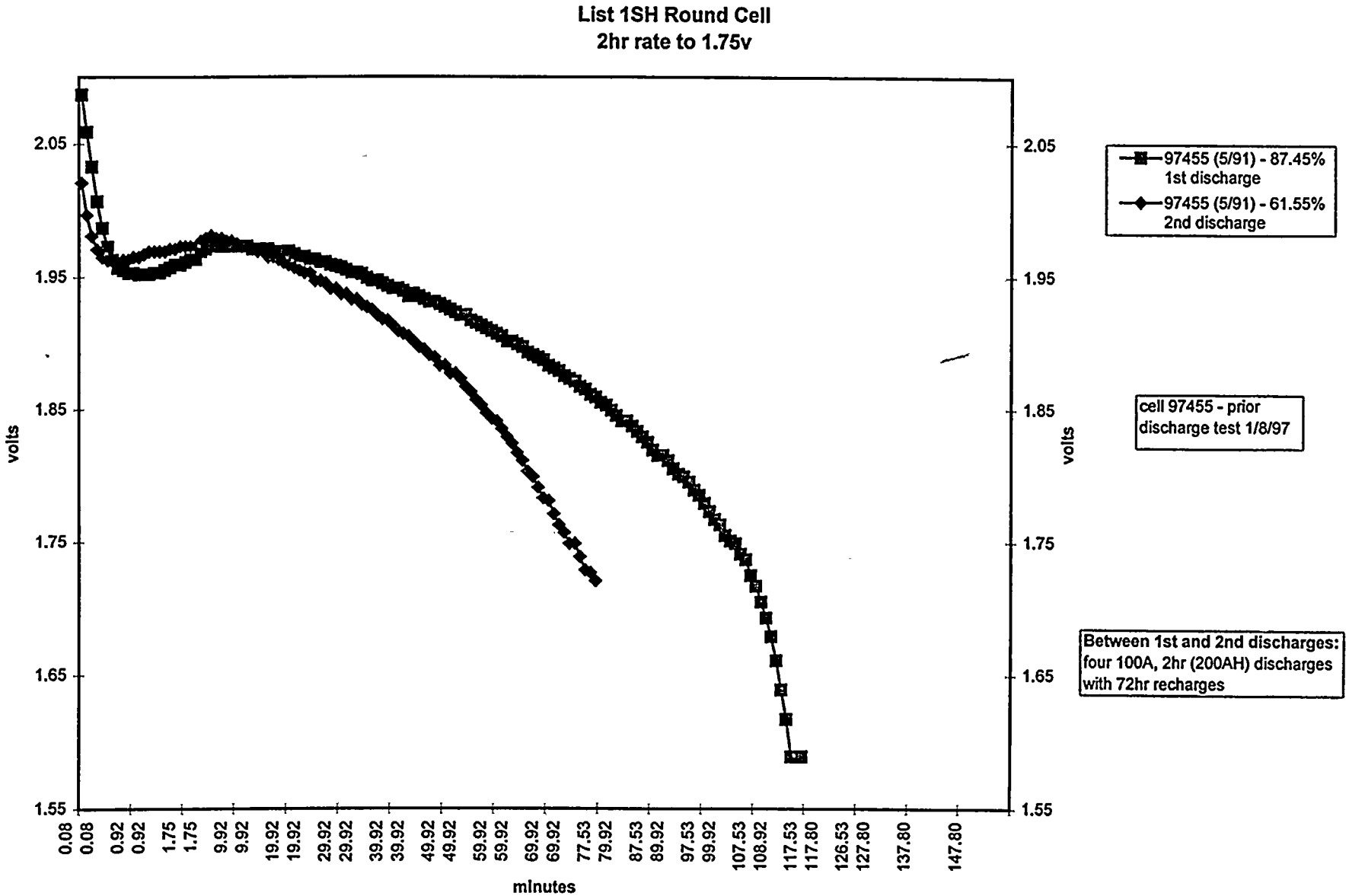

1st discharge 2/19/97
2nd discharge 3/12/97

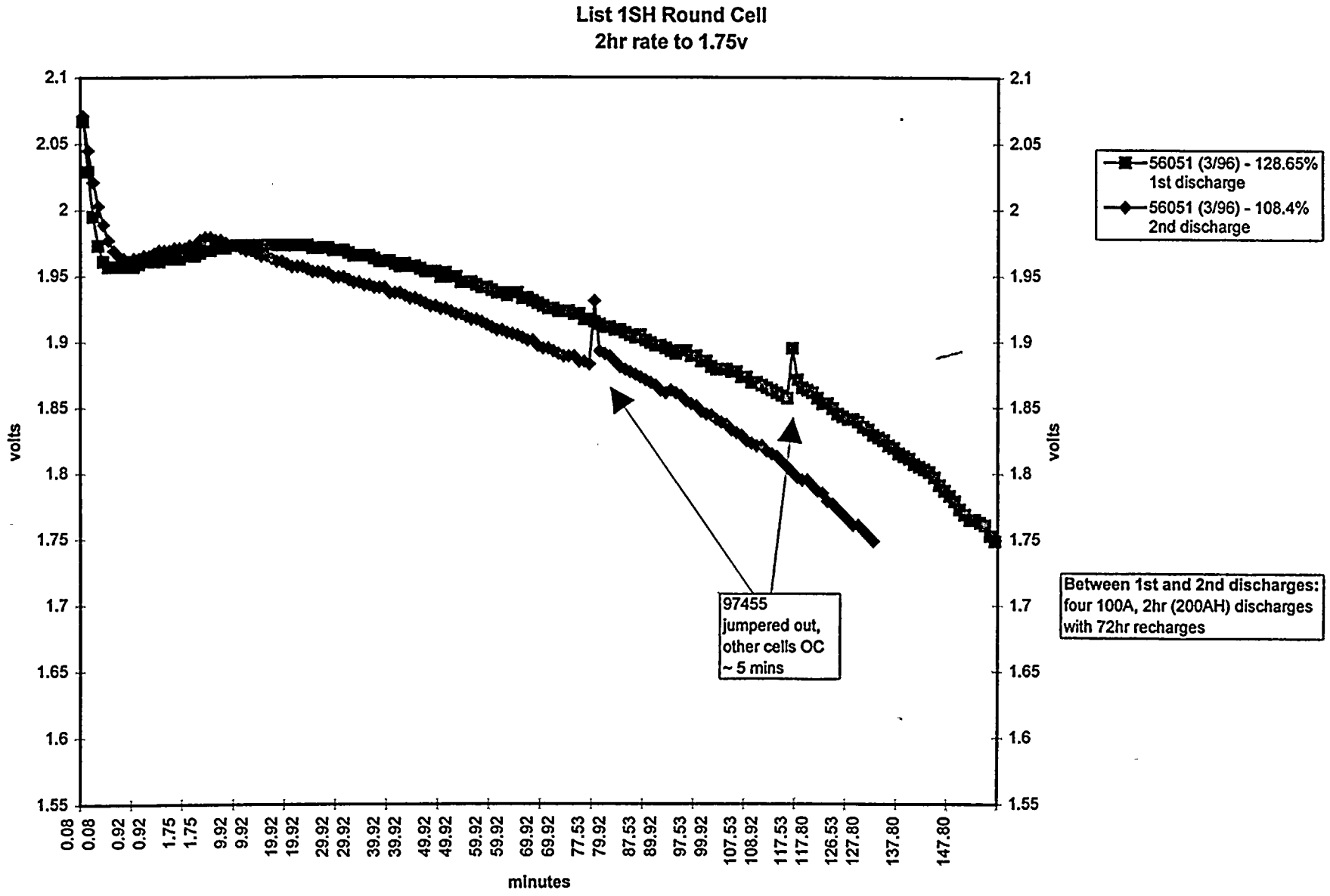

1st discharge 2/19/97
2nd discharge 3/12/97

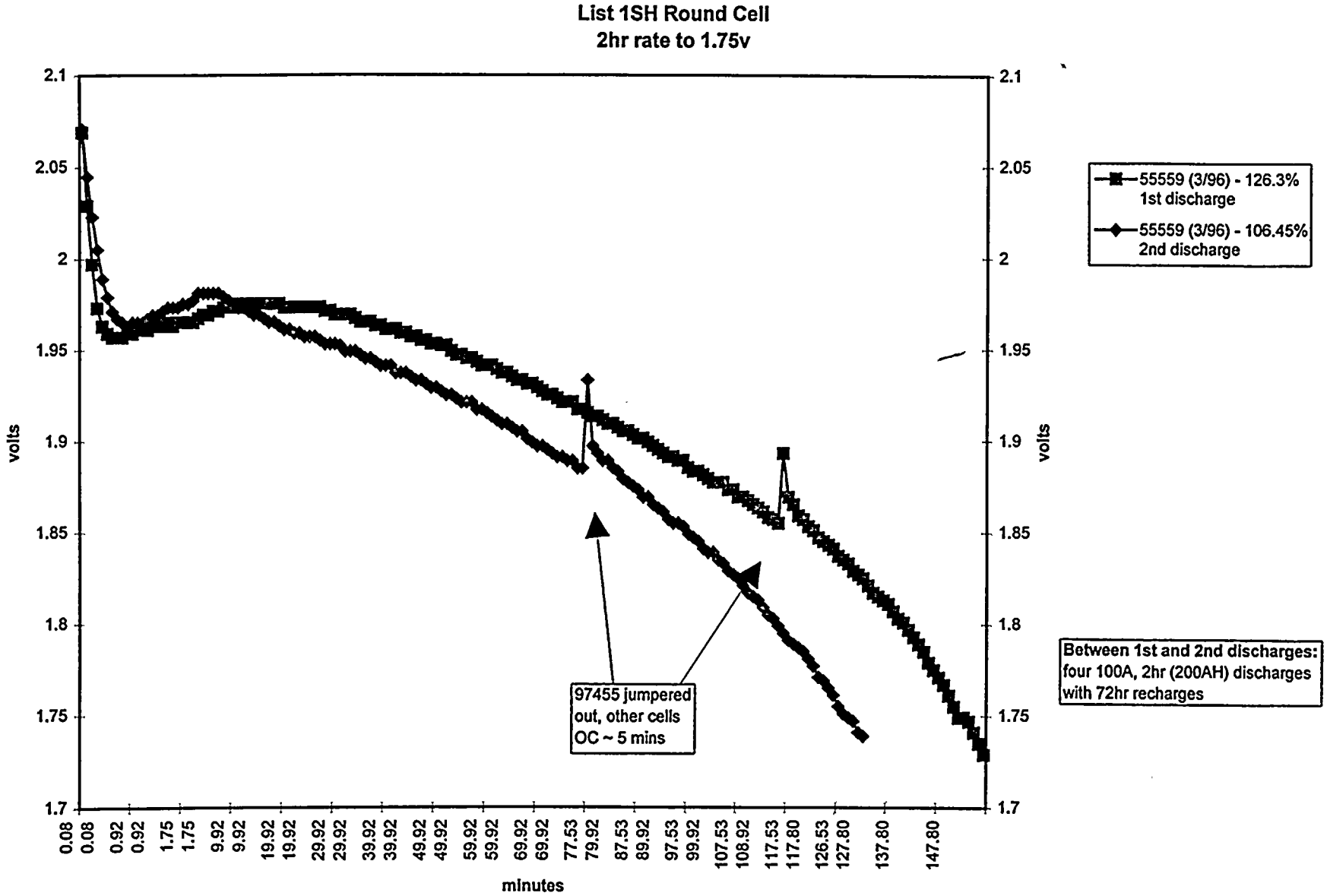

1st discharge 2/19/97
2nd discharge 3/12/97

Round Cell Multiple C[illegible]ne Shallow Discharges

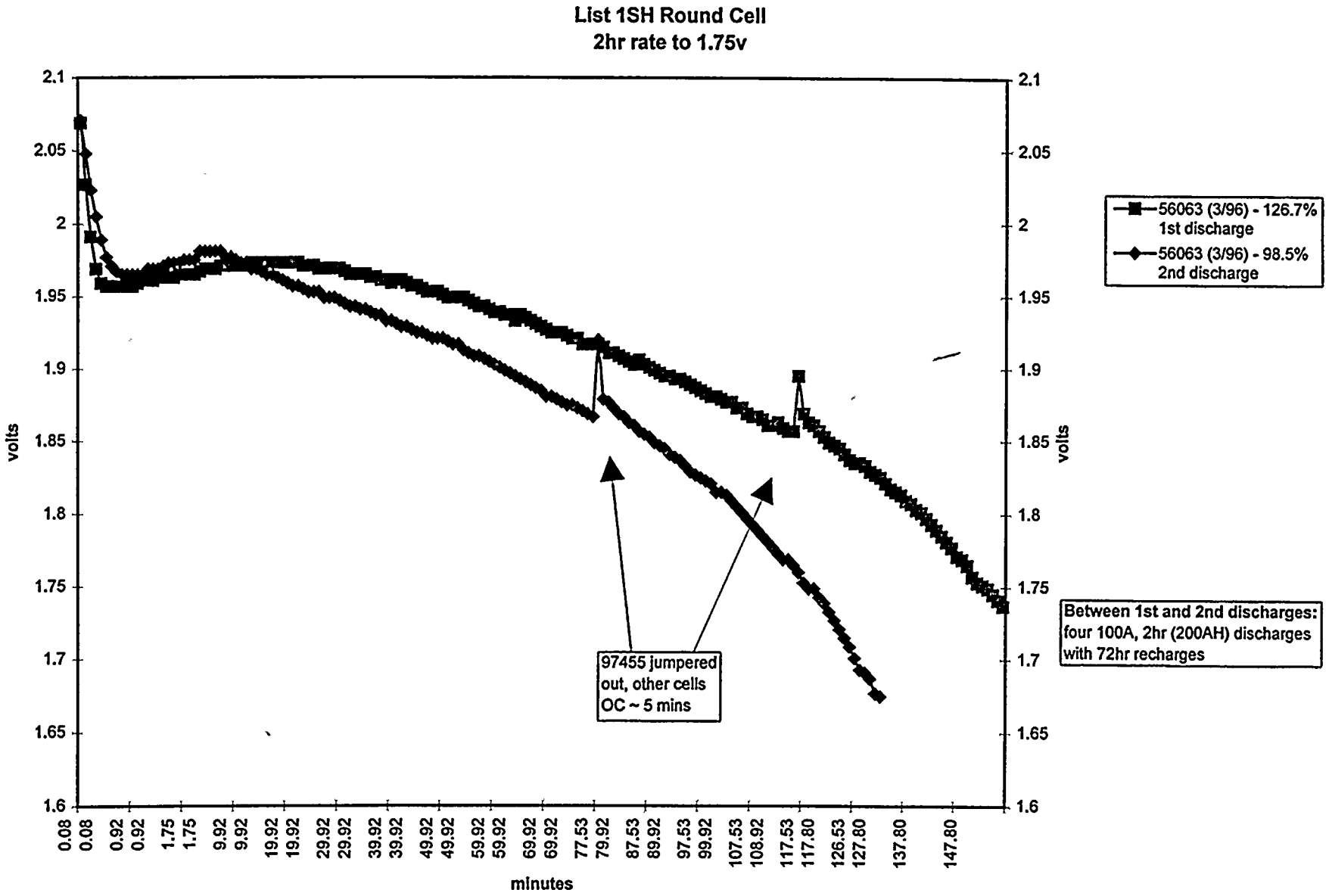

1st discharge 2/19/97
2nd discharge 3/12/97

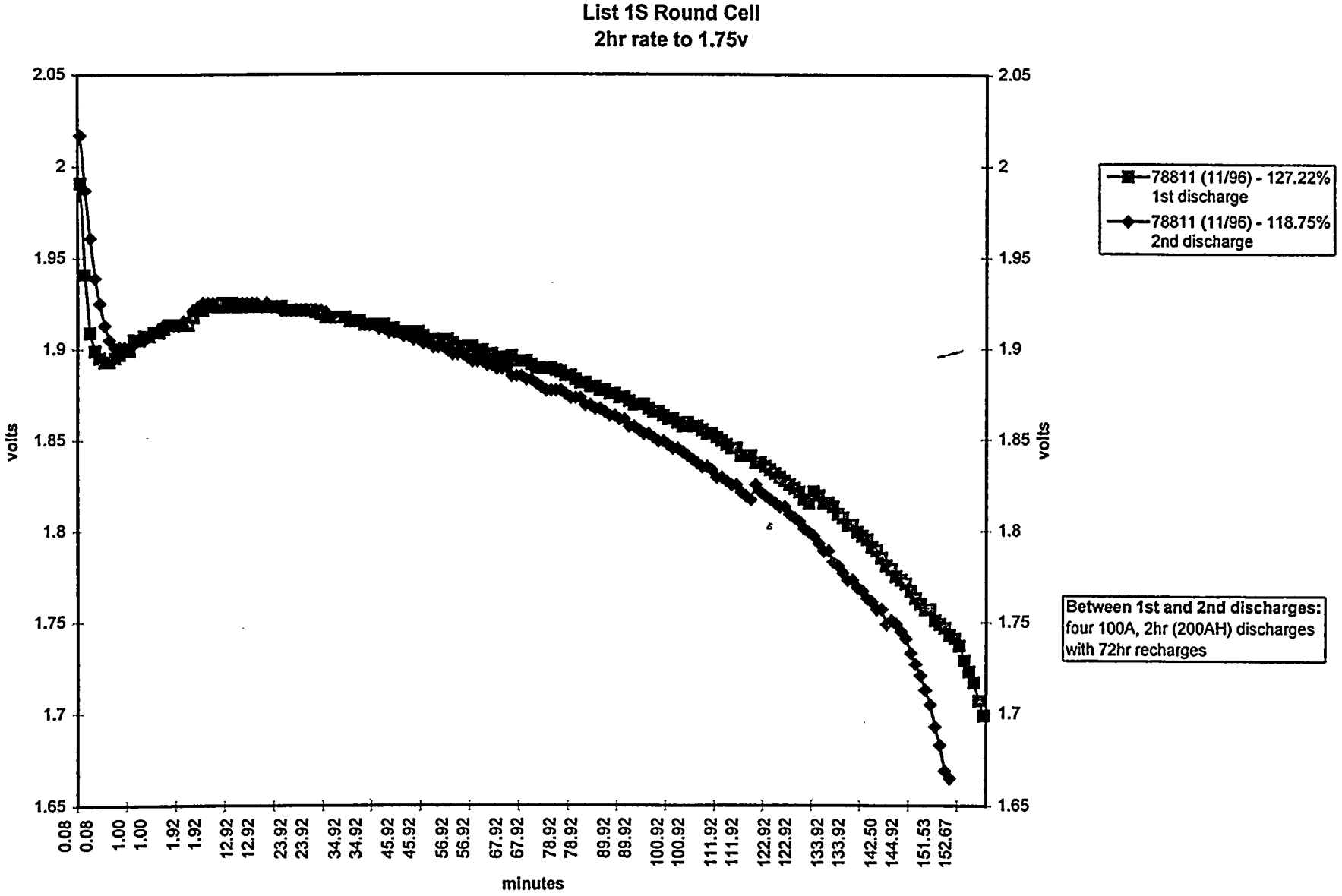

1st discharge 2/12/97
2nd discharge 3/12/97

Round Cell Multiple [redacted]ne Shallow Discharges

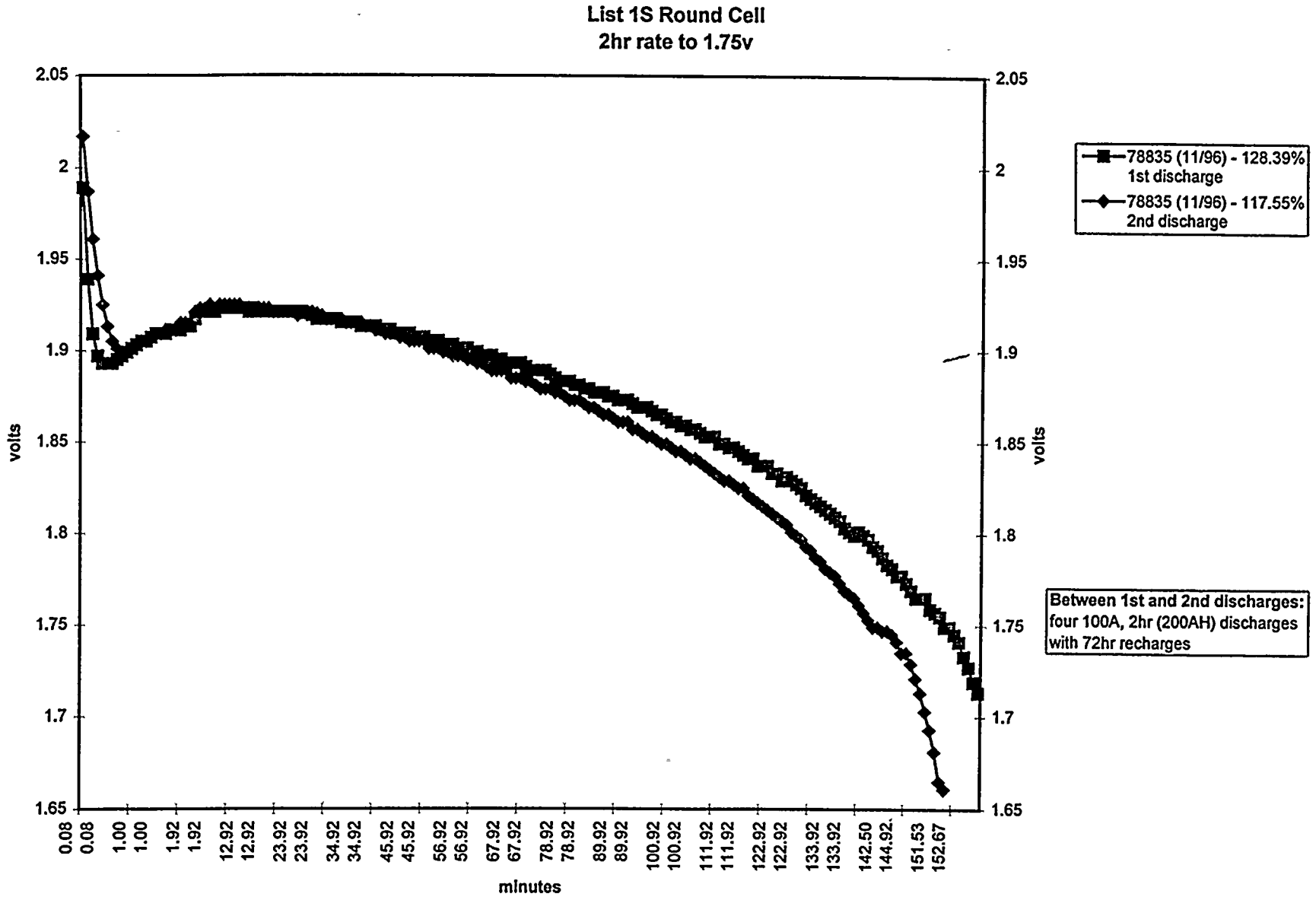

1st discharge 2/12/97
2nd discharge 3/12/97

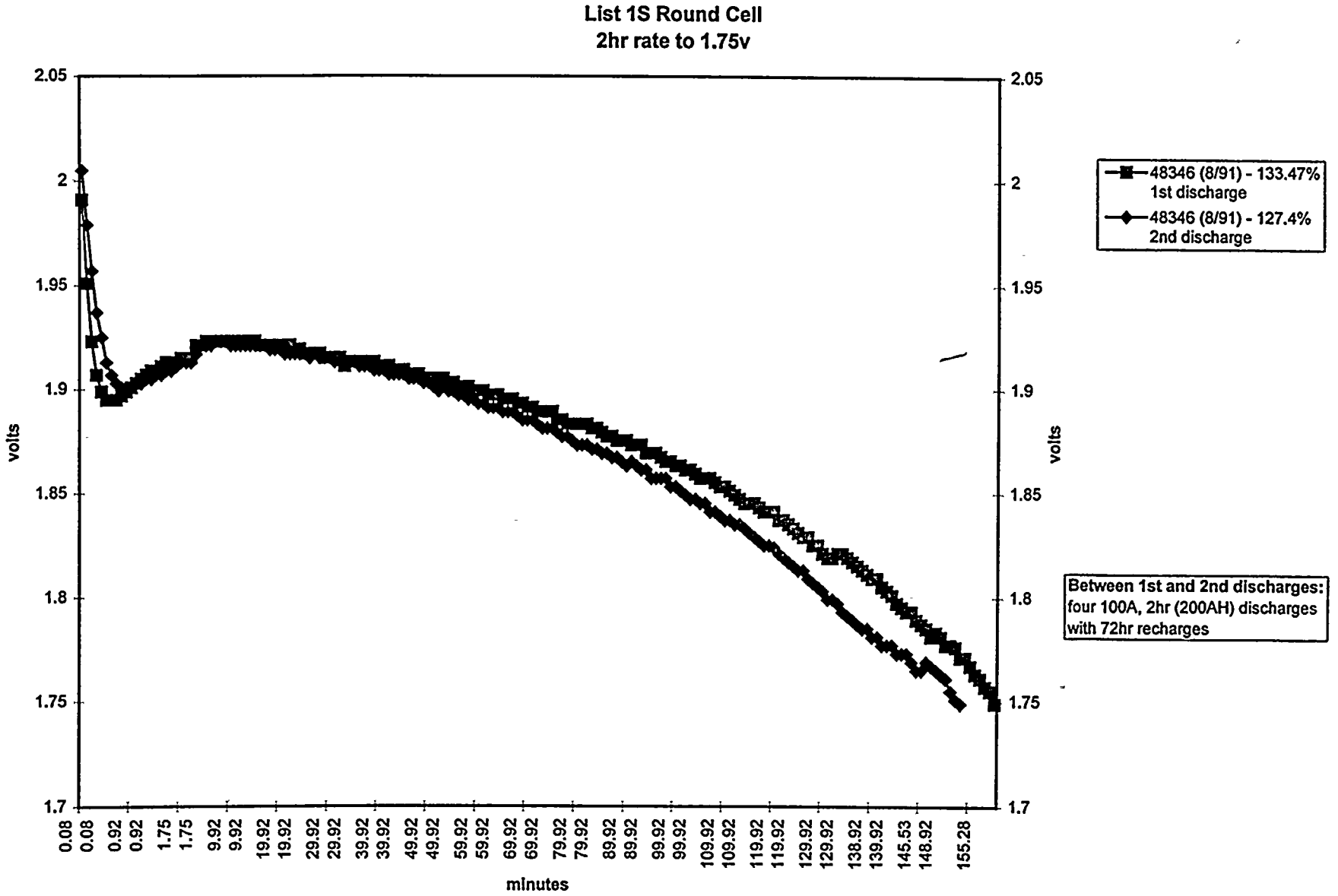

1st discharge 2/12/97
2nd discharge 3/12/97

Round Cell Multiple C[illegible]ne Shallow Discharges

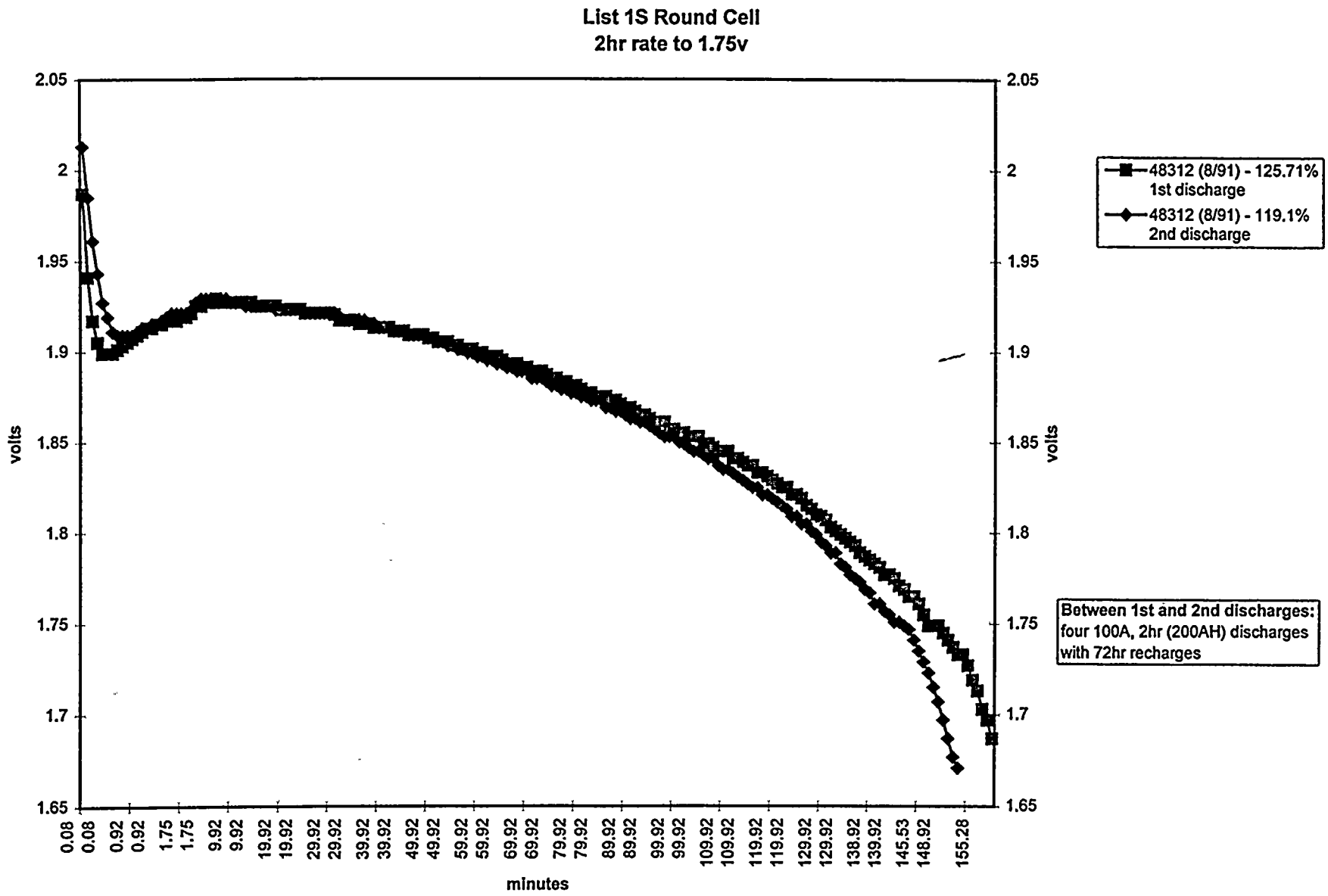

1st discharge 2/12/97
2nd discharge 3/12/97

Round Cell Multiple C[illegible]ne Shallow Discharges

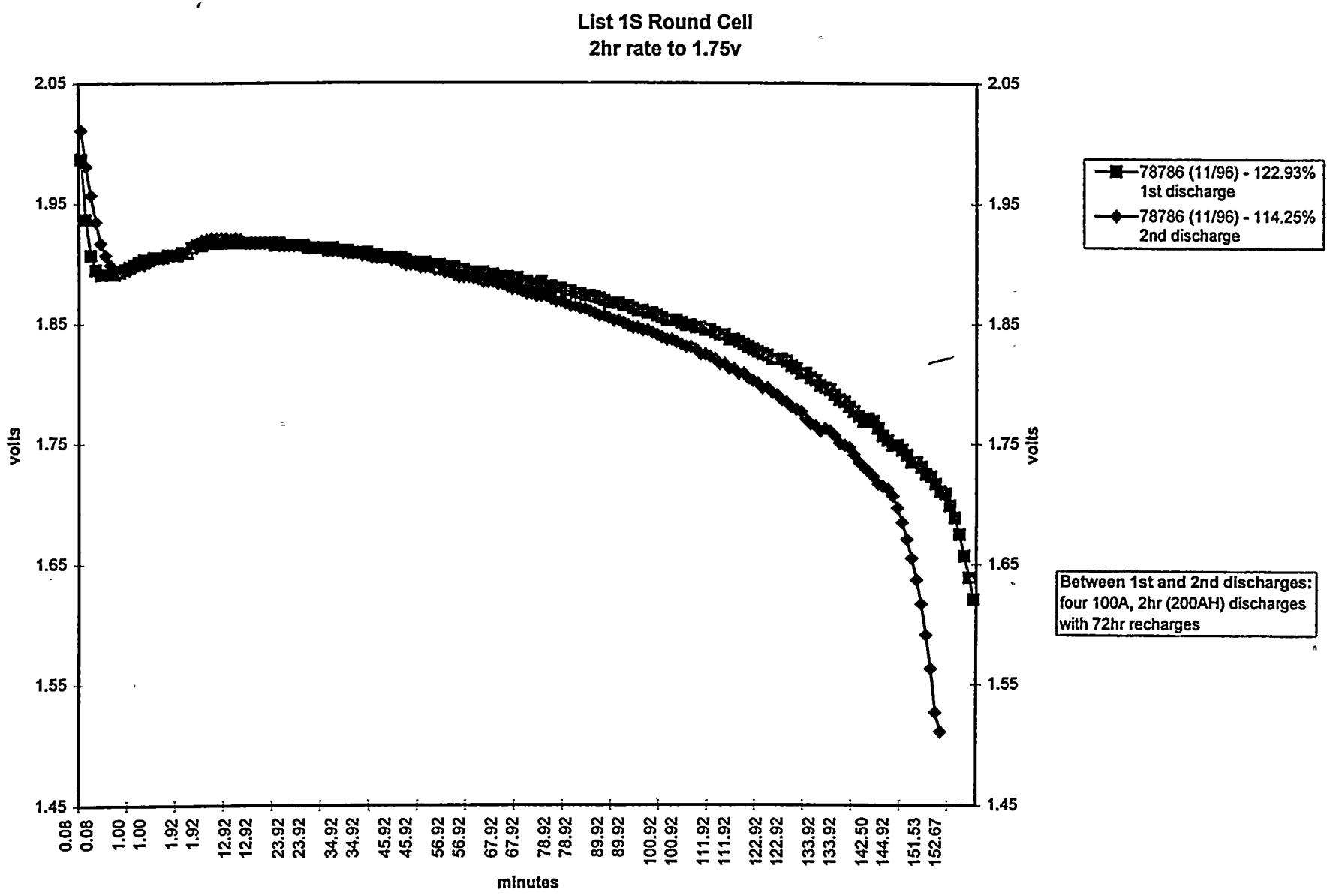

1st discharge 2/12/97
2nd discharge 3/12/97

Round Cell Multiple On-Line Shallow Discharges

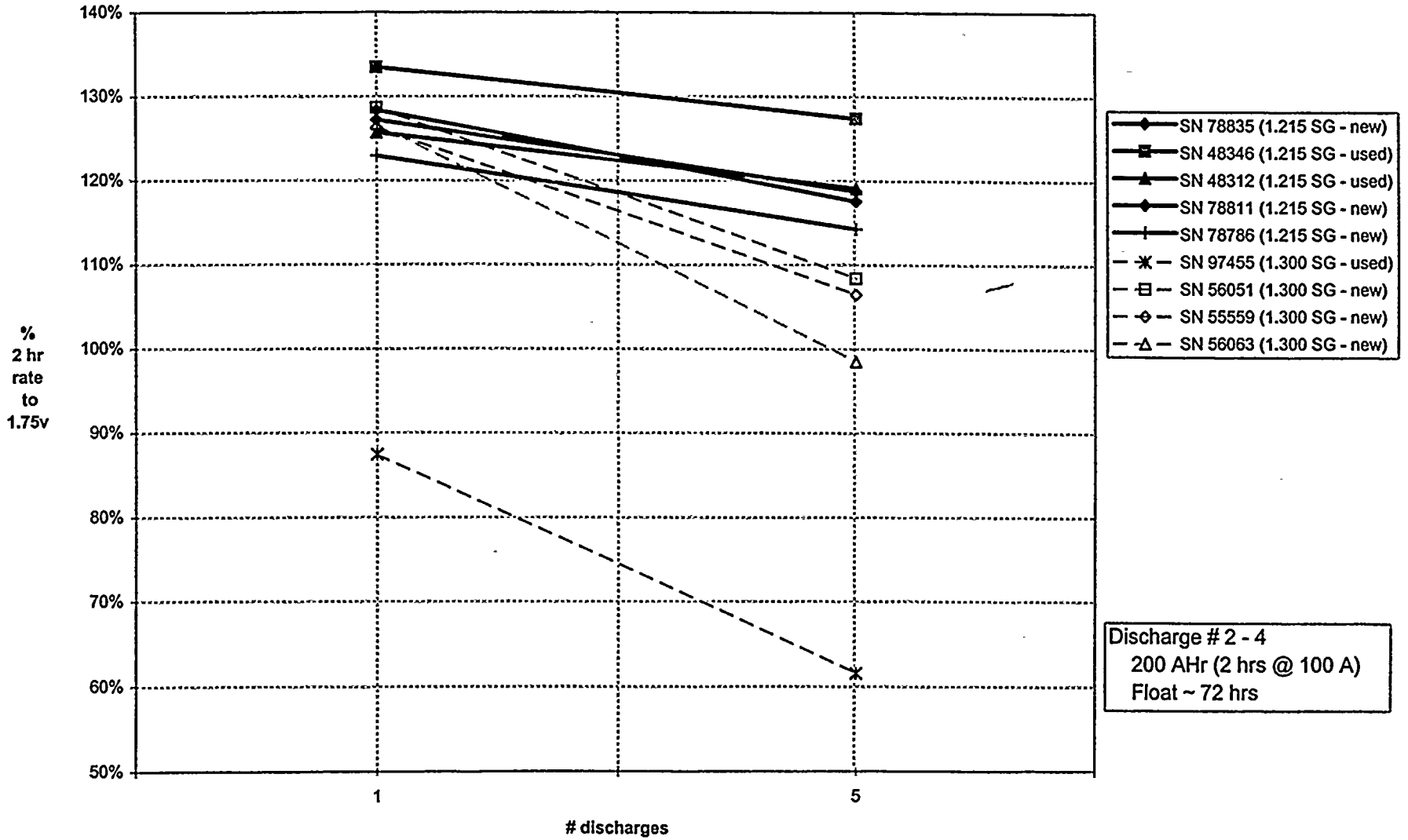

Industry Performance Test Examples
High-Gravity Round Cells

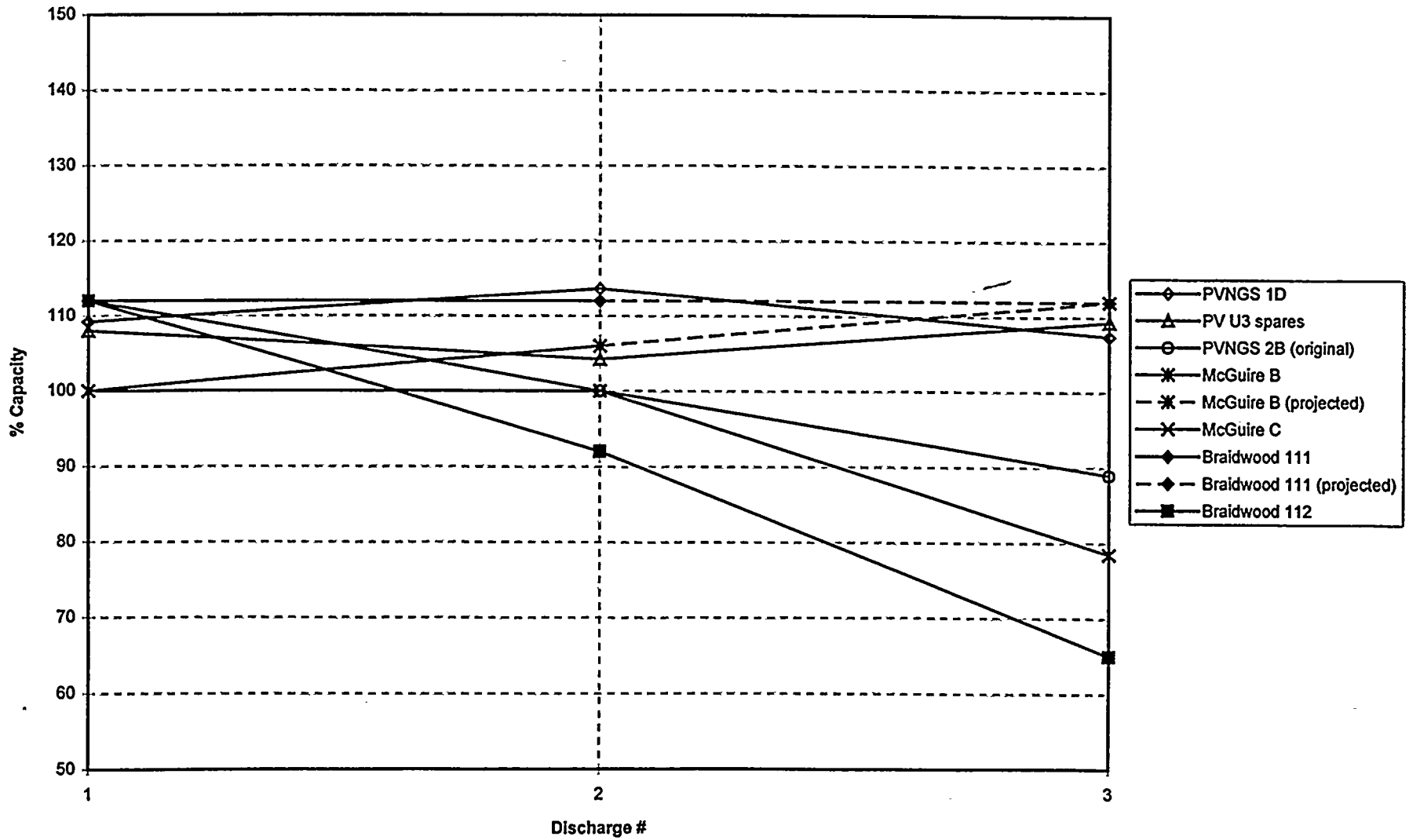

Lucent Technologies
Bell Labs Innovations

Microelectronics
Lucent Technologies Inc.
3000 Skyline Drive
Mesquite, TX 75149-1802

July 26, 1996

Memorandum of Record - Nuclear Utility Market Sales

After considerable evaluation, Lucent Technologies Inc., Microelectronics Group - Power Systems Division has decided to discontinue manufacturing the High Gravity Round Cell Flooded Batteries. Further, we have decided to discontinue marketing and sales activities of all power products into the nuclear utility market.

Lucent Technologies has earned a reputation of quality and customer satisfaction through the most technologically advanced power products, service and delivery available today. Because of this focus, we want to emphasize our intention of continued quality product and support for our existing customers. We will work with each of our five nuclear utility customers individually to establish plans for going forward. Options for consideration and evaluation include migration to another product or the use of our Low Gravity Round Cell Flooded Batteries.

We plan to initiate discussions with each of our customers immediately. Questions may be directed to me or the individuals listed below.

Sincerely,

E. B. Kahn
Director, Business Operations

Additional Contacts:

Ms Tracey Altman, Public Relations	(214) 284-2195
Mr. Jeff Bomaster, Product Management	(214) 284-3570
Mr. Frank Cavallaro, Sales Support	(214) 284-2482

Distribution List

To: Arizona Public Service Company
Commonwealth Edison Company
Duke Power
General Public Utilities Nuclear
Wolf Creek Nuclear Operating Group

Copies: Tracey Altman, Lucent Technologies
John Allen, Lucent Technologies
Whit Allen, Lucent Technologies
Jim Anderson, Wyle Laboratories
John Baldasty, Lucent Technologies
Jeff Bomaster, Lucent Technologies
Kathryn Bullock, Lucent Technologies
Kevin Burnett, Lucent Technologies
Frank Cavallaro, Lucent Technologies
Steve Clark, Lucent Technologies
Maureen Denton, Lucent Technologies
Frank Geosits, Lucent Technologies
Chuck Harm, Lucent Technologies
Dan Hill, Lucent Technologies
Pam Jackson, Lucent Technologies
Harold Kelly, H. Kelly Associates
Fred Laman, Lucent Technologies
Burt Lewis, Lucent Technologies
Greg Mathiesen, Lucent Technologies
Kieth McMillen, Lucent Technologies
Kevin Mortazavi, Lucent Technologies
MuMu Murugesamoorthi, Lucent Technologies
Erika Nannis, Lucent Technologies
Maureen O'Brien, Lucent Technologies
John Pendergrass, Lucent Technologies
Keith Schmidt, Lucent Technologies
Steve Voss, Lucent Technologies
Jay Walters, Lucent Technologies
Mike Weeks, Lucent Technologies
Bill Yeates, Lucent Technologies

Power Systems

Statement of Intent

- Discontinue Manufacturing High Gravity Round Cell Product Line
- Discontinue All Sales and Marketing Efforts
- Continue Limited Technical Support
- Individualized Customer Support and Warranty Administration
- Continue Representation on Round Cell Nuclear Utility User's Council

Power Systems

Key Decision Factors

- Past and Current Customer Concerns
- Capacity Loss
  - Repetitive/Frequent Deep Discharge Testing in this Application
- Amount of Support Required
- Focus on Core Telecommunications Markets and Customers
- Financial Contributions to the Business

Power Systems

Next Steps

- Discontinue All High Gravity Round Cell Battery Products
- Address All Outstanding Customer Issues
- Schedule Individual Customer Meetings to Determine Appropriate Approach
- Define Warranty, Based on Customer Requirements, Sizing, Other Factors